SERINE-451 PHOSPHORYLATION OF BACTERIAL-TYPE PHOSPHOENOLPYRUVATE CARBOXYLASE BY A CALCIUM-DEPENDENT PROTEIN KINASE LINKS CALCIUM SIGNALING WITH ANAPLEROTIC PATHWAY CONTROL IN DEVELOPING CASTOR OIL SEEDS

by

Allyson Tarah Hill

A thesis submitted to the Department of Biology

in conformity with the requirements for

the degree of Master of Science

Queen's University

Kingston, Ontario, Canada

August 2013

Abstract

Phospho*enol*pyruvate (PEP) carboxylase (PEPC) is a tightly controlled enzyme situated at a pivotal branchpoint of plant C-metabolism. Two physically and kinetically distinct oligomeric classes of PEPC exist in the endosperm of developing castor oil seeds (COS). Class-1 PEPC is a typical homotetramer composed of 107-kDa plant-type PEPC (PTPC) subunits, whereas the 910-kDa Class-2 PEPC hetero-octameric complex arises from a tight interaction between Class-1 PEPC and distantly related 118-kDa bacterial-type PEPC (BTPC) subunits. BTPC functions as both a catalytic and regulatory subunit of the allosterically-desensitized Class-2 PEPC, which has been hypothesized to support massive PEP-flux to malate for leucoplast fatty acid synthesis. Previous studies established that BTPC: (i) subunits of COS Class-2 PEPC are subject to inhibitory phosphorylation *in vivo,* and (ii) at Ser^{425} and Ser^{451} within an intrinsically disordered region. This study focuses on characterization of the COS protein kinase (BTPC-K) that phosphorylates BTPC at Ser^{451}. BTPC-K, having a native molecular mass of 63 kDa, was purified ~500-fold from developing COS endosperm. Its activity was absolutely dependent upon the presence of Ca^{2+} (K_a= 2.7 μM) and millimolar Mg^{2+}. BTPC-K phosphorylated BTPC subunits of Class-2 PEPC strictly at Ser^{451} (K_m= 1.1 μM), as well as histone type III-S (K_m= 1.7 μM), but did not phosphorylate a BTPC S451D phosphomimetic mutant, native COS PTPC or sucrose synthase, or α-casein. BTPC-K displayed a broad pH-activity optima of pH 7.3, a K_m for Mg^{2+}-ATP of 6.6 μM, and marked inhibition by 3-P-glycerate and PEP. The possible control of BTPC-K by disulfide-dithiol interconversion was suggested by its rapid inactivation and subsequent reactivation when incubated with oxidized glutathione and then dithiothreitol. BTPC-K activity was insensitive to exogenous calmodulin, but potently inhibited by 100 μM trifluoperazine (a calmodulin antagonist). BTPC-K-mediated Ser^{451} phosphorylation of BTPC

subunits of Class-2 PEPC inhibited BTPC activity by ~50% when assayed under suboptimal conditions (pH 7.3, 1 mM PEP with 10 mM L-malate). Overall the results of this study have led to the hypothesis that *in vivo* phosphorylation of COS BTPC at Ser^{451} is mediated by a dedicated calcium-dependent protein kinase (CDPK).

Co-Authorship

My collaborator in Chapter 2 was Dr. Sheng Ying who performed the bioinformatics analysis of the castor CDPK gene family. All other experiments reported in Chapter 2 were performed by myself.

Acknowledgements

I would first and foremost like to acknowledge the dedicated and unwavering support I have received from Dr. Plaxton throughout the entirety of my time as a student in his lab. His commitment to excellence in science and his belief that innovative scientific research should be used for the benefit of Canadian society have been both inspirational to me and the basis for my decision to pursue a career in scientific public policy. I am also very grateful to Dr. Wayne Snedden and Dr. Andrew Craig for their excellent guidance and constant encouragement throughout my thesis project. Thank you also to Dr. Ken Ko for kindly serving on my defense committee at the last minute. I would also like to thank all of the members of the Plaxton lab I have been privileged to work with over these past three years. Firstly to Brendan O'Leary, thank you for being a fantastic teacher and mentor. I owe all of my successes to your patience and hard work training me, and your continued support while at Oxford has been invaluable. To Eric Fedosejevs, thank you very much for your constant help in the lab, in particular thank you for the all of the time and effort you have taken to help me with protein purification troubleshooting. To Sheng Ying, thank you for help with my bioinformatic analyses and the delicious authentic Chinese cuisine! To the rest of the Plaxton lab, members past and present, thank you for your friendship and support. To all of the undergraduate volunteers who have helped with my project, thank you for your time and effort. A very special thanks to Malvika Dasani and Kisa Iqbal for being both great friends and phenomenal volunteers. To Kyle Bender and Trevor Snider, thank you for all of the excellent advice and help you have given me with various aspects of my project. To Michal Pyc, thank you not only for your help grinding innumerable batches of castor tissue, but for everything else you have done to help me finish my project.

I would also like to acknowledge my loving parents and family, without whom achieving this degree would not have been possible. In particular to Mum and Dad, thank you for the years of unconditional support you have given me, I am incredibly blessed to have parents as wonderful as you. Lastly, thank you to all of the friends old and new, near and far who have been with me however long, on this stretch of my academic journey! My research has been generously supported by an NSERC graduate scholarship, as well as NSERC Discovery and RTI funding for the Plaxton lab.

Table of Contents

Abstract……...ii

Co-Authorship……iv

Acknowledgements……v

Table of Contents……vi

List of Figures……..viii

List of Tables……..ix

List of Abbreviations……...x

Chapter 1. Literature Review and Introduction……1

1.1 General Background and Genetics of PEPC……1

1.2 Physiological Roles of PEPC……3

1.3 The role of PEPC in Carbon Partitioning in Developing Seeds……4

1.4 Post-translational Control of Plant-Type PEPC……7

Allosteric Effectors……7
Regulatory Phosphorylation……...7
Monoubiquitination……..10

1.5 Class-2 PEPC complexes……12

Discovery of the Bacterial-Type PEPC (BTPC) Gene……12.
Discovery of Bacterial-Type PEPC (BTPC) Polypeptides……..13
Tissue-Specific Expression of Bacterial-Type PEPC (BTPC) in Castor Plant……16
Post-Translational Modification of BTPC in Castor Oil Seed……17

1.6 Thesis Objectives……18

Chapter 2. A calcium-dependent protein kinase (CDPK) *in vivo* phosphorylates bacterial-type phosphoenolpyruvate carboxylase at serine-451 in developing castor oil seeds……...26

2.1 Introduction……27

2.2 Materials and Methods……31

Plant Material……...31
Preparation of Clarified Extracts……31
PEPC and Protein Assays……31
Electrophoresis and Immunoblotting……...32
Microsomal Membrane Preparation……33
BTPC-K Assay and Kinetic Studies……33
Partial Purification of BTPC-K from Developing COS……...35
Estimation of Native Molecular Mass by Gel Filtration FPLC……36

2.3 Results and Discussion……37

Detection of BTPC-K Activity in Clarified COS extracts……...37
Monitoring BTPC-K Activity throughout COS Development and Following Pod Excision.....37
Partial Purification of BTPC-K from Developing COS……...39
Native Molecular Mass Estimation of BTPC-K……...40
In vitro Phosphorylation-Inhibition of Recombinant Class-2 PEPC by BTPC-K……...40
Kinetic Characterization of BTPC-K……...42
Substrate Specificity of BTPC-K…….43
Metabolite Effectors and Redox Control of BTPC-K……..44
Effects of Calmodulin, 14-3-3s and a Calmodulin Antagonist on BTPC-K Activity……..45
Bioinformatic Analysis of Castor CDPK Family…….47

2.4 Concluding Remarks……...48

2.5 Acknowledgments……...52

Chapter 3. General Discussion……65

3.1 Overview……65

3.2 Future Directions……70.

References……74

Appendices……83

List of Figures

Figure 1.1 The phospho*enol*pyruvate carboxylase reaction……20

Figure 1.2 The diverse functions of plant PEPC……..21

Figure 1.3 Models illustrating several metabolic functions of plant PEPC……..22

Figure 1.4 Amino acid sequence alignment of Arabidopsis and castor oil plant PEPC isoenzymes…….23

Figure 1.5 Model illustrating the biochemical complexity of castor bean PEPC…….25

Figure 2.1 Time course for COS BTPC-K and ATP-dependent phosphorylation and λ-phosphatase-dependent dephosphorylation at Ser^{451} of the BTPC (p118) subunit of recombinant Class-2 PEPC ……53

Figure 2.2 Developmental profile of BTPC-K activity during COS development and influence of seed pod excision on BTPC-K activity……..54

Figure 2.3 Time-course for BTPC-K-mediated phosphorylation of COS BTPC at Ser^{451}……..55

Figure 2.4 Kinetic effect of Ser^{451} phosphorylation on BTPC activity of mutant Class-2 PEPC……..57

Figure 2.5 Effect of calcium, divalent metal cations, and assay pH, on relative BTPC-K activity……58

Figure 2.6 Substrate specificity of BTPC-K…….59

Figure 2.7 Effect of 3-P-glycerate (3PGA) and PEP on BTPC-K activity……...60

Figure 2.8 BTPC-K is partially inactivated by GSGG and reactivated by DTT……..61

Figure 2.9 Phylogenetic analysis of castor CDPKs……..62

Figure 2.10 BTPC-K is a soluble protein kinase……..63

Appendix 5 Exogenous bovine PK-A is unable to phosphorylate COS BTPC subunits of Class-2 PEPC at Ser^{451}……86

Appendix 6 Native molecular mass determination for purified BTPC-K……...87

Appendix 7 Analysis of purified COS BTPC-K by SDS-PAGE……..88

Appendix 8 Determination of COS BTPC-K specific activity…….89

Appendix 9 BTPC-K is unable to phosphorylate synthetic peptide containing residues flanking the BTPC Ser^{451} phospho-site……..90

Appendix 11 Domain structure of a CDPK……..91

Appendix 13 Partial alignment of COS BTPC Ser^{425} and Ser^{451} phosphorylation domains with other vascular plant BTPCs……...…94

List of Tables

Table 2.1 Purification of BTPC-K from stage V-VII developing COS endosperm…….64
Appendix 10 Effect of exogenous proteins and CaM antagonist on BTPC-K activity……90
Appendix 12 Predicted properties of deduced castor CDPKs……..92

List of Abbreviations

A_{280}	absorbance at 280 nanometers
BTPC	bacterial type phospho*enol*pyruvate carboxylase
BTPC-K	bacterial type phospho*enol*pyruvate carboxylase kinase
CAD	calcium-dependent protein kinase activation domain
CaM	calmodulin
CAM	Crassulacean acid metabolism
CDPK	calcium-dependent protein kinase
CoA	coenzyme A
COS	castor oil seed
Co-IP	co-immunopurification
DDL	dawdle protein
DTT	dithiothreitol
EGTA	ethylene glycol tetraacetic acid
FPLC	fast protein liquid chromatography
Glu-6-P	glucose-6-phosphate
GSSG	oxidized glutathione
I_{50}	inhibitor concentration yielding 50% activity
kDa	kilodalton
LC	liquid chromatography
MC-LR	microcystin-LR
MDH	malate dehydrogenase
M_r	molecular mass
MS	mass spectrometry
MS/MS	tandem mass spectrometry
NCBI	National Center for Biotechnology Information
OAA	oxaloacetate
PAGE	polyacrylamide gel electrophoresis
PEP	phospho*enol*pyruvate
PEPC	phospho*enol*pyrvuate carboxylase

Pi	inorganic phosphate
PK_c	cytosolic pyruvate kinase
PK_p	plastidic pyruvate kinase
PP2A	protein phosphatase type 2A
PPCK	PEPC protein kinase
PTM	post-translational modification
PTPC	plant type phospho*enol*pyruvate carboxylase
SnRK1	sucrose non-fermenting related kinase
TCA	trichloroacetic acid

Chapter 1. Introduction and Literature Review

1.1 GENERAL BACKGROUND AND GENETICS OF PEPC

PEPC [PEP(phosphoenolpyruvate) carboxylase] (EC 4.1.1.31) is an important, tightly controlled enzyme situated at a critical branch point in plant carbohydrate metabolism. It catalyzes the irreversible conversion of phosphoenolpyruvate (PEP) to oxaloacetate (OAA) and inorganic phosphate (Pi) in the presence of a divalent metal cation (Mg^{2+}, Mn^{2+}) and HCO_3^- (Figure 1.1)(O'Leary *et al.,* 2011b). PEPC is present in all vascular plants, green algae and most bacteria, but is absent in fungi and animals (Patel *et al.,* 2004; Ettema *et al.,* 2004; Izui *et al.,* 2004). It is best known for catalyzing atmospheric CO_2 fixation in C_4 and crassulacean acid metabolism photosynthesis (CAM) (Chollet *et al.,* 1996). In C_3 leaves and non-green tissues such as developing fruits and seeds, PEPC has a crucial non-photosynthetic role: it catalyzes the anaplerotic replenishment of carbon skeletons withdrawn from the Kreb's cycle for biosynthesis and nitrogen assimilation (Figure 1.2) (Chollet *et al.,* 1996; O'Leary *et al.,* 2011b).

Plant PEPCs belong to a small multigene family that encodes several "plant-type" PEPCs (PTPC), as well as one distantly related "bacterial-type" PEPC (BTPC) (O'Leary *et al.,* 2011b; Sanchez and Cejudo, 2003; Gennidakis *et al.,* 2007; Mamedov *et al.,* 2005; Sullivan *et al.,* 2004; Igawa *et al.,* 2010). PTPC genes encode closely related 105-110 kDa polypeptides which are distinguished by their conserved N-terminal seryl-phosphorylation domain, and that typically exist as 400-440 kDa homotetrameric Class-1 PEPCs (O'Leary *et al.,* 2011b; Izui *et al.,* 2004; Kai *et al.,* 2003). PTPCs are categorized as being either photosynthetic (C_4 and CAM PEPCs) or non-photosynthetic (C_3) isozymes. All PTPCs evolved from a common ancestral gene and thus exhibit a high degree of conservation at the genetic level (Izui *et al.,* 2004).

Extensive genetic and biochemical studies of photosynthetic and non-photosynthetic PTPC isozymes have determined that PTPC and thus Class-1 PEPC activity is subject to several types of post-translational controls. Allosteric activation and inhibition by glucose-6-P and malate, respectively (among other metabolic intermediates), along with phosphorylation-activation catalyzed by a dedicated Ca^{2+}-independent Ser/Thr kinase known as PEPC protein kinase (PPCK), and dephosphorylation by a protein phosphatase type-2A (PP2A) account for the most significant post-translational control of Class-1 PEPC (Izui *et al.,* 2004; Vidal *et al.,* 1997; Chollet *et al.,* 1996; Nimmo, 2003; O'Leary *et al.,* 2011b). More recent work on non-photosynthetic PEPCs has implicated reversible monoubiquitination as yet another tier of Class-1 PEPC control (O'Leary *et al.,* 2011b; Uhrig *et al.,* 2008b; Shane *et al.,* 2013). The crystal structures for *Zea mays* (maize) C_4 PEPC and *Escherichia coli* PEPC have also been solved, and this information in conjunction with site-directed mutagenesis studies have furthered our understanding of the structure-function relationships of Class-1 PEPC catalysis, as well as the control exerted by post-translational modifications (PTMs) and allosteric effectors (Izui *et al.,*2004; Kai *et al.,* 2004; O'Leary *et al.,* 2011b).

All plant genomes sequenced to date as well as that of ancestral green algae, also contain at least one *BTPC* gene. *BTPC* genes encode single, distantly related 116-118 kDa (130-kDa in green algae) polypeptides that are immunologically distinct from PTPCs and whose amino acid sequence shares a higher degree of similarity with PEPCs from proteobacteria than with PTPCs (Sanchez and Cejudo, 2003; O'Leary *et al.,* 2011b). These novel PEPC isozymes were therefore designated as "BTPCs" whereas all other C_3, C_4, and CAM PEPCs were subsequently classified as PTPCs. While PTPC isozymes are ubiquitously expressed in all plant tissues, BTPC isozymes appear to be mainly expressed in rapidly growing and/or biosynthetically active tissues

(Gennidakis *et al.,* 2007; Igawa *et al.,* 2010; O'Leary *et al.,* 2011a; O'Leary *et al.,* 2011b). BTPCs also have regulatory and structural characteristics that distinguish them from PTPCs and which will be discussed below. Additionally, green algal and vascular plant BTPCs physically interact with the corresponding Class-1 PEPC homotetramer to produce an unusual ~ 900-kDa hetero-octameric Class-2 PEPC (Figure 1.5) (Blonde and Plaxton, 2003; Gennidakis *et al.,* 2007; O'Leary *et al.,* 2009; Rivoal *et al.,* 1998; Rivoal *et al.,* 2001).

1.2 PHYSIOLOGICAL ROLES OF PEPC

Photosynthetic PTPCs in C_4 and CAM leaves function as a mechanism of concentrating atmospheric CO_2 via the assimilation of HCO_3^- (newly converted from CO_2 and H_2O by carbonic anhydrase) into OAA. Photosynthetic PEPCs thus reduce photorespiration and improve overall photosynthetic efficiency by as much as 2-fold relative to C_3 leaves (Svensson *et al.,* 2003; Nimmo, 2000; Vidal *et al.,* 1997; Hibberd *et al.,* 2010). Apart from its fundamental role in the initial fixation of CO_2 in C_4 and CAM photosynthesis, PEPC also has a wide-range of non-photosynthetic roles including supporting C/N interactions, seed formation and germination, guard cell metabolism during stomatal opening, fruit ripening, and the provision of malate as a respiratory substrate for symbiotic N_2-fixing bacteroids of legume root nodules (Figure 1.2) (O'Leary *et al.,* 2011b). Of these many functions, the focus of this thesis pertains to PEPC's role in the control of carbon partitioning to various storage end products in developing oil seeds. PEP metabolism via PEPC as well as cytosolic pyruvate kinase (PK_c) and plastidic pyruvate kinase (PK_p) plays a crucial role in partitioning photosynthate towards either leucoplast fatty acid biosynthesis or the mitochondrial production of carbon skeletons and ATP needed for amino acid interconversion to facilitate storage protein biosynthesis (Figure 1.3) (O'Leary *et al.,* 2011b; Plaxton and O'Leary *et al.,* 2011).

1.3 THE ROLE OF PEPC IN CARBON PARTITIONING IN DEVELOPING SEEDS

Developing seeds are important metabolic sinks which import large quantities of sugars and amino acids from metabolic source tissues (i.e. leaves) that must be metabolized into the starches, triglycerides and storage proteins which will eventually support seed germination. The partitioning of photosynthate into these three storage reserves is of great agronomic significance. Therefore, a detailed understanding of the metabolism of the developing seed is highly relevant for crop breeding and metabolic engineering. As was previously mentioned, PEP-metabolism via PEPC, PK_c and PK_p plays an important role in the partitioning of imported photosynthate to either leucoplast fatty acid biosynthesis or the mitochondrial production of C-skeletons and ATP needed for storage protein biosynthesis (Figure 1.3). It has been postulated that PEPC may also aid in refixing respired CO_2 to improve overall seed C economy (Golombek *et al.,* 1999; Uhrig *et al.,* 2008a; Singal *et al.,* 1995, King *et al.,* 1998; Chopra *et al.,* 2000; Park *et al.,* 2012). Increases in PEPC and PPCK activity as well as PTPC phosphorylation status during seed development are coincident with the main stages of storage oil and protein biosynthesis and have been shown to be controlled by photosynthate supply (Tripodi *et al.,* 2005, Murmu and Plaxton, 2007; Feria *et al.,* 2008; Singal *et al.,* 1995; King *et al.,* 1998; Sangwan *et al.,* 1992; Blonde and Plaxton, 2003; Sebei *et al.,* 2006; Lebouteiller *et al.,* 2007).

In regards to seed storage protein synthesis, PEPC is believed to be an important enzyme in this process owing to the requirement for OAA and 2-oxoglutarate (2-OG) needed to assimilate N during amino acid formation (Figure 1.3A) (Rolletschek *et al.,* 2004; Radchuk *et al.,* 2007; Weber *et al.,* 2005). Additional C-skeletons are necessary when seeds import N in the form of amino acids because (1) glutamine (Gln), a major component of the amino acids imported into the developing seed contains two amino groups per 2-OG skeleton, and (2) several

amino acids such as alanine (Ala) can be deaminated and respired through the Krebs cycle, yielding NH_4^+ that must then be re-assimilated into Gln and/or glutamate (Glu) via glutamine synthetase and glutamate-oxoglutarate amino transferase (GS/GOGAT)(Figure 1.3A) (O'Leary *et al.*, 2011b).

Considerable research has also shown that PEPC supports triacylglyceride (storage oil) synthesis in non-green developing oil seeds via the production of metabolite precursors and reducing power. *De novo* fatty acid biosynthesis occurs within leucoplasts, a process which depends upon both ATP and NAD(P)H, and utilizes acetyl-CoA as an immediate precursor (Figure 1.3B). However, the pathway leading from sucrose-derived cytosolic hexose-Ps to plastidial acetyl-CoA is quite flexible and varies within and between species. Thus the relative importance of PEPC-derived metabolite precursors (i.e. malate) in this process varies as well (Figure 1.3B) (Baud and Lepiniec, 2010; Rawsthorne, 2002). Studies using isolated leucoplasts from developing castor oil seeds (COS) and *Helianthus annus* (sunflower) seeds showed that exogenous malate supported maximal rates of triacylglyceride biosynthesis relative to other precursors (Pleite *et al.*, 2005; Smith *et al.*, 1992). Malate imported into the leucoplast is subsequently oxidized into acetyl-CoA via the plastidial isozymes of NADP-ME and pyruvate dehydrogenase complex (PDC), resulting in the production of all the reductant (NADPH and NADH) and acetyl-CoA necessary for C incorporation into fatty acids (Figure 1.3B). Additionally, storage lipid accumulation in COS is closely correlated with both PEPC and NADP-ME protein abundance and activity (Sangwan *et al.*, 1992; Houston *et al.*, 2009; Benedict and Beevers, 1961; Gennidakis *et al.*, 2007; Blonde and Plaxton, 2003; Shearer *et al.*, 2004) and a specific malate-Pi antiporter has been identified within the leucoplast envelope of developing COS and maize embryos (Eastmond *et al.*, 1997; Lara-Nunez and Rodriguez-Sotres, 2004).

Metabolic flux studies have reported that in developing green oil seeds such as rapeseed, flux from malate to plastidial acetyl-CoA appears to be negligible (Schwender *et al.,* 2006) despite a strong correlation between PEPC expression and oil synthesis rates (Sebei *et al.,* 2006). In contrast, in non-green oil seeds such as maize and sunflower, 30% and 10% respectively, of C flux into fatty acids was reported to be derived from PEPC generated malate (Alonso *et al.,* 2007; Alonso *et al.,* 2010). Taken together, these results support the hypothesis that PEPC plays an important role in controlling sucrose partitioning at the cytosolic PEP branchpoint to produce C-skeletons and reductant required for fatty acid biosynthesis in developing non-green oil seeds such as COS (Figure 1.3B) (O'Leary *et al.,* 2011b). The metabolic flux studies have revealed that PEPC provisioning of malate appears to be more important for fatty acid biosynthesis in non-green oil seeds versus green oil seeds. Since fatty acid synthesis in green oil seeds is light-dependent (Baud and Lepiniec 2010; Goffman *et al.,* 2005; Ruuska *et al.,* 2004) most of the reducing power needed to assemble fatty acids from acetyl-CoA is generated by the light reactions of leucoplast photosynthesis. Non-green oil seeds however do not photosynthesize; thus they must rely upon the reductant produced by the oxidation of malate and other metabolite precursors of acetyl-CoA to fuel triacylglyceride synthesis.

In the early 1960's, Harry Beevers (Purdue University), a celebrated plant physiologist, began a prolific body of work studying oilseed development and germination, carbon metabolism, and triacylglyceride storage and mobilization, using the castor plant as a model. COS has since become an important model system for studying non-green oilseed metabolism. Several desirable attributes of COS including its massive accumulation of storage oils during development (~64% of total seed weight) (Buchanan *et al.,* 2000; Eastmond and Graham, 2001), its easily harvestable endosperm tissue, and robust and rapid growth have also contributed to its

amenability as a model organism for studying oil seed metabolism. The recent sequencing and annotation of the castor genome have provided an important foundation for further investigation of regulatory and metabolic networks of castor-oil biosynthesis (Chan *et al.*, 2010).

1.4 POST-TRANSLATIONAL CONTROL OF CLASS-1 PEPCs

Allosteric Effectors

Plant Class-1 PEPCs are subject to a wide variety of post-translational controls, most of which were elucidated by 1990. Allosteric control of Class-1 PEPC is mediated by both feed-forward activation and feedback inhibition. Hexose and triose-phosphates including glucose-6-phosphate (Glu-6-P) and glycerol-3-phosphate (Gly-3-P) are allosteric activators, whereas L-malate, aspartate (Asp) and Glu are allosteric inhibitors (Figures 1.1 and 1.3A) (Chollet *et al.*, 1996; Blonde and Plaxton, 2003; O'Leary *et al.*, 2011b; Law and Plaxton, 1997; Moraes and Plaxton, 2000). Inhibition by Asp and Glu provides a regulatory link between N-metabolism and the control of respiratory C metabolism in plant tissues active in N-assimilation, through the concordant control of Class-1 PEPC (Figure 1.3A).

Regulatory Phosphorylation

Regulatory phosphorylation of Class- 1 PEPC was first documented through the study of C_4 and CAM photosynthetic Class-1 PEPC isozymes (Nimmo, 2003) and has since been implicated in the *in vivo* control of the enzyme from a wide range of non-photosynthetic tissues (O'Leary *et al.*, 2011b). Phosphorylation of PTPC occurs at a single, highly conserved serine (Ser) residue near the N-terminus of the protein (Figure 1.4). The phosphorylation of Class-1 PEPC results in enzyme activation at physiological pH by decreasing its sensitivity to allosteric inhibitors whilst simultaneously increasing its affinity for PEP and sensitivity to allosteric activators (Chollet *et al.*, 1996; Izui *et al.*, 2004; O'Leary *et al.*, 2011b, Nimmo, 2003; Nimmo,

2006). The phosphorylation status of Class-1 PEPCs is mediated by an endogenous Ca^{2+}-independent PEPC protein kinase (PPCK) and protein phosphatase type-2A (PP2A) (Nimmo, 2003; Nimmo, 2006; Li and Chollet, 1994; Wang and Chollet, 1993; Murmu and Plaxton, 2007). Due to the importance of phosphorylation as a regulatory mechanism of Class-1 PEPC, extensive studies of PPCK have been undertaken, including its cloning from CAM, C_4, and C_3 plants, as well as the purification and characterization of the native protein from several species (Nimmo, 2003; Nimmo, 2006). Consequently, PPCK-mediated phosphorylation of Class-1 PEPC continues to be one of the most well-understood paradigms of regulatory enzyme phosphorylation *in planta* (O'Leary *et al.,* 2011b).

With M_rs ranging from 31-33 kDa, PPCKs lack a regulatory domain and consist only of a core kinase catalytic domain; they are thus the smallest protein kinases yet to be reported (Izui *et al.,* 2004; Nimmo, 2006). Due to the lack of any regulatory domain, PPCK activity and ultimately Class-1 PEPC phosphorylation status appears to be largely controlled by rates of PPCK synthesis and degradation (Izui *et al.,* 2004; Nimmo, 2006; Murmu and Plaxton, 2007). This means of control is relatively unorthodox as most protein kinases are post-translationally controlled by second messengers such as Ca^{2+} ions, cyclic nucleotides, and/or phosphorylation by other protein kinases. However there is some evidence of additional post-translational PPCK controls including: (1) malate inhibition of PPCK activity, possibly through its interaction with PEPC (Murmu and Plaxton, 2007; Law and Plaxton, 1997; Wang and Chollet, 1997), (2) dithiol-disulfide interconversion (Murmu and Plaxton, 2007; Saze *et al.,* 2001; Tsuchida *et al.,* 2001), and (3) a proteinaceous inhibitor (Nimmo *et al.,* 2001).

PPCK expression is upregulated *in planta* in response to a variety of signals. These include light and N supply in C_3 leaves, light in C_4 leaves, a circadian rhythm in CAM leaves,

nutritional Pi deprivation in cell cultures and C_3 plants, and photosynthate supply in developing seeds and legume root nodules (Nimmo, 2003; Nimmo, 2006; Murmu and Plaxton, 2007; Feria *et al.,* 2008; Chen *et al.,* 2008; Fukayama *et al.,* 2006; Monreal *et al.,* 2010; Monreal *et al.,* 2007; Shenton *et al.,* 2006; Gregory *et al.,* 2009). In developing COS and soybean root nodules endogenous PPCK transcripts, activity, and PTPC phosphorylation are eliminated in response to prolonged darkness of intact plants. The reillumination of these plants led to the complete reversal of these effects (Murmu and Plaxton, 2007; Chen *et al.,* 2008; Tripodi *et al.,* 2005). It is clear from these results that there is a direct relationship between the delivery of photosynthate from illuminated leaves to these heterotrophic "sink-tissues" and the upregulation of PPCK activity and PTPC phosphorylation. Studies of the PP2A which dephosphorylates PTPC *in vivo* have shown constant expression levels throughout plant tissue, indicating that PTPC phosphorylation status is predominantly controlled by PPCK activity (Chollet *et al.,* 1996; Hartwell *et al.,* 1999; Dong *et al.,* 1998). However, PP2A is notoriously under-studied in comparison with PPCK. Therefore, additional research is necessary in order to determine whether the catalytic activities of PP2A subunits are controlled by associated regulatory subunits. Nevertheless, PPCK-mediated phosphorylation of PEPC appears to be one of the many ways in which plant cells sense sugars, allocate C between source and sink tissues, and subsequently partition it into various storage end products.

Aside from directly controlling enzymatic activity, protein phosphorylation can provide docking sites for other proteins and thus can be a crucial component in mediating protein:protein interactions. In particular, a highly conserved and abundant family of proteins collectively known as 14-3-3s, bind to phospho-sites on diverse target proteins and play a central regulatory role in eukaryotic cells (Plaxton and Podestá, 2006). The *Arabidopsis* PTPC isozyme AtPPC1

was recently identified as a putative 14-3-3 binding protein via the proteomic profiling of tandem affinity purified 14-3-3 protein complexes from transgenic *Arabidopsis* seedlings (Chang *et al.,* 2009). However, AtPPC1, and PTPCs in general, do not contain any known 14-3-3 binding motifs and attempts to demonstrate 14-3-3 binding by pure native phospho- or dephosphorylated AtPPC1 have been unsuccessful (C. MacKintosh and W. Plaxton, unpublished data). Additional research is necessary to determine whether or not 14-3-3s do bind to any Class-1 PEPCs or have any effect on the enzyme's kinetic and regulatory properties.

Monoubiquitination

Ubiquitin is a small (8-kDa), highly conserved, regulatory protein found in all eukaryotic cells. It can be covalently attached to a target protein through an isopeptide bond between its C-terminal glycine (Gly) residue and the ε-amino group of a lysine (Lys) residue on its target. The attachment of ubiquitin to a protein is accomplished via a multi-enzyme system consisting of activating (E1), conjugating (E2), and ligating (E3) enzymes. Polyubiquitination is a well-studied, pervasive, eukaryotic PTM that targets proteins for degradation by the 26S proteasome. Unsurprisingly, the degradation of both PPCK and PTPC via the polyubiquitin-proteasome pathway has been reported (Agetsuma *et al.,* 2005; Schulz *et al.,* 1993). Less well-understood however, is protein monoubiquitination, a reversible and non-destructive PTM that mediates protein:protein interactions and protein subcellular localization to help control diverse cellular processes such as DNA repair, endocytosis, transcription and translation, and signal transduction (Schnell and Hicke, 2003; Mukhopadhay and Riezman, 2007).

Studies of Class-1 PEPC from germinating COS endosperm unexpectedly revealed that PTPC monoubiquitination is a further tier of post-translational control for this important metabolic enzyme (Uhrig *et al.,* 2008b). Germinating COS endosperm extracts contain two

immunoreactive PTPC polypeptides that migrate at 107- and 110-kDa, and which occur at a 1:1 ratio when PEPC is purified from these tissues. Through the use of N-terminal sequencing, mass spectrometry, and immunoblotting, it was established that both polypeptides are the products of the same *PTPC* gene (*RcPpc3*), and that the 110-kDa polypeptide is the monoubiquitinated form of the 107-kDa subunit (Figure 1.5) (Uhrig *et al.,* 2008b). Lys-628 was identified as the site of PTPC monoubiquitination in germinating COS endosperm; this residue is absolutely conserved in all sequenced PTPCs and BTPCs and is proximal to a PEP binding/catalytic domain (Uhrig *et al.,* 2008b). A recombinant human deubiquitinating enzyme [USP-2 (ubiquitin specific protease-2) core], when incubated with pure Class-1 PEPC from germinating COS endosperm, effectively cleaved ubiquitin from the 110-kDa PTPC subunit, converting it back into the 107-kDa subunit (Uhrig *et al.,* 2008b). Class-1 PEPC deubiquitination led to a significant reduction in the enzyme's K_m(PEP) and sensitivity to all allosteric effectors (Uhrig *et al.,* 2008b). PTPC monoubiquitination has since been demonstrated in *Lilium longiflorum* (lily) pollen (Igawa *et al.,* 2010) and the hallmark immunoreactive PTPC "doublet" that is characteristic of monoubiquitinated Class-1 PEPC from germinating COS endosperm has been reported on PTPC immunoblots of extracts from a wide variety of plants and tissues (Gonzalez *et al.*, 1998; Osuna *et al.,* 1999; Nhiri *et al.,* 2000; O'Leary *et al.,* 2011b). The most recent development in our understanding of PEPC monoubiquitination comes from a study of Class-1 PEPC in the proteoid roots of Pi-deprived *Hakea prostrata* (harsh hakea), a non-mycorrhizal species adapted to the nutrient-impoverished soils of Western Australia (Shane *et al.,* 2013). In early root development, *Hakea* Class-1 PEPC exists as a heterotetramer containing an equivalent ratio of monoubiquitinated 110-kDa and phosphorylated 107-kDa PTPC subunits. As root maturation proceeds, *Hakea* 110-kDa PTPC subunits become deubiquitinated and subsequently

phosphorylated *in vivo*. These PTMs correlate with PEPC activation as well as increased production of organic acid anions such as malate and citrate which are excreted in copious amounts by the roots in response to Pi-deficiency (Shane *et al.,* 2013). This study represents the first evidence for the simultaneous monoubiquitination and phosphorylation of individual but otherwise identical subunits of an oligomeric native enzyme. In contrast, previous studies of Class-1 PEPC PTMs in various castor plant tissues indicated that PTPC monoubiquitination and phosphorylation may be mutually exclusive (O'Leary *et al.,* 2011b; O'Leary *et al.,* 2009). It is clear that additional research is necessary to fully understand both the prevalence, metabolic functions and "cross-talk" between PTPC monoubiquitination and phosphorylation.

1.5 CLASS-2 PEPC COMPLEXES

The Discovery of the BTPC Gene

The advent of genome sequencing led to the interrogation of *Arabidopsis* and rice *PEPC* gene families in 2003, which resulted in the surprising discovery that both species contained a *PEPC* gene whose deduced amino acid sequence was quite divergent from those of PTPCs (Sanchez and Cejudo, 2003). These novel PEPC isoenzymes shared a slightly higher sequence similarity with PEPCs from proteobacteria than with vascular PTPCs and this led to their subsequent classification as BTPCs while the remaining C_3, C_4, and CAM PEPCs became known thereafter as PTPCs. BTPCs constitute a monophyletic group, are believed to have evolved in green algae, and are present in every plant or algal genome that has been sequenced to date (O'Leary *et al.,* 2011b).

The Discovery and Characterization of BTPC polypeptides

Prior to the identification of the gene encoding the BTPC polypeptide, a series of papers published in the 1990's, describing the purification and characterization of PEPCs from unicellular green algae (*Selenastrum minutum* and *Chlamydomonas reinhardtii*), unknowingly provided the first empirical evidence of the BTPC subunit. Two distinct PEPC classes which shared an identical PTPC subunit but exhibited highly dissimilar physical and kinetic properties were purified from both algal species (Rivoal *et al.,* 1996; Rivoal *et al.,* 1998; Rivoal *et al.,* 2001; Rivoal *et al.,* 2002; Schuller *et al.,* 1990). The expected 400-kDa PEPC homotetramers composed exclusively of identical PTPC subunits were classified as Class-1 PEPCs, whereas novel, higher M_r complexes composed of PTPC subunits in tight association with an immunologically unrelated 130-kDa subunit (subsequently shown to be BTPC) were designated as Class-2 PEPCs. In comparison with Class-1 PEPCs, Class-2 PEPCs displayed enhanced thermal stability, a broader pH-activity profile, biphasic PEP saturation kinetics, and a significantly reduced sensitivity to allosteric effectors. Changes in the supply of inorganic N were shown to have an effect on the levels of gene and protein expression of both algal PEPC subunits. However this effect was more pronounced for the PTPC subunits, which supports the hypothesis that Class-1 PEPC has an important anaplerotic function during N-assimilation (Mamedov *et al.,* 2004; Moellering *et al.,* 2007). From these and other studies of BTPC, deduced PEPC polypeptides can now be easily classified as a BTPC or PTPC based on three main criteria: (1) the C-terminal tetrapeptide is (R/K)NTG for BTPCs and QNTG for PTPCs, (2) BTPCs lack the N-terminal serine phosphorylation motif (acidic-basic-XX-[pS]-IDAQLR) that is a hallmark of all PTPCs (Sanchez and Cejudo, 2003; Mamedov *et al.,* 2005; Gennidakis *et al.,*

2007), and (3) all BTPCs contain a unique and highly divergent approximate 10-kDa insertion known as an "intrinsically disordered region" (Figure 1.4) (O'Leary *et al.,* 2011c).

Purification and characterization of low- and high-M_r PEPC isoforms from the endosperm of developing COS revealed that these distinct PEPC complexes shared incredibly similar physical, kinetic, and regulatory properties with the Class-1 and Class-2 PEPCs present in green algae (Blonde and Plaxton, 2003). Native COS Class-1 PEPC is a classic 410-kDa homotetramer consisting of phosphorylated 107-kDa PTPC subunits, whereas native COS Class-2 PEPC is a 910-kDa hetero-octamer composed of the same Class-1 PEPC core tightly associated with four 118-kDa BTPC subunits (Figure 1.5) (Gennidakis *et al.,* 2007; Blonde and Plaxton, 2003). Relative to COS Class-1 PEPC, COS Class-2 PEPC displayed the enhanced thermal stability, decreased allosteric effector sensitivity, a broader pH-activity profile, and biphasic PEP saturation kinetics characteristic of algal Class-2 PEPCs (Blonde and Plaxton, 2003; O'Leary *et al.,* 2009). A suite of additional *in vitro* techniques including co-immunopurification (co-IP) and non-denaturing PAGE of clarified extracts, in conjunction with in-gel PEPC activity staining and parallel immunoblotting with BTPC- and PTPC-specific antibodies, have been used to further document Class-1 and Class-2 PEPCs in developing COS, lily pollen, and expanding castor leaves (Gennidakis *et al.,* 2007; Tripodi *et al.,* 2005; Uhrig *et al.,* 2008a, O'Leary *et al.,* 2009; Kai *et al.,* 2003; O'Leary *et al.,* 2011a).

Native BTPC subunits of vascular plant and algal Class-2 PEPCs are highly susceptible to *in vitro* proteolytic cleavage by an endogenous thiol endopeptidase at a specific site in their intrinsically disordered region (Figure 1.4) (Gennidakis *et al.,* 2007; Rivoal *et al.,* 1998; Rivoal *et al.,* 2001). This rapid proteolytic degradation has rendered the purification of native COS Class-2 PEPC with non-truncated BTPC subunits virtually impossible, despite the use of a wide-

range of protease inhibitors and cocktails. Limited protection against the proteolysis of BTPC from clarified COS extracts via the use of phenylmethylsulfonyl fluoride (PMSF) and the ProteCEASE 100 Cocktail produced by G Biosciences has allowed for immunoblotting and co-IP of the non-graded 118-kDa BTPC polypeptide (Gennidakis *et al.,* 2007; Uhrig *et al.,* 2008a). To circumvent the difficulties posed by the *in vitro* proteolysis of BTPC, two additional techniques have been employed to allow for the characterization of non-degraded, native BTPC. Co-IP of highly enriched native BTPC via the use of an anti-(castor PTPC)-IgG immunoaffinity column allowed for the purification of relatively large quantities of the native protein which facilitated detailed MS characterization of its *in vivo* phosphorylation sites (Uhrig *et al.,* 2008a; O'Leary *et al.,* 2011c). Alternatively, recombinant wild-type and phosphomimetic mutant versions of COS BTPC (RcPPC4) and Arabidopsis PTPC (AtPPC3) were heterologously expressed in *Escherichia coli*, and cell lysates mixed together to form stable, chimeric, Class-2 PEPCs which were then successfully purified and characterized (O'Leary *et al.,* 2009; O'Leary *et al.,* 2011c; Dalziel *et al.,* 2012). Analysis of wild-type and mutant recombinant Class-2 PEPCs has led to (1) the kinetic characterization of the BTPC subunit, (2) an understanding of the regulatory effect BTPC subunits exert on PTPC subunits within the Class-2 PEPC complex, and (3) insights into the regulatory role of multi-site phosphorylation of the BTPC subunit via the use of phosphomimetic mutagenesis (O'Leary *et al.,* 2009; O'Leary *et al.,* 2011c; Dalziel *et al.,* 2012).

Although the BTPC polypeptide retains full PEPC catalytic activity, there are several lines of evidence which strongly suggest that PTPC subunits are essential binding partners of BTPC *in vivo*. For example: (1) native BTPC subunits have only ever been observed in association with PTPC subunits as a Class-2 PEPC complex, (2) BTPC subunits tightly associate

with PTPC subunits during purification, (3) recombinant COS BTPC forms insoluble aggregates when left in isolation (i.e. without PTPC binding partners), and (4) transient co-expression studies of FP (fluorescent protein)-tagged castor oil plant PTPC and BTPC subunits in tobacco BY2 cells have demonstrated their *in vivo* interaction and dynamic association with the surface of mitochondria, mediated by BTPC's intrinsically disordered region (Igawa *et al.*, 2010; Gennidakis *et al.*, 2007; Blonde and Plaxton, 2003; Rivoal *et al.*, 1998; Rivoal *et al.*, 2001; O'Leary *et al.*, 2011b; Park *et al.*, 2012).

Tissue-Specific Expression of BTPC in the Castor Plant

Recent work has characterized the tissue-specific expression of BTPC in the castor plant, in an attempt to further discern the physiological role of this protein. BTPC transcripts and polypeptides: (1) are abundant in the inner integument, cotyledon and endosperm of developing COS, (2) occur at low levels in roots and cotyledons of germinating COS, and (3) exhibit a distinct developmental profile pattern in leaves, with detectable expression levels found only in leaf buds and young, expanding leaves (O'Leary *et al.*, 2011a). It appears that BTPC and thus Class-2 PEPC expression is limited to those tissues which are rapidly growing and/or very biosynthetically active, whereas PTPC and thus Class-1 PEPC exists as a 'housekeeping' form of PEPC that is constitutively expressed in all tissues (O'Leary *et al.*, 2011b). One of the main results from the aforementioned imaging studies done with FP-PEPCs in tobacco BY2 cells was that Class-1 PEPC appeared to localize diffusely throughout the cytosol, whereas Class-2 PEPC dynamically associates with the outer mitochondrial envelope in response to mitochondrial respiration (Park *et al.*, 2012). Class-2 PEPC's unique kinetic and regulatory properties, in conjunction with its restriction to biosynthetically active tissues and its subcellular localization to the mitochondrial surface has to the hypothesis that it functions as a "metabolic overflow

mechanism" that facilitates rapid refixation of respiratory CO_2 while sustaining a large anaplerotic flux to replenish Kreb's cycle C-skeletons withdrawn for biosynthesis (O'Leary *et al.,* 2011b; Park *et al.,* 2012).

Post-Translational Modification of BTPC in the Developing COS

As BTPC subunits lack the traditional PTPC N-terminal seryl-phospho-site, it was erroneously assumed that plant BTPCs are not phosphorylatable *in vivo* (Sanchez and Cejudo, 2003; Nimmo, 2006). However, preliminary studies of co-IP'd COS BTPC using the phosphoprotein stain Pro-Q Diamond, revealed that the native BTPC from developing COS endosperm was in fact highly phosphorylated *in vivo* (Uhrig *et al.,* 2008a). Moreover, Pi-affinity PAGE using Phos-Tag acrylamide in conjunction with λ-phosphatase treatment demonstrated that COS BTPC phosphorylation occurs at multiple sites (Uhrig *et al.,* 2008a). Fourier-transform MS of highly enriched co-IP'd BTPC identified three novel phosphorylation sites: Thr^{4} at the N-terminus along with Ser^{425} and Ser^{451} within BTPC's intrinsically disordered region (respectively corresponding to acidophilic, proline-directed and basophilic kinase recognition motifs) (Figures 1.4 and 1.5) (O'Leary *et al.,* 2011b; Uhrig *et al.,* 2008a; O'Leary *et al.,* 2011c, Dalziel *et al.,* 2012). Thr^{4} and Ser^{451} are conserved in all other BTPC orthologues, whereas Ser^{425} is only partially conserved (Figure 1.4) (O'Leary *et al.,* 2011b; O'Leary *et al.,* 2011c; Dalziel *et al.,* 2012).

Kinetic analyses of phosphomimetic mutants (Ser to Asp) of COS BTPC at Ser^{425} and Ser^{451} indicated that phosphorylation at both sites causes inhibition of BTPC catalytic activity within the Class-2 PEPC complex by increasing their K_m(PEP) as well as their sensitivity to feedback inhibition by Asp and malate (O'Leary *et al.,* 2011c; Dalziel *et al.,* 2012). Phospho-site specific antibodies raised against short, synthetic phosphopeptides corresponding to the sequence

flanking the Ser^{425} and Ser^{451} phospho-sites have been crucial tools for studying the *in vivo* phosphorylation of BTPC in COS at both sites. The developmental patterns of BTPC phosphorylation at Ser^{425} and Ser^{451}, determined via immunoblotting of clarified COS extracts with the respective phospho-site specific antibodies, have been shown to be quite distinct from the *in vivo* phosphorylation of COS Class-1 PEPC's PTPC subunits at Ser^{11} (Murmu and Plaxton, 2007; O'Leary *et al.,* 2011c; Dalziel *et al.,* 2012). Phosphorylation of BTPC at both sites in the developing COS endosperm increases from Stage III-IX, which are the stages coincident with storage oil production (O'Leary *et al.,* 2011c; Dalziel *et al.,* 2012). Additionally, the removal of photosynthate supply via seed pod excision (depodding), leads to the increase in Ser^{425} and Ser^{451} phosphorylation (O'Leary *et al.,* 2011c; Dalziel *et al.,* 2012), but rapid PTPC dephosphorylation (Murmu and Plaxton, 2007). Taken together, these results as well as distinctive phosphorylation motifs surrounding the respective seryl residues clearly imply that phosphorylation of COS PTPC at Ser^{11} and BTPC at Ser^{425} and Ser^{451} are subject to control by different protein kinases and signaling pathways. Similar phosphomimetic analyses of the Thr^{4} phospho-site have not found any discernible kinetic effect of phosphorylation at this site (O'Leary *et al.,* 2011b). However, the Thr^{4} phospho-site exists in a conserved FHA (forkhead-associated)-binding domain (pTXXD), which are known phosphothreonine-dependent protein interaction modules (Chevalier *et al.,* 2009). It will thus be of interest to establish whether BTPC phosphorylation at Thr^{4} mediates the interaction of Class-2 PEPCs with any FHA domain-containing proteins (O'Leary *et al.,* 2011b).

1.6 THESIS OBJECTIVES

While significant advances have been made in our understanding of the existence and regulatory role of *in vivo* COS BTPC phosphorylation at Ser^{451} and Ser^{425}, nothing is known

about the identity, biochemical properties, or control of the protein kinase(s) responsible for these PTMs. Thus, the main objective for my thesis was to address this knowledge gap by purifying and characterizing the protein kinase that phosphorylates BTPC at Ser^{451} in developing COS endosperm. This knowledge will aid in further understanding the role BTPC phosphorylation plays in Class-2 PEPC function within COS, and ultimately, the role Class-2 PEPC plays in carbon partitioning to important storage end products in developing non-green oilseeds.

A relatively novel, non-radioactive, semi-quantitative assay of BTPC Ser^{451} kinase (BTPC-K) activity was initially employed to facilitate the purification of the BTPC-K from developing COS endosperm. This assay is based upon the use of BTPC Ser^{451} phospho-site specific antibodies and immunoblotting to assess Pi incorporation from unlabeled ATP into the conserved Ser^{451} residue of the BTPC subunits of recombinant Class-2 PEPC. This immunological-based assay will also be used for various clarified extract studies of BTPC-K. The successful purification of the COS BTPC-K allowed for the kinetic characterization of the partially purified kinase via the use of a more traditional, quantitative kinase assay using [γ-^{32}P]-ATP, and possibly facilitate its identification via mass spectrometry.

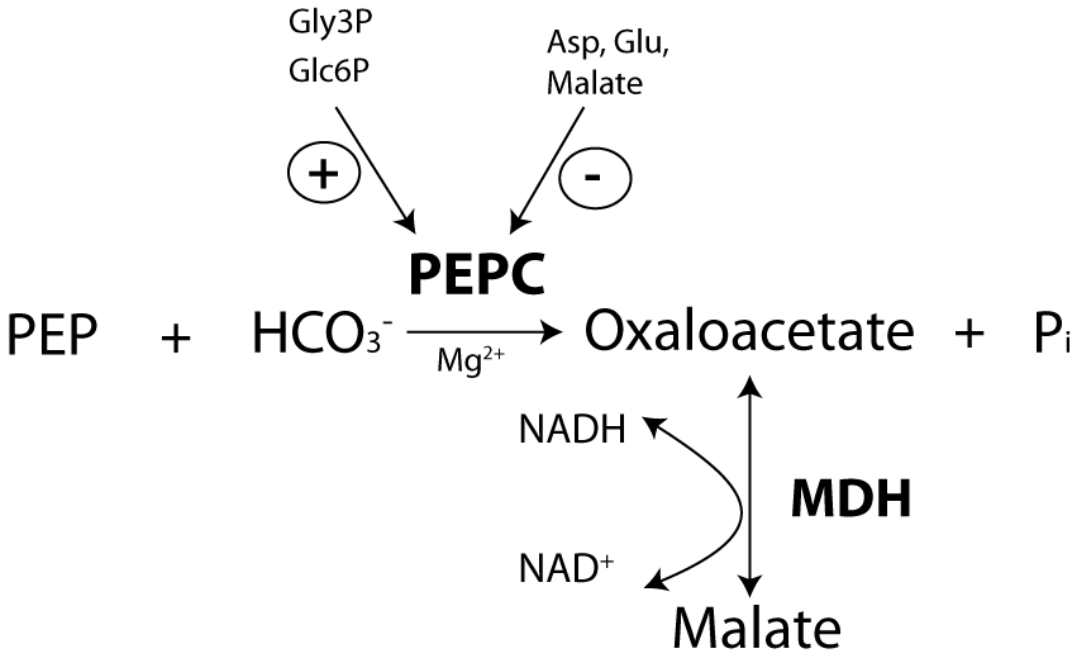

Figure 1.1: The phospho*enol*pyruvate carboxylase reaction. The carboxylation of PEP to oxaloacetate releasing Pi by PEPC requires the presence of both HCO_3^- and the metal cofactor Mg^{2+}. Glycerol-3-P and glucose-6-P act as allosteric activators of Class-1 PEPC from vascular plants whereas L-Asp, L-Glu, and L-malate act as allosteric inhibitors.

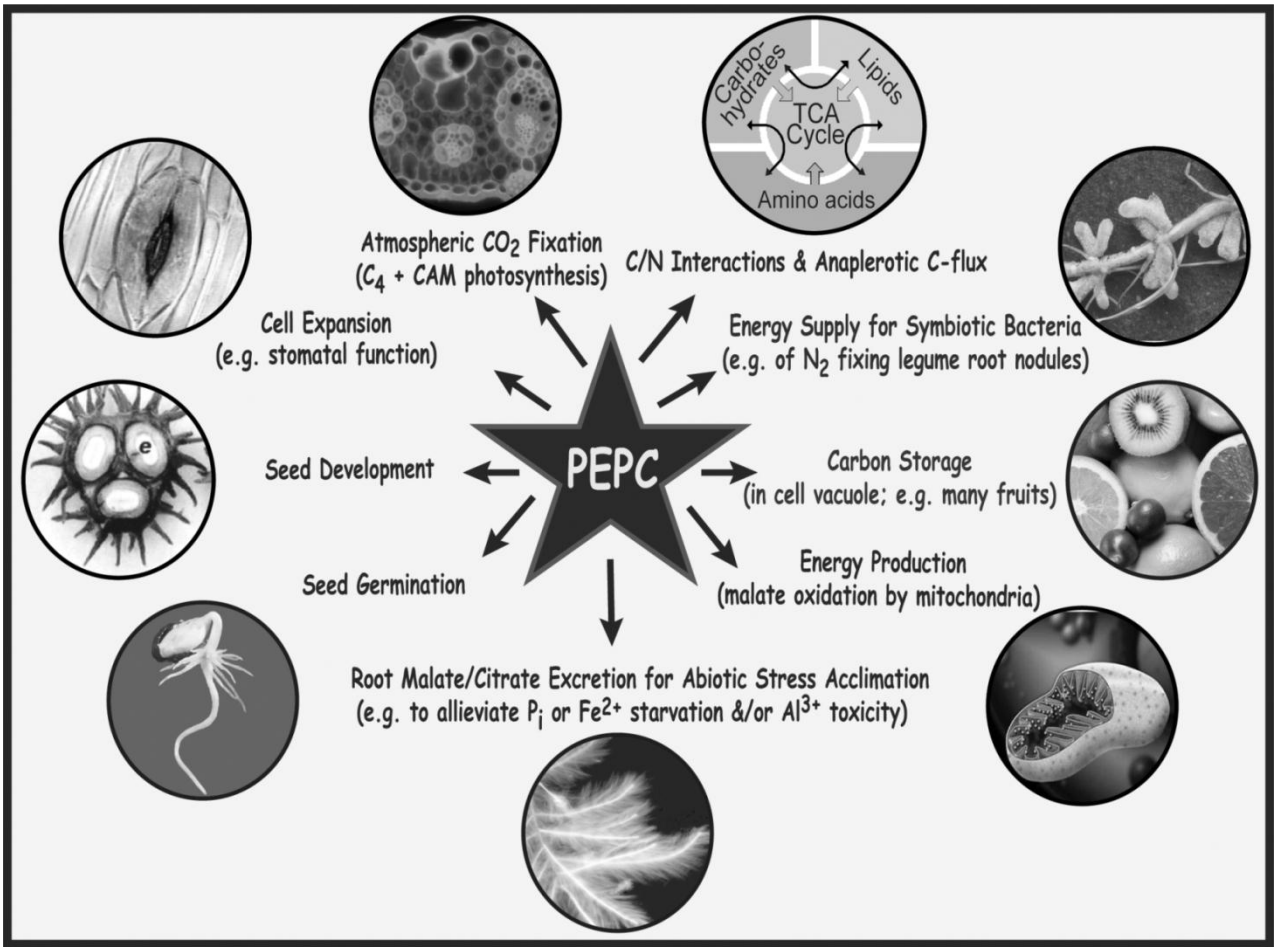

Figure 1.2 The diverse functions of plant PEPCs. Plant PEPC isozymes have a variety of functions including: atmospheric CO_2 fixation in C_4 and CAM plants, C/N interactions, anaplerotic replenishment of TCA cycle intermediates, carbon storage, N_2 fixation, energy supply for symbiotic bacteria, energy production, abiotic stress acclimation, seed development, seed germination, and cell expansion. (taken from O'Leary *et al.*, 2011b).

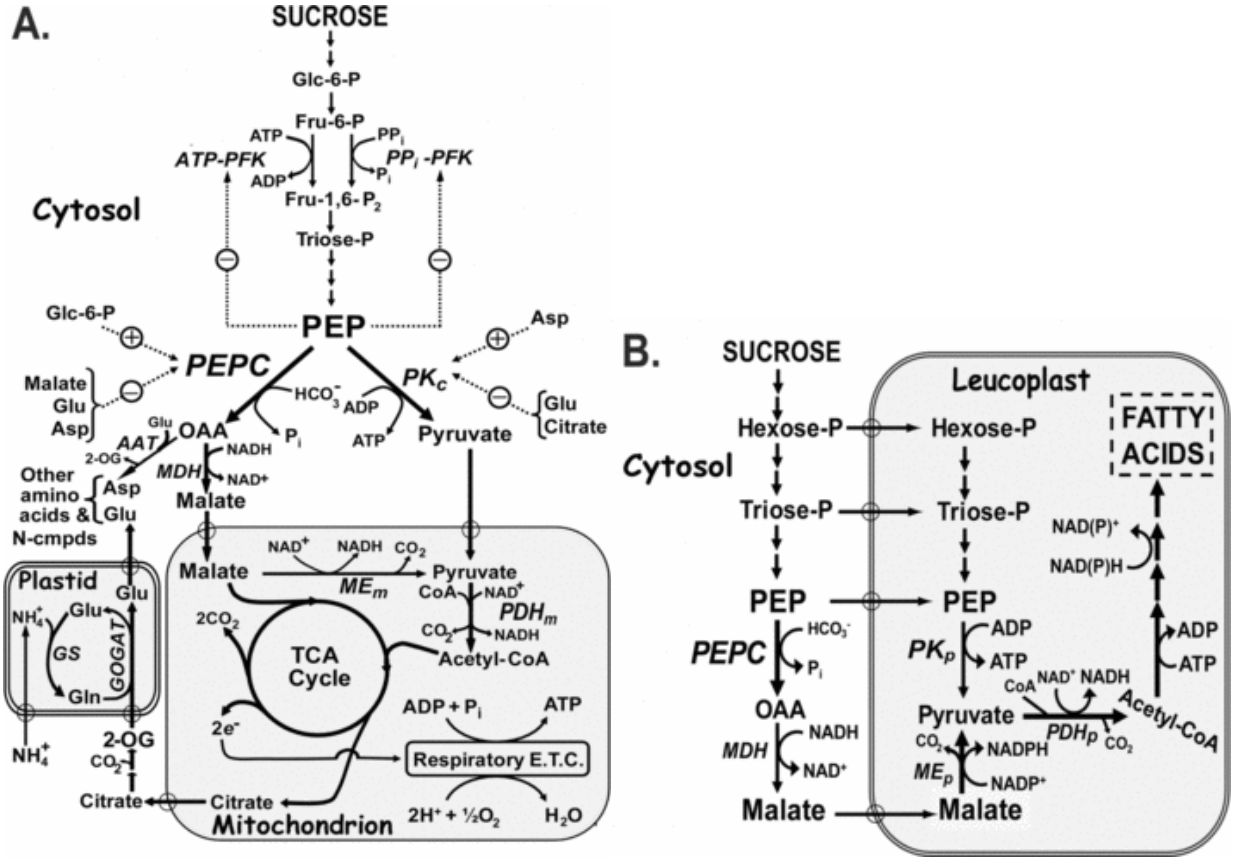

Figure 1.3 Models illustrating several metabolic functions of plant PEPCs. (A) Interactions between carbon and nitrogen metabolism involve three compartments in plant cells. This scheme highlights the critical roles of the two terminal enzymes of plant cytosolic glycolysis, PEPC and PK_c, in controlling the provision of the mitochondria with respiratory substrates, as well as for generating the 2-OG and OAA respectively required for NH_4^+-assimilation via GS/GOGAT in plastids and aspartate amino transferase in the cytosol. The co-ordinate control of PEPC and PK_c by allosteric effectors, in particular Glu and Asp, provides a mechanism for the regulation of cytosolic glycolytic flux and PEP partitioning during and following NH_4^+-assimilation. (**B**) Alternative metabolic routes for the conversion of sucrose to fatty acids in developing oilseeds. This model illustrates the role of PEPC in controlling PEP partitioning to malate as a source of both carbon skeletons and reducing power for leucoplast fatty acid synthesis. Abbreviations are as defined in the text, in addition to the following: AAT, Asp aminotransferase; E.T.C., electron transport chain; ME_m/PDH_m and ME_p/PDH_p, mitochondrial and plastidic isoenzymes of ME and PDH respectively (taken from O'Leary *et al.*, 2011b).

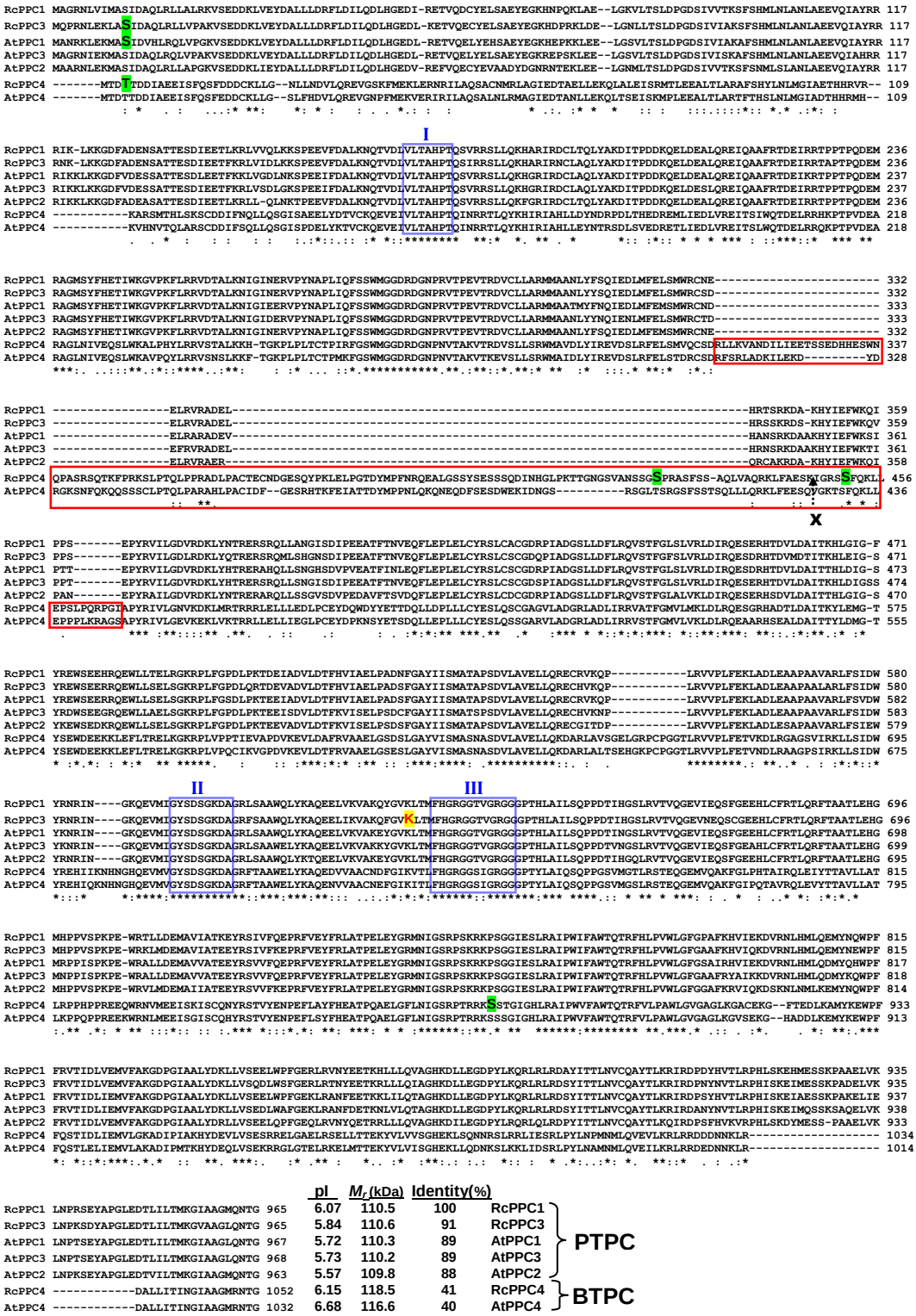

		pI	M_r (kDa)	Identity(%)		
RcPPC1	LNPRSEYAPGLEDTLILTMKGIAAGMQNTG 965	6.07	110.5	100	RcPPC1	PTPC
RcPPC3	LNPKSDYAPGLEDTLILTMKGVAAGLQNTG 965	5.84	110.6	91	RcPPC3	
AtPPC1	LNPTSEYAPGLEDTLILTMKGIAAGLQNTG 967	5.72	110.3	89	AtPPC1	
AtPPC3	LNPTSEYAPGLEDTLILTMKGIAAGLQNTG 968	5.73	110.2	89	AtPPC3	
AtPPC2	LNPKSEYAPGLEDTVILTMKGIAAGMQNTG 963	5.57	109.8	88	AtPPC2	
RcPPC4	------------DALLITINGIAAGMRNTG 1052	6.15	118.5	41	RcPPC4	BTPC
AtPPC4	------------DALLITINGIAAGMRNTG 1032	6.68	116.6	40	AtPPC4	

Figure 1.4 Amino acid sequence alignment of *Arabidopsis* and castor oil plant PEPC isoenzymes. Known *in vivo* phosphorylation sites of castor oil plant and *Arabidopsis* PTPCs (RcPPC3 and AtPPC1 respectively) and castor oil plant BTPC (RcPPC4) are highlighted in green. RcPPC3's conserved Lys^{628} monoubiquitination site is marked with red font. BTPC's highly divergent ~10-kDa intrinsically disordered region is designated by the red rectangle. The RcPPC4 site that is susceptible to *in vitro* proteolytic cleavage (Lys^{446}- Ile^{467}) is marked with an X. Conserved subdomains essential for PEPC catalysis are designated with Boxes I-III. The predicted pI, molecular mass and sequence identity (%) of the various PEPCs are shown. Deduced *Arabidopsis* and castor PEPC sequences were aligned with the use of ClustalW software (http://www.ebi.ac.uk/Tools/clustalw2/index.html). Semi-colons and asterisks indicate identical and conserved amino acids respectively (adapted from O'Leary *et al.,* 2011b).

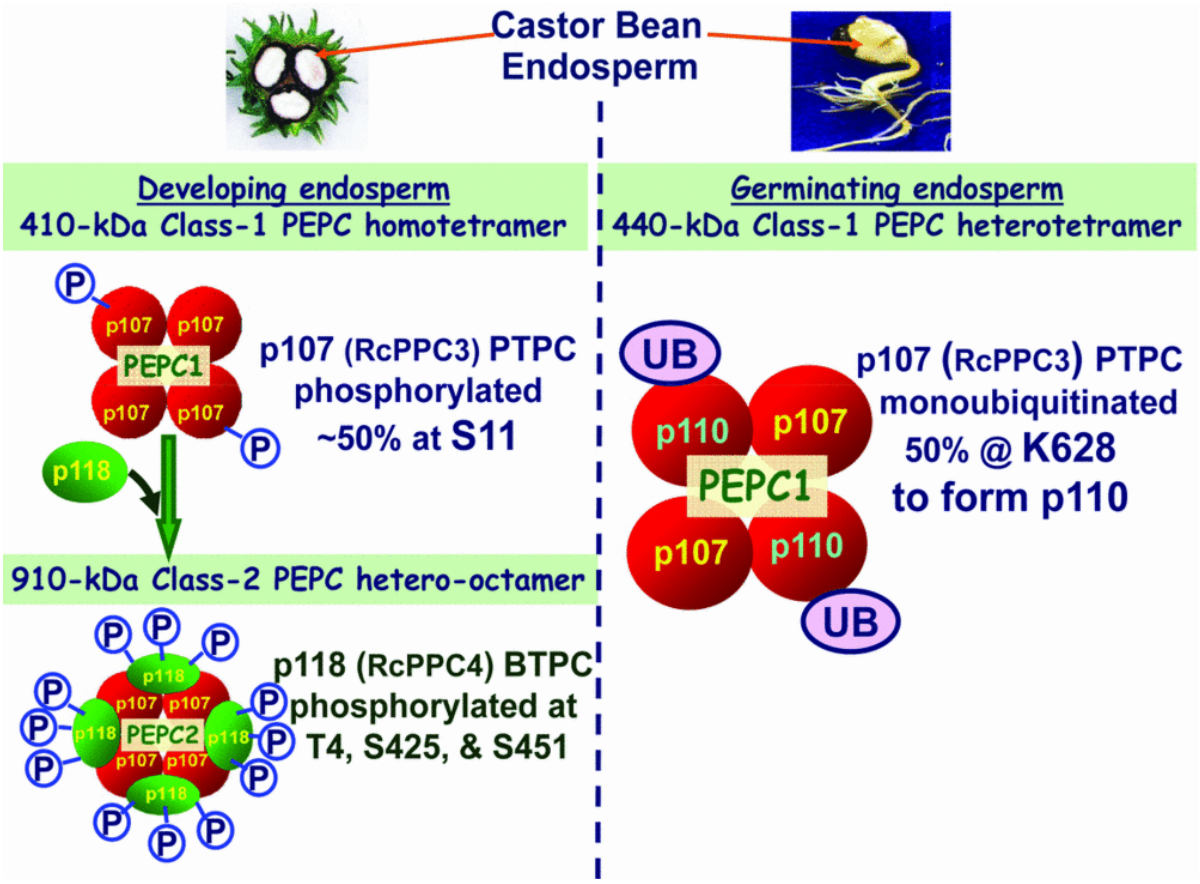

Figure 1.5 Model illustrating the complexity of COS PEPC. In developing COS endosperm the PTPC RcPPC3 exists as a typical Class-1 PEPC homotetramer (PEPC1) which is subject to sucrose-dependent *in vivo* phosphorylation of its 107-kDa subunit (p107) at Ser[11]. Class-1 PEPC can also tightly associate with 118-kDa BTPC (RcPPC4) subunits (p118) to form the novel allosterically desensitized Class-2 PEPC hetero-octameric complex (PEPC2). The BTPC subunit of Class-2 PEPC is subject to *in vivo* multi-site regulatory phosphorylation at Thr[4], Ser[425] and Ser[451] (Uhrig *et al.*, 2008a; O'Leary *et al.*, 2009; O'Leary *et al.*, 2011c; Dalziel *et al.*, 2012). In germinating COS, the same Class-1 PEPC isozyme (RcPPC3) also undergoes regulatory monoubiquitination at Lys[628] (Uhrig *et al.*, 2008b) (adapted from O'Leary *et al.*, 2011b).

Chapter 2. Serine-451 phosphorylation of bacterial-type phosphoenolpyruvate carboxylase by a calcium-dependent protein kinase links calcium signaling with anaplerotic pathway control in developing castor oil seeds

A.T. Hill and W. C. Plaxton (2013)

Manuscript in preparation

2.1 INTRODUCTION

PEPC [PEP(phosphoenolpyruvate) carboxylase] (EC 4.1.1.31) is an important, tightly controlled enzyme situated at a critical branch point in plant carbohydrate metabolism that catalyzes the irreversible β- carboxylation of phosphoenolpyruvate (PEP) to oxaloacetate (OAA) and inorganic phosphate (Pi) in the presence of a divalent metal cation (Mg^{2+}, Mn^{2+}) and HCO_3^-. C_4 and crassulacean acid metabolism (CAM) photosynthetic PEPCs have been extensively characterized at the structural and regulatory level due to their critical role in atmospheric CO_2 fixation (Izui *et al.,* 2004; Nimmo, 2003). However, PEPC also has a variety of particularly essential, non-photosynthetic functions which have received considerable attention, among them the anaplerotic replenishment of Kreb's cycle intermediates consumed during biosynthesis and N-assimilation (O'Leary *et al.,* 2011b). Plant PEPCs belong to a small, multi-gene family encoding several plant-type PEPCs (PTPC), as well as one, distantly related, bacterial-type PEPC (BTPC) (Gennidakis *et al.,* 2007; Igawa *et al.,* 2010; Mamedov *et al.,* 2005; O'Leary *et al.,* 2011b; Sullivan *et al.,* 2004). *PTPC* genes encode closely related 100-110-kDa polypeptides that typically assemble as homotetrameric Class-1 PEPCs controlled by a variety of allosteric effectors in conjunction with reversible phosphorylation and monoubiquitination (Nimmo, 2003; O'Leary *et al.,* 2011b; Uhrig *et al.,* 2008b; Shane *et al.,* 2013). Phosphorylation of PTPC occurs at a conserved N-terminal seryl residue and is catalyzed by a dedicated Ca^{2+}-independent PTPC protein kinase (PPCK) and protein phosphatase type-2A (PP2A) (O'Leary *et al.,* 2011b; Izui *et al.,* 2004; Murmu and Plaxton, 2007). PTPC phosphorylation enhances its allosteric activation by hexose-phosphates whilst simultaneously reducing allosteric inhibition by L-malate and L-Asp (O'Leary *et al.,* 2011b). Due to the importance of phosphorylation as a regulatory mechanism of Class-1 PEPC activity, extensive studies of PPCK have been undertaken, including its cloning

from CAM, C_4, and C_3 plants, as well as the purification and characterization of the native protein from several species (Nimmo, 2003; Nimmo, 2006; Wang and Chollet, 1993; Murmu and Plaxton, 2007). Consequently, PPCK-mediated phosphorylation of PTPC continues to be one of the most well-understood examples of regulatory enzyme phosphorylation *in planta* (O'Leary *et al.,* 2011b).

Plant *BTPC* genes encode 116-118-kDa polypeptides that share a higher sequence identity with prokaryotic PEPCs than PTPCs (O'Leary *et al.,* 2011b). Purification of native PEPCs from unicellular green algae and the triacylglyceride-rich endosperm of developing castor oil seeds (COS) led to the discovery of unusual high-M_r Class-2 PEPC hetero-octameric complexes composed of a Class-1 PEPC core tightly associated with four BTPC subunits (Rivoal *et al.,* 1998; Rivoal *et al.,* 2001; Mamedov *et al.,* 2005; Moellering *et al.,* 2007; Blonde and Plaxton, 2003; Gennidakis *et al.,* 2007). Despite BTPC subunits retaining PEPC catalytic activity, there are several lines of evidence which suggest that BTPCs only exist *in vivo* as part of a Class-2 PEPC complex (Moellering *et al.,* 2007; Blonde and Plaxton, 2003; Gennidakis *et al.,* 2007; Igawa *et al.,* 2010; O'Leary *et al.,* 2009; Uhrig *et al.,* 2008a; Park *et al.,* 2012). Relative to Class-1 PEPC, Class-2 PEPCs display enhanced thermal stability, a broader pH-activity profile, biphasic PEP saturation kinetics and a remarkable insensitivity to Class-1 PEPC allosteric effectors (Rivoal *et al.,* 2001; O'Leary *et al.,* 2009). Within the Class-2 PEPC complex, BTPC functions as both a catalytic and regulatory subunit as it modulates the PEP binding, catalytic activity, and allosteric sensitivity of its PTPC interacting partners (Blonde and Plaxton, 2003; O'Leary *et al.,* 2009). Tissue-specific expression studies in castor have discerned that *BTPC* transcript and polypeptide expression (and thus Class-2 PEPC complexes) is restricted to biosynthetically active tissues as opposed to PTPC which is ubiquitously expressed in all tissues

(O'Leary *et al.,* 2011a). Transient expression of FP (fluorescent protein)-tagged PEPCs in tobacco BY2 cells have shown that while Class-1 PEPC appears to be localized diffusely throughout the cytosol, Class-2 PEPC dynamically associates with the outer mitochondrial envelope in response to mitochondrial respiration (Park *et al.,* 2012). Class-2 PEPC's unique kinetic and regulatory properties, in conjunction with its restriction to biosynthetically active tissues and its subcellular targeting to the mitochondrial surface, has led to the current hypothesis that it functions as a "metabolic overflow mechanism" that facilitates rapid refixation of respiratory CO_2 while sustaining a large anaplerotic flux to replenish tricarboxylic acid cycle C-skeletons withdrawn for biosynthesis (O'Leary *et al.,* 2011b; Park *et al.,* 2012).

Although BTPCs lack the N-terminal seryl phosphorylation motif characteristic of PTPCs, BTPC is *in vivo* phosphorylated at multiple sites during COS development (Uhrig *et al.,* 2008a). Fourier-transform mass spectrometry (MS) of native COS BTPC identified three novel *in vivo* phosphorylation sites: Thr^{4} at the N-terminus, and Ser^{425} and Ser^{451} within a unique ~10-kDa intrinsically disordered region (respectively corresponding to acidophilic, proline-directed, and basophilic kinase recognition motifs) (O'Leary *et al.,* 2011b; Uhrig *et al.,* 2008a; O'Leary *et al.,* 2011c; Dalziel *et al.,* 2012). The phospho-sites at Thr^{4} and Ser^{451} are conserved in all other BTPC orthologues whereas the Ser^{425} phosphorylation site is only partially conserved (O'Leary *et al.,* 2011b; O'Leary *et al.,* 2011c; Dalziel *et al.,* 2012). Kinetic analyses of Ser^{425} and Ser^{451} phosphomimetic mutants (Ser to Asp) of COS BTPC indicated that phosphorylation at both sites causes inhibition of the BTPC subunits within the Class-2 PEPC complex by increasing their K_m(PEP) as well as their sensitivity to feedback inhibition by Asp and malate (O'Leary *et al.,* 2011c; Dalziel *et al.,* 2012). The function of BTPC phosphorylation at Thr^{4} remains unknown (O'Leary *et al.,* 2011b). Phospho-site specific antibodies raised against synthetic

phosphopeptides corresponding to the sequence surrounding the Ser^{425} and Ser^{451} phospho-sites have been crucial tools for studying the *in vivo* phosphorylation of BTPC in COS at both of these sites (O'Leary *et al.,* 2011c; Dalziel *et al.,* 2012). The developmental patterns of BTPC phosphorylation at Ser^{425} and Ser^{451} have been shown to be quite distinct from the *in vivo* phosphorylation of Class-1 PEPC's PTPC subunits at Ser^{11} (Murmu and Plaxton, 2007). Additionally, the removal of photosynthate supply via seed pod excision (depodding), leads to an increase in Ser^{425} and Ser^{451} phosphorylation (O'Leary *et al.,* 2011c**;** Dalziel *et al.,* 2012), whereas PTPC has been shown to be rapidly dephosphorylated and promptly monoubiquitinated following seed pod excision (Murmu and Plaxton, 2007, O'Leary *et al.,* 2011a**).** Taken together, these results clearly imply that phosphorylation of PTPC at Ser^{11} and BTPC at Ser^{425} and Ser^{451} are subject to control by different protein kinases and signaling pathways.

While significant advances have been made in our understanding of the regulatory role of COS BTPC phosphorylation at Ser^{451} and Ser^{425}, nothing is known about the identity, biochemical properties, or control of the protein kinase(s) responsible for these PTMs. The current study begins to addresses this gap in knowledge by employing a non-radioactive semi-quantitative assay to monitor BTPC Ser^{451} kinase (BTPC-K) activity from developing COS extracts. This BTPC-K assay is based upon the use of Ser^{451} phospho-site specific antibodies and immunoblotting to assess P incorporation from unlabeled ATP into the BTPC subunits of Class-2 PEPC at Ser^{451}. We also report the partial purification of the BTPC-K, its dissimilarity to PPCKs, and discovery that it belongs to the Ca^{2+}-dependent protein kinases (CDPK) family. Also described are physical and kinetic properties, substrate specificities, and other characteristics of this unique and previously unknown protein kinase.

2.2 MATERIALS AND METHODS

Plant Material

Castor plants (*Ricinus communis;* cv Baker 296) were cultivated in a greenhouse at 24°C and 70% humidity under natural light supplemented with 16 h of artificial light. Pods containing developing COS at various stages of development (Greenwood and Bewley, 1985) were harvested at midday unless otherwise indicated. For depodding experiments, stems containing intact pods of developing COS were excised and placed in water in the dark for various periods of time. Developing endosperm tissue was rapidly dissected, frozen in liquid-N_2 and stored at -80°C until used.

Preparation of Clarified Extracts

Quick-frozen COS endosperm was homogenized (1:2, w/v) using a Brinkmann PT-3100 Polytron in ice-cold Buffer A which contained 50 mM Hepes-KOH (pH 7.3), 1 mM EDTA, 1 mM EGTA, 10 mM $MgCl_2$, 20% (v/v) glycerol, 20 mM NaF, 2 mM Na_3VO_4, 2 mM Na_2MoO_4, 5 mM thiourea, 1mM dithiothreitol (DTT), 1 % (w/v) polyvinyl(polypyrrolidone) (PVPP), 1 mM 2,2'-dipyridyl disulfide (DPDS), 1 mM phenylmethylsulfonyl fluoride (PMSF), 5 µl ml^{-1}ProteCEASE-100 (G-Biosciences), and 50 nM microcystin-LR (MC-LR). Homogenates were centrifuged at 15,000 *g* for 15 min at 4°C. Supernatants were desalted in 3 ml Sephadex G-50 'spin columns' equilibrated in the standard kinase assay buffer described below.

PEPC and Protein Assays

PEPC activity was assayed at 25°C by following NADH oxidation at 340 nm using a Molecular Devices microplate spectrophotometer. The following optimized 200 µl assay mixture was used: 50 mM Hepes-KOH (pH 8.0) containing 10% (v/v) glycerol, 10 mM PEP, 5 mM $KHCO_3$, 10 mM $MgCl_2$, 2 mM DTT, 0.15 mM NADH, and 5 units ml^{-1} of porcine muscle malate

dehydrogenase (Roche). One unit of PEPC is defined as the amount of PEPC resulting in the production of 1 μmol of oxaloacetate min^{-1}. Apparent $K_{m,}$ I_{50} and K_a values (concentrations of inhibitors and activators producing 50% inhibition and activation, respectively) were calculated using a non-linear least-square regression computer program (Brooks, 1992). All kinetic parameters represent means of at least three independent experiments and are reproducible to within ±15% S.E.M. of the mean value. Metabolite stock solutions were made equimolar with $MgCl_2$ and adjusted to pH 7.3. Protein concentrations were determined by Coomassie Blue G-250 dye-binding using bovine γ-globulin as the protein standard (Blonde and Plaxton, 2003).

Electrophoresis and Immunoblotting

SDS-PAGE using a Bio-Rad Protean III mini-gel rig, subunit estimates via SDS-PAGE, and immunoblotting were conducted as previously described (Blonde and Plaxton, 2003). Antigenic polypeptides were visualized using an alkaline phosphatase-conjugated secondary antibody and chromogenic detection (Plaxton, 1989). Rabbit anti-BTPC [anti-(COS BTPC)-IgG] was raised against homogeneous recombinant RcPPC4 as described previously (O'Leary *et al.*, 2009). Rabbit anti-pSer451 [anti-(COS BTPC Ser451 phosphorylation site specific)]-IgG was raised against a synthetic phosphopeptide, corresponding to residues 447-457 of COS BTPC, as described previously (Dalziel *et al.,* 2012). For all anti-pSer451 immunoblots, the corresponding dephosphopeptide (10 μg ml^{-1}) was used to block any nonspecific antibodies raised against the non-phosphorylated portions of the sequence. All immunoblot results were replicated a minimum of three times with representative results shown in the various figures.

Microsomal Membrane Preparation

Quick-frozen stage VII (full-cotyledon) COS endosperm (2 g) was homogenized in 4 ml of ice cold Buffer A. The homogenate was filtered through Miracloth (Calbiochem) and

centrifuged at 10,000 *g* for 20 min at 4°C. The supernatant was centrifuged at 96,000 *g* for 1 h at 4°C. An aliquot of the initial supernatant (total protein fraction) was taken prior to re-centrifugation, desalted and assayed for BTPC-K activity and protein. The final supernatant (soluble fraction) was removed, desalted, and assayed for BTPC-K activity and protein. The remaining pellet was re-suspended in Buffer A containing 0.5% (v/v) Triton X-100 and without PVPP or thiourea, using a Teflon homogenizer. This membrane fraction was then desalted and assayed for BTPC-K activity and protein.

BTPC-K Assay and Kinetic Studies

The *in vitro* activity of BTPC-K was assayed by monitoring P incorporation from either non-radioactive ATP (for semi-quantitative assays of BTPC-K activity in desalted COS extracts or during BTPC-K purification) or [γ-^{32}P]ATP (for kinetic studies of partially purified BTPC-K) into the BTPC subunit of purified, heterologously expressed Class-2 PEPC (O'Leary *et al.,* 2009; O'Leary *et al.,* 2011c). The standard BTPC-K assay mix contained 50 mM Hepes-KOH (pH 7.3), 10 mM $MgCl_2$, 1 mM DTT, 0.1 mM Na_3VO_4, 0.1 mM Na_2MoO_4, 50 nM MC-LR, 0.5 µl ml^{-1} ProteCEASE-100, 10% (v/v) glycerol, 0.2 mM $CaCl_2$, 20 µg purified recombinant Class-2 PEPC (corresponds to 10 µg BTPC subunit) (O'Leary *et al.,* 2009' O'Leary *et al.,* 2011c; Dalziel *et al.,* 2012), the appropriate amount of kinase sample, and 0.1 mM ATP or 0.1 mM [γ-^{32}P]ATP (specific activity 1000 cpm/pmol), in a final volume of 50 µl. Where necessary, free Ca^{2+} was controlled by modifying the standard kinase assay mix to contain 0.5 mM EGTA and varying amounts of $CaCl_2$. Free Ca^{2+} concentrations were calculated using software available at http://www.stanford.edu/~cpatton/webmaxc/webmaxcE.htm. Assays were initiated by the addition of ATP and reactions were incubated at 30°C. Aliquots were withdrawn at specified

times and assayed for Class-2 PEPC activity and/or P incorporation into Class-2 PEPC's 118-kDa BTPC subunit (p118).

For non-radioactive BTPC-K assays, relative P incorporation into the BTPC subunit from unlabeled ATP was estimated by subjecting aliquots of kinase assays to SDS-PAGE and immunoblotting with anti-pSer451 and anti-BTPC. The relative amount of P incorporation into the BTPC subunit of Class-2 PEPC was estimated by quantification of the anti-pSer451 immunoreactive p118 subunits on immunoblots after scanning using Image J software (http://rsbweb.nih.gov/ij/); derived values were linear with respect to the amount of immunoblotted extracts. Immunoquantification data are presented as means ± S.E.M. Several values were compared using the Student's *t*-test; *P* values <0.05 were considered to be statistically significant.

For all radioactive BTPC-K assays, relative ^{32}P incorporation from [γ-^{32}P]ATP into the BTPC subunit was visualized by subjecting aliquots of kinase assays to SDS-PAGE and developing Coomassie Blue R-250 stained and dried gels for 2 h in a phosphorimager cassette (Molecular Dynamics, Piscataway NJ, USA) followed by scanning of the cassette using a Typhoon 6000 (GE Healthcare). ^{32}P incorporation into BTPC was quantified either by (1) digestion of excised Coomassie blue stained p118 bands from SDS gels with H_2O_2 and liquid scintillation counting as described by Law and Plaxton (1997) (Appendix 2) or (2) by trichloroacetic acid (TCA) precipitation of protein in BTPC-K reaction mixtures and Cerenkov counting as described in Hardie *et al.* (1999) (Appendix 3).

Partial Purification of BTPC-K from Developing COS

All chromatography steps were carried out at room temperature using an ÄKTA Purifier-FPLC system (GE Healthcare). All buffers were adjusted to their respective pH at 25°C and

contained a phosphatase inhibitor cocktail (25 mM NaF, 1 mM EDTA, 1 mM $NaMoO_4$, and 1 mM $NaVO_3$), whereas 50 nM MC-LR and 2.5 µl ml^{-1} ProteCEASE-100 were added to all pooled fractions to further inhibit any co-purifying phosphatase or protease activity. Quick-frozen stage V-VII (mid- to full-cotyledon) developing COS endosperm (150 g) was Polytron extracted in 300 ml Buffer A containing 4% (w/v) polyethylene glycol (PEG-8000) and centrifuged at 20,000 *g* for 30 min at 4°C. The supernatant was filtered through 4 layers of Miracloth and re-centrifuged as above. A 50% (w/v) solution of PEG-8000 was added to the supernatant fraction to a final concentration of 26%, followed by stirring for 20 min at 4°C. Precipitated proteins were pelleted as above. Pellets were dissolved in Buffer B which contained 50 mM Hepes-KOH (pH 7.3), 1 mM EDTA, 1 mM EGTA, 2 mM $MgCl_2$ and 20% (saturation) $(NH_4)_2SO_4$. Re-suspended pellets were clarified by centrifugation and loaded at 2 ml min^{-1} onto a Butyl Sepharose 4 Fast Flow column (1.6 x 12.5 cm) (GE Healthcare) pre-equilibrated in Buffer B. The column was washed with Buffer B until the A_{280} approached baseline. Bound proteins were eluted during the first step gradient consisting of 50 ml of 30% Buffer B and 70% Buffer C which contained 50 mM Hepes-KOH (pH 7.3), 1 mM EDTA, 1 mM EGTA, and 10% (v/v) ethylene glycol. All BTPC-K activity was subsequently eluted in the second step gradient of 30 ml of 100% Buffer C. The peak BTPC-K activity fractions were pooled and concentrated in an Amicon Ultra-15 Centrifugal Filter Unit (30-kDa cutoff). This sample was loaded at 0.5 ml min^{-1} onto a HiLoad 16/60 Superdex-200 gel filtration column that was pre-equilibrated and subsequently eluted with Buffer D containing 50 mM Tris-HCl (pH 7.3), 1 mM EDTA, 0.5 mM EGTA, 10% (v/v) glycerol, and 0.1 M KCl. Pooled kinase fractions from the Superdex-200 column were concentrated to 1 ml and then diluted to 5 ml in Buffer E containing 20 mM Tris-HCl (pH 7.4), 15% (v/v) glycerol, and 1 mM $CaCl_2$. This sample was loaded at 0.5 ml min^{-1} onto

a Mono Q 5/50 GL column (GE Healthcare) pre-equilibrated in Buffer E. BTPC-K activity was eluted with a linear gradient (25 ml) of 0-0.5 M NaCl in Buffer E. Peak BTPC-K fractions were pooled and concentrated in an Amicon Ultra-15 Centrifugal Filter Unit (30-kDa cutoff) to 150 µl. $MgCl_2$ was added (final concentration = 5.5 mM) to this sample, and it was loaded at 0.3 ml min^{-1} onto a Cibacron Blue Sepharose Fast Flow column (1 x 2 cm) (GE Healthcare) equilibrated in Buffer F which contained 20 mM Tris-HCl (pH 8), 5.5 mM $MgCl_2$ and 2.5 mM EDTA. The column was washed with Buffer F containing 0.15 M NaCl, and BTPC-K eluted in Buffer F containing 0.3 M NaCl and 0.2% (w/v) CHAPS. Pooled fractions were concentrated to 200 µl in an Amicon Ultra-15 Centrifugal Filter Unit (30-kDa cutoff). For storage, 10% (v/v) glycerol was added to final preparation which was then divided into 20 µl aliquots and frozen at -80°C until use. BTPC-K activity was stable for at least 4 months when stored at -80°C.

Estimation of Native Molecular Mass by Gel Filtration FPLC

Native M_r was determined by FPLC at 0.2 ml min^{-1} on both Superdex-200 10/300 GL and Superdex-75 10/30 GL columns calibrated in Buffer D and calculated from a plot of K_{av} (partition coefficient) against log (M_r) using the following protein standards: ferritin (440-kDa), catalase (250-kDa), aldolase (158-kDa), bovine serum albumin (66-kDa), ovalbumin (44-kDa), carbonic anhydrase (29-kDa), chymotrypsinogen A (25-kDa), ribonuclease A (13.7-kDa) and cytochrome C (12.4-kDa).

2.3 RESULTS AND DISCUSSION

Detection of BTPC-K Activity in Clarified COS Extracts

The production of a phospho-site specific antibody that specifically cross-reacts with the conserved Ser^{451} phosphorylation site of the p118 subunit of Class-2 PEPC (Dalziel *et al.*, 2012),

along with the purification of recombinant Class-2 PEPCs from *E. coli* (O'Leary *et al.,* 2009; Dalziel *et al.,* 2012), facilitated the development of a semi-quantitative immunological assay for BTPC-K activity in COS extracts. Figure 2.1 demonstrates a typical *in vitro* BTPC-K assay using desalted extracts from stage V developing COS endosperm as the kinase source, purified recombinant Class-2 PEPC as the kinase substrate, and anti-pSer451 versus anti-BTPC immunoblots. Phosphorylation of p118 at Ser^{451} by BTPC-K activity present in the COS extracts was absolutely dependent upon the presence of ATP and Mg^{2+} (Figure 2.1a). Specificity of the anti-pSer451 for the phospho-form of p118 in Class-2 PEPC was demonstrated by the time-dependent elimination of its cross-reaction following λ-phosphatase treatment (Figure 2.1b). Complete dephosphorylation of p118 occurred 20 min following its incubation with λ-phosphatase, without influencing the total amount of p118 as revealed by parallel immunoblotting with anti-BTPC (Figure 2.1b). Unlike the Ser^{11} phospho-site of COS PTPC (Tripodi *et al.,* 2005), the BTPC Ser^{451} phospho-site was unable to be phosphorylated by protein kinase A (PK-A) or dephosphorylated by the catalytic subunit of bovine heart PP2A (Appendix 5). This implies that BTPC's Ser^{451} phospho-status is controlled by a separate protein kinase and phosphatase than PTPC's Ser^{11} *in vivo*.

Monitoring BTPC-K Activity throughout COS Development and Following Pod Excision

Relative BTPC-K activity in desalted endosperm extracts prepared at each stage of COS development was determined using the anti-pSer451 based immunological assay. These results are interpreted in comparison with those previously attained using phospho-site specific antibodies to determine PPCK activity (Murmu and Plaxton, 2007) and BTPC's Ser^{451} and Ser^{425} phosphorylation status (Dalziel *et al.,* 2012; O'Leary *et al.,* 2011c) during COS development. A distinct developmental pattern of BTPC-K activity was observed such that it was relatively

constant during early endosperm development, increased at stage VII, and then markedly decreased by stage IX (Figure 2.2a). In COS endosperm, developmental stage III marks rapid cell expansion, stage V–VII represent the major phases of oil and protein accumulation, and at stage IX the seed is almost mature, has lost vascular connection with the parent plant, and has begun to desiccate (Sangwan *et al.,* 1992; Greenwood and Bewley, 1982; Simcox *et al.,* 1979). The developmental profiles of COS PPCK activity and BTPC-K activity were dissimilar; COS PPCK activity rapidly increased during COS development, becoming maximal in stage V to VII, and was barely detectable at stages III and IX (Murmu and Plaxton, 2007). BTPC-K activity showed some correlation with the *in vivo* phosphorylation statuses of Ser^{451} and Ser^{425}, which increase throughout development becoming maximal at stage IX (Dalziel *et al.,* 2012, O'Leary *et al.,* 2011c).

COS pod excision, which eliminates photosynthate import, caused a significant increase in BPTC-K activity after 48 h (Figure 2.2b). This parallels the *in vivo* phosphorylation status of Ser^{451} which increased 72 h after COS depodding (Dalziel *et al.,* 2012). In contrast, COS PPCK activity is dependent upon the presence of imported photosynthate such that depodding or prolonged darkness of intact plants caused the complete elimination of PPCK activity (Murmu and Plaxton, 2007). The results presented in Figures 2.2a and 2.2b: (1) support the conclusion that PPCK does not phosphorylate BTPC at Ser^{451}, and (2) unlike PPCK, the BTPC-K appears to be controlled by factors other than up/down regulation as its kinase activity does not always parallel *in vivo* BTPC Ser^{451} phosphorylation status.

Partial Purification of BTPC-K from Developing COS

BTPC-K was highly purified using a combination of PEG-fractionation and FPLC on butyl-Sepharose, Superdex-200, Mono-Q, and Cibacron Blue Sepharose columns. BTPC-K was separated from its endogenous substrate during the initial chromatography on butyl-Sepharose. FPLC of peak BTPC-K activity fractions on HiLoad 16/60 Superdex-200 gel filtration and Mono-Q 5/50 GL columns provided significant purification as the majority of contaminating protein was separated from BTPC-K on these matrices (Table 2.1). Final partial purification of BTPC-K was achieved by fractionation on Cibracron Blue Sepharose. The decision to use Blue-Sepharose as an affinity resin was made because BTPC-K activity exhibited a Ca^{2+}-dependency during purification (Table 2.1), and Blue-Sepharose is effective for the purification of Ca^{2+}-dependent protein kinases (CDPKs) from various plant tissues (Putnam-Evans *et al.,* 1990; Harmon *et al.,* 1987; Anil and Rao, 2001). CDPKs are typically eluted from Blue-Sepharose with 0.2% (w/v) CHAPS after a 0.6 M NaCl wash step (Putnam-Evans *et al.,* 1990; Anil and Rao, 2001). However, BTPC-K activity was eluted from this matrix in the presence of 0.3 M NaCl and 0.2% (w/v) CHAPS, following a 0.15 M NaCl wash.

The standard purification of BTPC-K was ~500-fold, yielding 0.1 mg protein (Table 2.1). The percent recovery of BTPC-K activity was 1%, the final specific activity in the presence of micromolar Ca^{2+} being 707 pmol min^{-1} mg^{-1} (Table 2.1). Blue dextran agarose affinity chromatography is effective for PPCK purifications from leaves, soybean root nodules, and developing COS (Murmu and Plaxton, 2007; Zhang and Chollet, 1997; Wang and Chollet, 1993). However, it proved ineffective for purifying BTPC-K as no activity bound to this matrix.

Native Molecular Mass Estimation of BTPC-K

Calibration of both the Superdex-200 column used during BTPC-K purification and a Superdex-75 column with M_r standards yielded a native M_r of approximately 63±1 kDa (mean ± S.E.M. of n=6 determinations) (Appendix 6). Although we achieved a ~500-fold purification of BTPC-K, it is still relatively impure since SDS-PAGE followed by Sypro Red staining resulted in at least 6 distinct protein staining bands (Appendix 7). Notably, an approximate 1.4 million-fold purification was required to isolate 0.1 μg of homogenous PPCK from 2.6 kg of illuminated maize leaves (Saze *et al.*, 2001). It thus appears that BTPC-K polypeptides, similar to PPCK polypeptides from species such as maize, tomato, COS, and soybean (Murmu and Plaxton, 2007; Marsh *et al.*, 2003; Xu *et al.*, 2003; Saze *et al.*, 2001), occur at extremely low levels *in planta.*

In vitro Phosphorylation-Inhibition of Recombinant Class-2 PEPC by BTPC-K

Purified BTPC-K activity was quantified by monitoring P incorporation from either [γ-^{32}P]ATP [and either: (1) SDS-PAGE followed by phosphorimaging or gel band excision and scintillation counting, or (2) TCA precipitation of proteins and scintillation counting] or unlabeled ATP (and anti-pSer451 immunoblotting) into the p118 subunit of pure recombinant Class-2 PEPC (Figure 2.3a,b). Experiments were performed to validate and optimize the BTPC-K assay as well as to determine maximal stoichiometric P incorporation into p118 (Appendix 8). Thus, phosphorylation assays were run at variable quantities of the partially purified BTPC-K or its substrate BTPC (as part of the Class-2 PEPC complex) (Appendix 8a). Based on these results we selected 250 ng of partially purified BTPC-K and a saturating amount (0.2 μg μl^{-1}) of BTPC and performed phosphorylation time-courses to establish linearity of the BTPC-K assay (Figure 2.3a,b; Appendix 8b). These reaction conditions were used for kinetic studies of the partially purified BTPC-K. The parallel radioactive and non-radioactive BTPC-K assays yielded identical

time-courses such that maximal p118 phosphorylation at Ser^{451} was achieved ~100 min following assay initiation. The maximal stoichiometry of ^{32}P incorporation into BTPC subunits of Class-2 PEPC was estimated to be approximately 0.6 mol/mol p118 subunit. BTPC-K activity was absolutely dependent upon the presence of Mg^{2+} and Ca^{2+} (Figure 2.3a, b). Ca^{2+}-dependence of the partially purified BTPC-K was examined by performing BTPC-K assays in the presence of exogenous Ca^{2+} or EGTA. The results of Figures 2.3a and b indicate that unlike most PPCKs examined to date (Chollet *et al.*, 1996; Izui *et al.*, 2004; Nimmo, 2006; Murmu and Plaxton, 2007) COS BTPC-K is likely a Ca^{2+}-dependent protein kinase (CDPK). Additionally, no measurable ^{32}P was incorporated into the BTPC subunits of either S451D phosphomimetic mutant Class-2 PEPC, nor the PTPC subunits of Class-2 PEPC (Figure 2.3a). Thus, all radioactivity measured was strictly due to BTPC-K-mediated phosphorylation of BTPC at Ser^{451}.

No significant influence of BTPC-K-mediated phosphorylation on BTPC activity of mutant Class-2 PEPC (containing catalytically inactive $AtPPC3^{R644A}$ PTPC subunits) occurred when Class-2 PEPC was assayed under optimal conditions (pH 8.0, 20 mM PEP) (Figure 2.3c). However, when assayed under two sub-optimal conditions (pH 7.3, 1 mM PEP with or without 10 mM L-malate), Class-2 PEPC activity decreased by approximately 50% and 40%, respectively (Figure 2.3c). Phosphorylation of p118 at Ser^{451} caused an approximate two-fold increase in BTPC's K_m(PEP) at pH 7.3 (K_m=1.6±0.2 mM and 0.71±0.1 mM for phospho- and dephospho-BTPC respectively) (Figure 2.4a). Ser^{451} phosphorylation by BTPC-K also elicited significant reductions in BTPC's I_{50}(malate) and I_{50}(Asp) values [I_{50}(malate) = 5.8±0.5 mM and I_{50}(Asp) = 18.7±2 mM for phospho-BTPC, and I_{50}(malate) = 8.1±1 mM and I_{50}(Asp) = 29.6±3.5 mM for dephospho-BTPC] (Figure 2.4b,c). These results corroborate our previous work with phosphomimetic Ser^{451} Class-2 PEPC mutants (containing heterologously expressed

RcPPC4^{S451D} and AtPPC3 ^{R644A} subunits), where the S451D mutation, while not altering $V_{max,}$ caused a three-fold increase in BTPC's K_m(PEP) at pH 7.3 and elicited a significant reduction in BTPC's I_{50}(malate) and I_{50}(Asp) (Figure 2.4a-c) (Dalziel *et al.*, 2012; O'Leary *et al.*, 2011c). The difference in the degree of attenuation of BTPC's kinetic properties between the S451D mutant and the pSer^{451} Class-2 PEPCs may be due to the *in vitro* stoichiometric incorporation of P into p118; only approximately 60% phosphorylation of total BTPC subunits at Ser^{451} was achieved with the partially purified BTPC-K, while 100% of the BTPC subunits of the S451D Class-2 PEPC contained the phosphomimetic mutation

Kinetic Characterization of BTPC-K

The influence of pH on the activity of purified BTPC-K was determined over the range of pH 6.0-9.5 using a mixture of 25 mM Mes and 25 mM Bistris-propane as the assay buffer. BTPC-K exhibited a broad pH profile with maximal activity occurring at ~pH 7.3 (Figure 2.5c), in contrast to plant PPCKs which exhibit maximal activity at ~pH 8.0-8.5 (Law and Plaxton, 1997, Murmu and Plaxton, 2007, Wang and Chollet, 1993**,** Saze *et al.*, 2001). Subsequent BTPC-K assays were conducted at pH 7.3 unless otherwise indicated. The K_m value of COS BTPC-K for BTPC was 1.1 μM while its K_m value for Mg^{2+}-ATP was 6.6 μM. The optimal concentration of Mg^{2+} for maximal BTPC-K activity was 10 mM, with inhibition occurring above 10 mM (Figure 2.5b). Mn^{2+} also served as an adequate divalent cation cofactor in place of Mg^{2+}. However maximal BTPC-K activity in the presence of 10 mM Mn^{2+} was approximately 20% less than that attained in the presence of 10 mM Mg^{2+}(Figure 2.5b). BTPC-K displayed negligible activity in the absence of free Ca^{2+} ions (Figure 2.5a) and required 2.7 μM free Ca^{2+} for half-maximal activity (Figure 2.5a). A recent analysis of several recombinant *Arabidopsis* CDPKs found that they exhibited a wide range of sensitivities to Ca^{2+} *in vitro*, i.e. $K_a(Ca^{2+})$

values ranged from 200 nM to complete Ca^{2+}-independence (Boudsocq *et al.,* 2012). Based on the results of Boudsocq *et al.* (2012), COS BTPC-K activity exhibits moderate Ca^{2+} sensitivity *in vitro.*

Substrate Specificity of BTPC-K

BTPC-K exhibited a narrow substrate specificity *in vitro.* BTPC-K was unable to phosphorylate any of the following proteins assayed at 0.2 mg ml^{-1}: S451D mutant BTPC subunits of Class-2 PEPC, PTPC subunits of either recombinant Class-2 PEPC or native dephospho-COS Class-1 PEPC, dephosphorylated-sucrose synthase (SuSy) from developing COS, or α-casein (Figure 2.6a,b). Nor did BTPC-K phosphorylate a variety of synthetic peptide variants containing the sequences flanking the Ser^{451} phospho-site (Appendix 9). Lysine-rich Histone Type III-S (isolated from calf thymus), however, served as a good substrate for BTPC-K (K_m=1.72 μM) (Figure 2.6a,b). Our results indicate that we have successfully purified BTPC-K to relative homogeneity (with respect to other protein kinases), as a variety of substrates with known phospho-sites were not phosphorylated despite most protein kinases having the propensity to phosphorylate a wide range of proteins relatively indiscriminately when isolated *in vitro.* BTPC-K, in a similar fashion to other plant CDPKs, appears unable to phosphorylate acidic proteins such as α-casein, whereas basic proteins such as histone type III-S serve as a good substrate (Szczegielniak *et al.,* 2000; Harmon *et al.,* 1987), lending further support to the hypothesis that BTPC-K is a bonafide CDPK. Additionally, it appears that the BTPC-K may be dedicated to phosphorylating BTPC's Ser^{451} residue of the Class-2 PEPC complex since no other residues, including known Class-2 PEPC phospho-sites (Thr^{4} and Ser^{425} on BTPC, and Ser^{11} on PTPC, respectively) were phosphorylated when Ser^{451} was mutated to Asp. Furthermore, BTPC-K's inability to phosphorylate synthetic peptides containing the Ser^{451} phosphorylation motif

indicates that the BTPC phosphorylation activity of BTPC-K is influenced not only by the linear sequence of the intrinsically disordered region of BTPC wherein Ser^{451} is located, but also by the overall conformation of the target enzyme. This is reminiscent of COS PPCK which displayed a marked preference for phosphorylating native COS Class-1 PEPC as compared to a variety of C_3 and C_4 leaf PEPCs, despite all of the enzymes possessing the highly conserved N-terminal seryl phosphorylation motif characteristic of PTPCs (Murmu and Plaxton, 2007). Finally, it appears that at least two distinct CDPKs are operating in developing COS endosperm, as COS SuSy and the corresponding SuSy dephospho-peptide containing its *in vivo* Ser^{11} phospho-site are phosphorylated *in vivo* by an abundant CDPK activity in clarified COS extracts that is apparently independent from BTPC-K activity (E. Fedosejevs and W. Plaxton, unpublished data).

Metabolite Effectors and Redox Control of BTPC-K Activity

BTPC-K activity was unaffected by the addition of malate, glucose-6-P, sucrose, glycerol-3-P, glucose, Glu, Gln, Asp, Asn, Pi, ribose-5-P, or fructose-1,6-P_2 (5 mM each), or fructose-2,6-P_2 (10 μM). However, 3-P-glycerate (3PGA) and PEP decreased BTPC-K activity by 42±1% and 57±2%, respectively (Figure 2.7a,b). 3PGA and PEP appear to have a direct effect on the kinase itself and do not indirectly affect BTPC-K activity though interaction with the substrate as inhibition of activity was evident when either BTPC or Histone Type III-S served as its substrate (Figure 2.7a,b). Since phosphorylation at Ser^{451} inhibits BTPC activity (Figure 2.3c) it is logical that increased cytosolic [3PGA] and [PEP] would inhibit the protein kinase responsible for this phosphorylation, in order to increase PEP-flux to malate via Class-2 PEPC under these conditions.

Redox-control of PPCK activity has been demonstrated in maize, *Flaveria trinervia*, and COS, where it was hypothesized that reversible dithiol-disulfide inter-conversion may down-

regulate PPCK activity under various environmental conditions that cause oxidative stress *in vivo* (Saze *et al.*, 2001; Tsuchida *et al.*, 2001; Murmu and Plaxton, 2007). Both C_4 leaf and COS PPCKs appear to contain reactive thiol groups that lead to potent inhibition of enzymatic activity when oxidized, but result in pronounced reactivation of the enzyme when re-reduced with DTT. Similarly, pre-incubation of partially purified BTPC-K with 5 mM GSSG versus 5 mM DTT for 10 min at 30^{o}C resulted in a ~57% decrease and ~10% increase in BTPC-K activity, respectively, relative to control BTPC-K incubations lacking added GSSG or DTT (Figure 2.8a). Moreover, the inhibition of BTPC-K by 5 mM GSGG was fully reversed when the GSGG-treated enzyme was pre-incubated with 10 mM DTT for an additional 10 min at 30^{o}C (Figure 2.8a). Identical experiments performed with Histone Type III-S as the substrate yielded similar but more pronounced oxidation-inactivation and reduction-activation of BTPC-K (~78% and 35%, respectively) indicating that redox-control occurs at BTPC-K and not indirectly via a substrate-specific effect. An *Arabidopsis* CDPK (AtCPK21) also exhibited oxidation-inactivation and thioredoxin-mediated reduction re-activation, and an intramolecular disulfide bond (Cys97-Cys108) was identified as the site of redox modulation (Ueoka-Nakanishi *et al.*, 2013). It is thus possible that redox control of plant CDPK activity is conserved amongst several members of the family.

Effects of Calmodulin, 14-3-3s, and a Calmodulin Antagonist on BTPC-K Activity

Lands plants, including COS, contain a suite of Ca^{2+}-regulated protein kinases encompassing CDPKs, chimeric Ca^{2+} and calmodulin-dependent protein kinases (CCaMKs), CDPK-related protein kinases (CRKs), and SNRK3s (SNF1-related protein kinase, type 3, some of which are regulated by Ca^{2+}-binding proteins) (Harper and Harmon, 2005). Calmodulin (CaM) can potentially regulate members of all of these kinase families with the exception of

CDPKs which are CaM-insensitive (Harmon *et al.*, 1987; Harper and Harmon, 2005). Certain CDPKs in turn, have been shown to be activated by 14-3-3 proteins (Lachaud *et al.*, 2013; Liese and Romeis, 2013). Thus, BTPC-K activity was assayed in the presence of exogenous CaM (heterologously expressed purified petunia CaM81) or 14-3-3 protein (heterologously expressed *Saccharomyces cerevisiae* BMH2) (1 μM each) (Appendix 10). BTPC-K activity decreased slightly in the presence of CaM and 14-3-3 protein (~20% and ~13%, respectively), however it also exhibited a ~15% decrease in activity in the presence of exogenous bovine serum albumin, which served as a control (Appendix 10). These results indicate that the effects of CaM and 14-3-3 protein on BTPC-K activity were non-specific, and that COS BTPC-K is a CaM and 14-3-3 –insensitive CDPK.

CDPKs are composed of three domains; the N-terminal variable domain, the serine/threonine protein kinase domain, and a CDPK activation domain (CAD) (Appendix 11) (Liese and Romeis, 2013). The CAD consists of a pseudosubstrate segment and a Ca^{2+}-binding domain which is highly similar to CaM as it contains four Ca^{2+}-binding EF-hand motifs (Liese and Romeis, 2013, Harper and Harmon, 2005). Due to the structural and biochemical similarity of CAD to CaM, many plant and protist CDPKs are inhibited by μM amounts of CaM antagonists such as trifluoperazine (TFP) (Abo-El-Saad and Wu, 1995; Cavagnino *et al.*, 2011; Harmon *et al.*, 1994; Szczegielniak *et al.*, 2000). BTPC-K activity was also strongly inhibited by TFP; at 100 μM BTPC-K activity was reduced by ~50%, a result consistent with other plant CDPKs (Appendix 10) (Abo-El-Saad and Wu, 1995; Szczegielnak *et al.*, 2000; Hetherington and Trewavas 1982; DasGupta, 1994).

BTPC-K is a Soluble Protein Kinase

The majority of *Arabidopsis* CDPKs have predicted N-terminal myristoylation and palmitoylation sites (Hrabak *et al.,* 2003). Myristoylation with or without palmitoylation has been shown to be responsible for membrane localization of some plant CDPKs, while others (often those lacking acylation sites) remain soluble/cytosolic (Martin and Busconi, 2000; Boudsocq *et al.,* 2012; Liese and Romeis, 2013). Putative COS CDPKs are also predicted to differ in their subcellular localization and solubility (Appendix 12). Using subcellular fractionation of clarified COS extracts, soluble and microsomal fractions were recovered after ultracentrifugation and BTPC-K activity assayed in the respective fractions (Figure 2.10). BTPC-K activity was only detected in the soluble fraction, suggesting that it has no N-terminal acylation sites. The cytosolic localization of BTPC-K is consistent with its maximal activity occurring at ~pH 7.3 as well as the cytosolic localization of its *in vivo* substrate, BTPC (Park *et al.,* 2012).

Bioinformatic Analysis of Castor CDPK Family

Interrogation of the castor genome revealed that it contains 34 putative *CDPK* genes (Figure 2.9, Appendix 12). The *Arabidopsis* genome also contains 34 predicted *CDPK* genes; however, three of these genes have not been shown to be expressed based on the existence of cDNA or expressed sequence tags (Liese and Romeis, 2013; Hrabak *et al.,* 2003). Alignment of the kinase catalytic domains as well as analysis of entire deduced sequences of the 34 putative *Arabidopsis* CDPKs has led to their organization into four subgroups (I-IV) (Hrabak *et al.,* 2003). The significance of these subgroupings with regards to biochemical or physiological function remains unknown. Similar analysis of deduced sequences of the 34 putative castor CDPK isoforms indicated that they cluster into three subgroups (I-III) (Figure 2.9, Appendix 12).

Subgroup III is the least complex with two members, whilst subgroups I and II are more complex as they contain further subdivisions within themselves; i.e. Ia and Ib and IIa and IIb (Figure 2.9, Appendix 12). The majority of predicted CDPK proteins have molecular masses between 51.5-72.1 kDa (Appendix 12), which is consistent with the predicted molecular masses for *Arabidopsis* CDPKs (Hrabak *et al.*, 2003). Molecular mass predictions outside of this range (i.e. between 34.6-12.3 kDa) may be due to the misidentification of pseudogenes as putative CDPKs, or due to truncated sequences within the castor genome database. Nevertheless, with a native molecular mass of ~63 kDa, COS BTPC-K falls well within the size range for a typical CDPK.

2.4 CONCLUDING REMARKS

To the best of our knowledge, this is the first report detailing the purification and biochemical characterization of a protein kinase that *in vivo* phosphorylates a plant BTPC. Results indicate that COS BTPC-K is an entirely distinct type of protein kinase from any previously studied PPCKs (including COS PPCK) owing to its unique physical, biochemical and kinetic properties.

Several lines of evidence suggest that BTPC-K is a CDPK as opposed to the archetypal PPCKs which are currently the only identified PEPC protein kinases. BTPC-K activity was absolutely dependent upon the presence of free Ca^{2+} and the kinase exhibited a Ca^{2+}- sensitivity which appears to be typical of many plant CDPKs studied to date (Figure 2.5a) (Boudsocq *et al.*, 2012; Harmon *et al.*, 1987, Liese and Romeis, 2013). In contrast, PPCKs are believed to be Ca^{2+}-independent (O'Leary *et al.*, 2011b). The native molecular mass estimated for BTPC-K at ~63-kDa falls within the range of plant CDPKs (Appendix 6, 12), and is much larger than PPCKs which have apparent molecular masses of ~30-kDa as they consist simply of a core catalytic

kinase domain (O'Leary *et al.*, 2011b, Nimmo, 2003; Chollet *et al.*, 1996). BTPC-K's substrate preference for basic proteins such as Histone Type III-S and its inability to phosphorylate acidic proteins such as α-casein is yet another characteristic of many plant CDPKs (Figure 2.6) (Harmon *et al.*, 1987; Szczegielniak *et al.*, 2000; Huang and Huber, 2001). COS PPCK can by comparison, phosphorylate Histone Type III-S to the same extent as α-casein (Murmu and Plaxton, 2007). Additionally, COS BTPC-K does not phosphorylate PTPC as either a subunit of recombinant Class-2 PEPC or native COS Class-1 PEPC (Figure 2.6), perhaps the most convincing evidence of the uniqueness of BTPC-K with respect to COS PPCK. Finally, BTPC-K activity is severely attenuated by the presence of CaM antagonist TFP, indicating that BTPC-K is either: (1) a CaM-dependent Ca^{2+}-sensitive protein kinase, or (2) a CDPK with a CAD region that is also sensitive to TFP given its sequence homology to CaM (Appendix 10). Since BTPC-K was not activated by exogenous CaM (Appendix 10), this leads us to conclude that it is a CDPK.

It is unsurprising that COS BTPC and PTPC phosphorylation should be controlled by distinct protein kinases. Physiologically, BTPC phosphorylation at Ser^{451} appears to inhibit Class-2 PEPC activity by increasing its apparent K_m(PEP) and sensitivity to allosteric inhibitors, while PTPC phosphorylation serves to activate the enzyme (Figure 2.3c) (O'Leary *et al.*, 2011b; Tripodi *et al.*, 2005; Murmu and Plaxton, 2007; Dalziel *et al.*, 2012). PPCK transcript and expression levels appear to be strongly controlled by sucrose supply (O'Leary *et al.*, 2011b); in non-green "sink" tissues such as COS, this is hypothesized to be a mechanism whereby plant cells can sense sugars in order to effectively partition imported carbon into seed storage products including protein and lipids when photosynthate supply is abundant. While BTPC-K expression and activity appears to be somewhat sensitive to photosynthate supply (Figure 2.2b), its relatively constitutive expression throughout COS development implies additional post-

translational control of its activity apart from mere synthesis/degradation. Ca^{2+} is known to play a central role in eukaryotic signal transduction with Ca^{2+}-sensor proteins, including plant CDPKs, being critical transducers of the many unique Ca^{2+}-signatures elicited in response to external stimuli or developmental cues, through the activation of phosphorylation cascades (Liese and Romeis, 2013). CDPKs are implicated in many different processes of plant biology, with several studies documenting critical *in vivo* roles for CDPKs in heterotrophic "sink" tissues such as developing seeds (Abo-El-Saad and Wu, 1995; Szczegielniak *et al.*, 2000; Anil *et al.*, 2003), pollen (Estruch *et al.*, 1994; Yoon *et al.*, 2006; Zhao *et al.*, 2013), and root nodules (Zhang and Chollet, 1997b). That BTPC-K is a CDPK thus appears to be a plausible scenario given its tissue-specific expression and purported role in the regulatory phosphorylation of a key enzyme at the crux of carbon and nitrogen metabolism in developing COS.

Despite being distinct protein kinases, COS BTPC-K activity was significantly attenuated by mM amounts of the glycolytic intermediates 3PGA and PEP, in a similar fashion to COS PPCK activity which is also affected by PEP (Figure 2.7) (Murmu and Plaxton, 2007). However, whereas PEP inhibited BTPC-K activity, it activated COS PPCK (Figure 2.7) (Murmu and Plaxton, 2007). Given that PPCK-mediated PEPC phosphorylation activates Class-1 PEPC, while BTPC-K-mediated phosphorylation inhibits Class-2 PEPC, it is logical that increased cytosolic PEP concentrations would serve to simultaneously activate the protein kinase responsible for increasing PEP-flux to malate (i.e. PPCK) via Class-1 PEPC, whilst inhibiting a distinct protein kinase responsible for decreasing PEP-flux through Class-2 PEPC (i.e BTPC-K). Plant CDPKs and PPCKs are classified as belonging to the same superfamily of serine-threonine protein kinases, the "CDPK-SnRK" superfamily, and an analysis of intron placements supports the hypothesis that CDPKs and PPCKs have a common evolutionary origin (Hrabak *et al.*,

2003). Thus the persistence of shared kinetic and biochemical properties would be physiologically relevant, particularly considering the distinct yet similar roles BTPC-K and PPCK must fulfill in the respective coordinate control of COS Class-1 and Class-2 PEPCs.

Apart from characterizing BTPC-K as a CDPK, this study has also served to validate previous work analyzing the kinetic properties of phosphorylated Class-2 PEPC performed with phosphomimetic S451D BTPC mutant subunits (O'Leary *et al.,* 2011c; Dalziel *et al.,* 2012). BTPC-K-mediated phosphorylation at Ser^{451} induced a similar increase in K_m(PEP) and decrease in I_{50}(malate) and I_{50}(Asp) values as the S451D phosphomimetic mutant when assayed under suboptimal conditions (Figure 2.4a-c) (Dalziel *et al.,* 2012). It is still unclear how phosphorylation at these sites contributes to the regulation of carbon metabolism *in vivo,* and the discovery of environmental stimuli or cellular conditions that modulate phosphorylation at these sites would thus be a major advancement. Nevertheless, BTPC-K's apparent dedication to the Ser^{451} phospho-site of BTPC (as is evidenced by its narrow substrate specificity *in vitro*), clearly implies a specific regulatory role for the kinase as well as for BTPC phosphorylation *in vivo*. Additional work to identify the castor *CDPK* gene encoding BTPC-K as well as an analysis of *BTPC-K* transcript expression levels and patterns will be necessary in order to further our understanding of regulatory Class-2 PEPC phosphorylation and the interplay between Ca^{2+}-signalling and storage oil and protein synthesis in COS.

2.5 ACKNOWLEDGEMENTS

We are grateful to Prof. Wayne Snedden (Queen's Univ.) for helpful advice, as well as the gift of recombinant petunia CaM81. We are also grateful to Prof. Greg Moorhead (Univ. of Calgary) for the gift of DH5α *E. coli* cells expressing His-tagged *S. cerevisiae* BMH2 (14-3-3 protein). Dr. Sheng Ying kindly performed the bioinformatics analysis of the castor *CDPK* gene family.

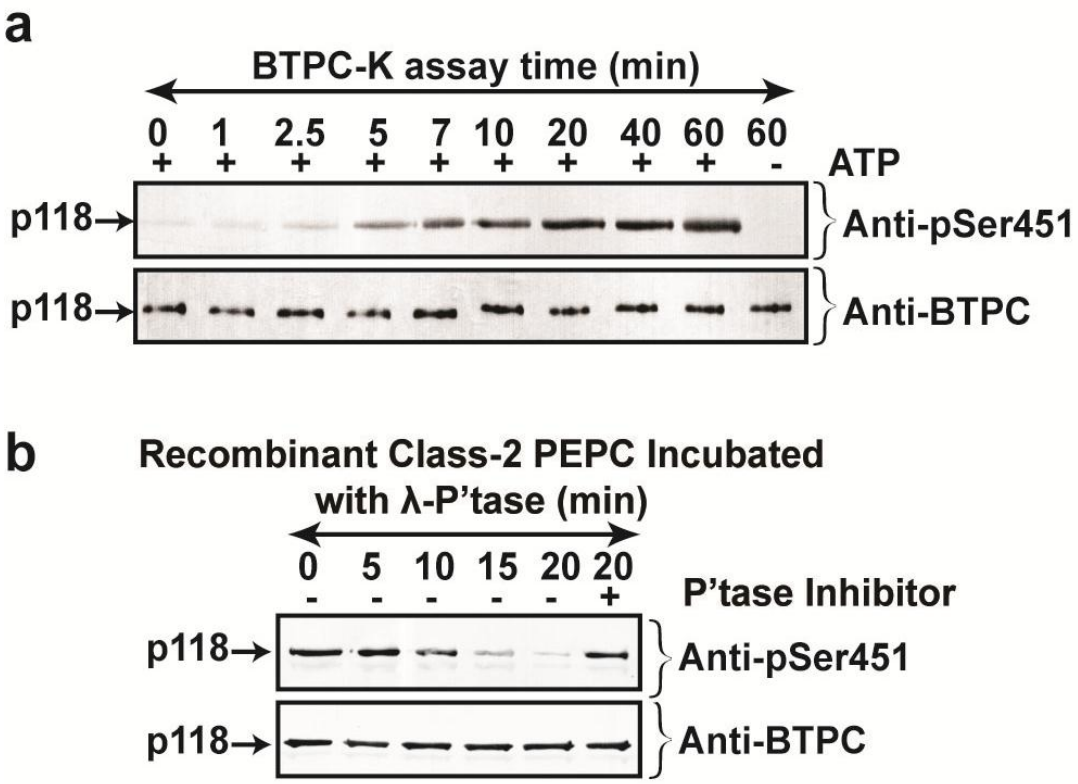

Figure 2.1. Time course for COS BTPC-K and ATP-dependent phosphorylation **(a)** and λ-phosphatase-dependent dephosphorylation (**b**) at Ser^{451} of the BTPC (p118) subunit of recombinant Class-2 PEPC. Aliquots were removed at various times and subjected to SDS-PAGE, followed by immunoblotting with either anti-pSer451 (1 µg BTPC/lane) or anti-BTPC-IgG (100 ng BTPC/lane), and chromogenic staining as in Tripodi *et al* (2005). **(a)** Pure recombinant Class-2 PEPC (40 µg) was incubated at 30° C in a reaction mixture (50 µl final volume) containing 10 mM $MgCl_2$, 0.2 mM $CaCl_2$, 50 nM MC-LR, 0.25 mM ATP, and a desalted clarified extract (10 µg protein) from stage V-VII developing COS. **(b)** Recombinant Class-2 PEPC whose BTPC subunits were *in vitro* phosphorylated at Ser^{451} (panel a) was dephosphorylated at 30 °C with 8,000 units ml^{-1} of λ-phosphatase in the presence of absence of a phosphatase inhibitor cocktail (25 mM NaF, 1 mM EDTA, 1 mM $NaMoO_4$, and 1 mM $NaVO_3$) as in Uhrig *et al* (2008a).

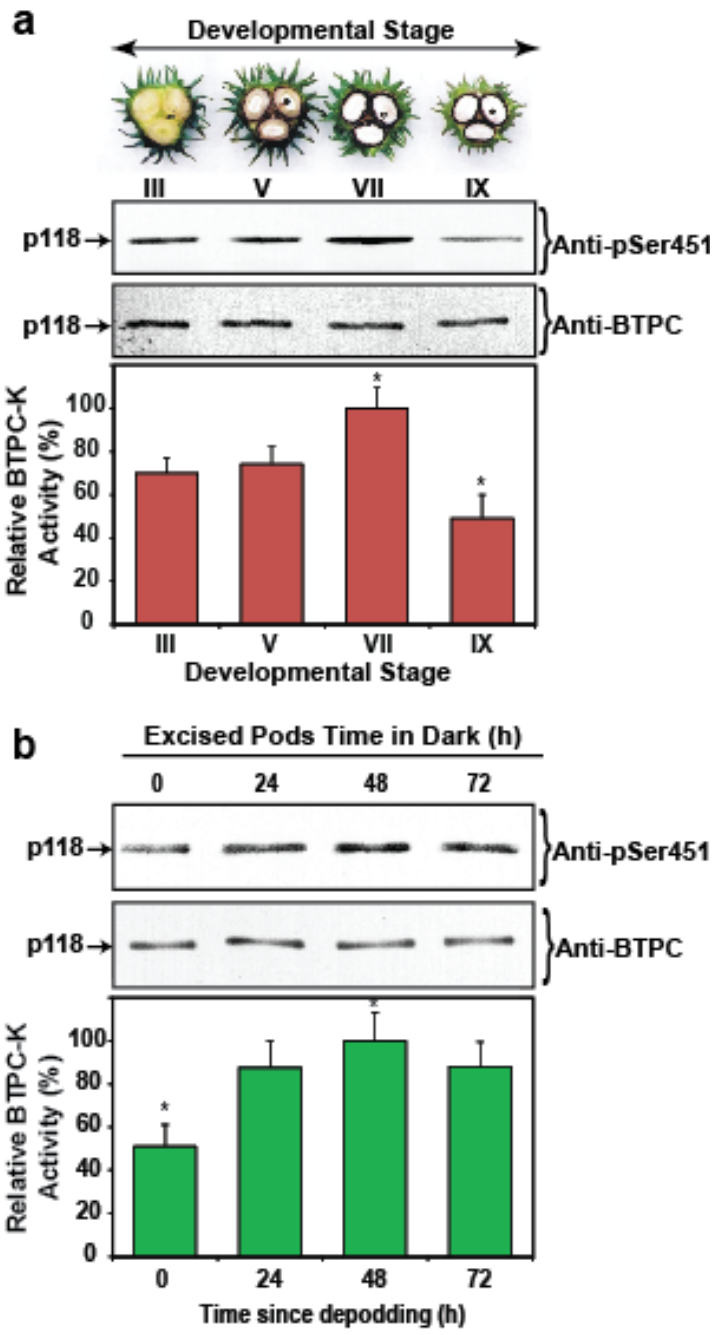

Figure 2.2. Developmental profile of BTPC-K activity during COS development (**a**) and influence of seed pod excision on BTPC-K activity (**b**). Purified recombinant Class-2 PEPC (40 µg) was incubated for 20 min at 30°C in reaction mixtures (50 µl final volume) containing 0.1 mM ATP, 50 nM MC-LR and a desalted clarified COS extract (1 µg protein) from **(a)** various stages of COS development or **(b)** from stage VII endosperm tissue harvested from intact, excised pods that were placed in the dark with water at 24°C and analyzed at the indicated times. Aliquots were subjected to SDS-PAGE and immunoblotting with either anti-pSer451 (1 µg BTPC/lane) or anti-BTPC (100 ng BTPC/lane). The immunoblots were scanned and quantified using Image J software. The ratios of signals from three independent biological replicates were compared as a semi-quantitative measure of relative BTPC-K activity. Maximal mean observed BTPC-K activity from **(a)** Stage VII developing COS endosperm or **(b)** Stage VII developing COS endosperm 48 h after seed pod excision, were used as standards and given a relative BTPC-K activity value of 100% to which all other values were normalized. *All values represent the means ± S.E.M. of three biological replicates.* **(a)** Relative BTPC-K activity at Stage VII was significantly different ($P < 0.05$, Student's *t*-test) from Stage IX. **(b)** Relative BTPC-K activity 48 h post seed pod excision was significantly different ($P < 0.05$, Student's *t*-test) from that obtained at 0 h.

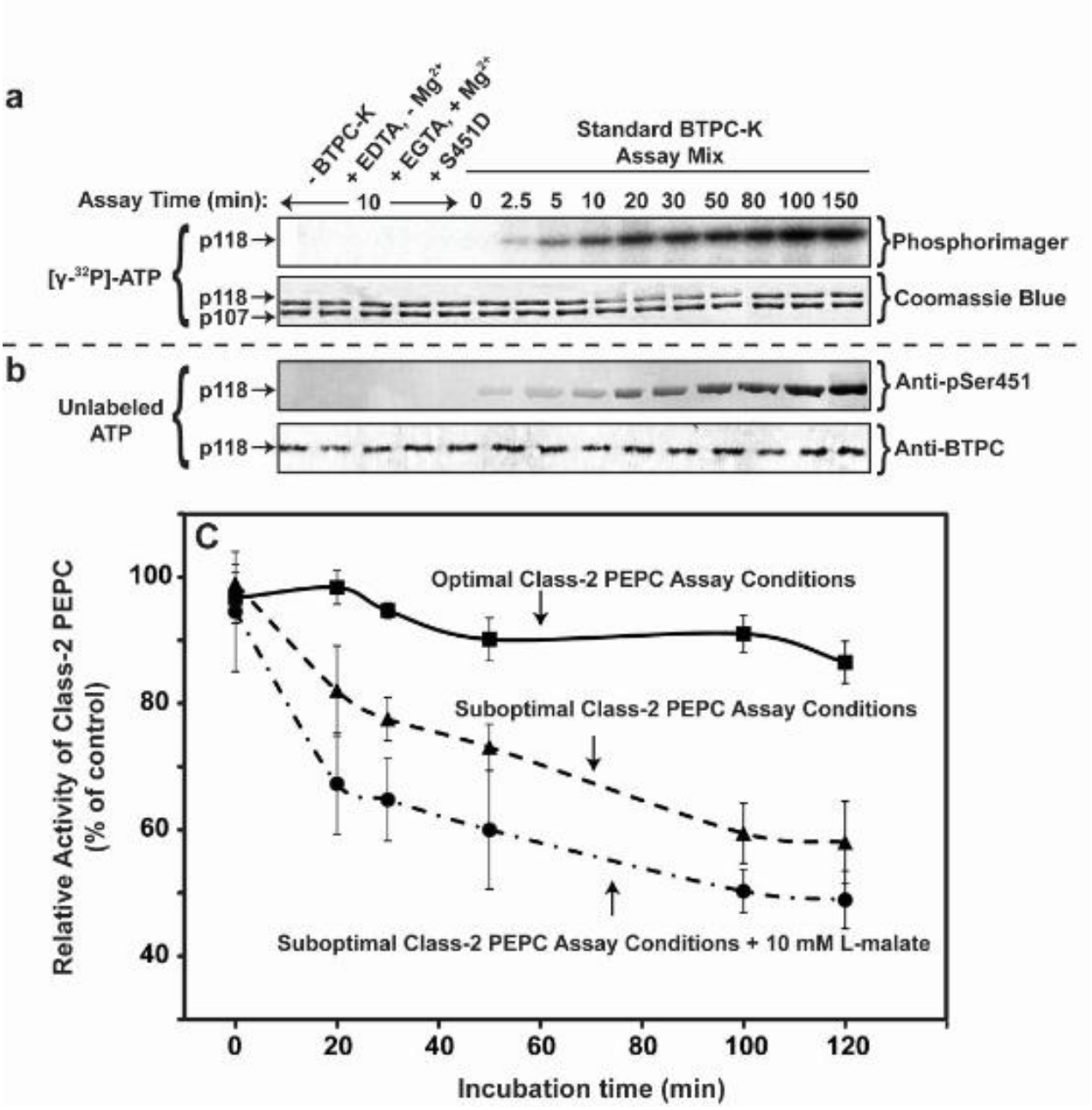
a
- BTPC-K
+ EDTA, - Mg2+
+ EGTA, + Mg2+
+ S451D
Standard BTPC-K Assay Mix
Assay Time (min):
10
0 2.5 5 10 20 30 50 80 100 150
[γ-32P]-ATP
p118
p118
p107
Phosphorimager
Coomassie Blue
b
Unlabeled ATP
p118
p118
Anti-pSer451
Anti-BTPC
C
Optimal Class-2 PEPC Assay Conditions
Suboptimal Class-2 PEPC Assay Conditions
Suboptimal Class-2 PEPC Assay Conditions + 10 mM L-malate
Relative Activity of Class-2 PEPC (% of control)
100
80
60
40
0
20
40
60
80
100
120
Incubation time (min)

Figure 2.3. Time-course for BTPC-K-mediated phosphorylation of COS BTPC at Ser^{451}. Pure recombinant Class-2 PEPC [40 µg, containing catalytically inactive PTPC ($AtPPC3^{R644A}$) subunits (O'Leary *et al.,* 2011c)] was incubated at 30 °C with partially purified BTPC-K (250 ng) in the presence of 0.1 mM of either [γ-^{32}P]ATP (specific radioactivity 1000 cpm/pmol) **(a)** or non-radioactive ATP **(b)**. Aliquots were removed at various times and subjected to SDS-PAGE, followed by Coomassie blue R-250 staining and phosphorimaging (**a**, 1 µg BTPC/lane) or immunoblotting with anti-pSer451 (**b,** 1 µg BTPC/lane) or anti-BTPC (**b,** 100 ng BTPC/lane), and chromogenic staining as in Tripodi *et al* (2005). Also shown is the extent of BTPC phosphorylation following parallel incubations in the absence of BTPC-K (lane 1); in the presence of 5 mM EDTA and absence of Mg^{2+} (lane 2); in the presence of 5 mM EGTA (lane 3); and in the presence of recombinant Class-2 PEPC containing phosphomimetic COS BTPC S451D subunits (O'Leary *et al.,* 2011 425c) (lane 4). **(c)** The activity of corresponding Class-2 PEPC [containing catalytically inactive mutant (R644A) PTPC subunits and active wild-type BTPC subunits] was determined from a non-radioactive ATP BTPC-K assay at optimal (pH 8.0, 20 mM PEP),and suboptimal (pH 7.3, 1 mM PEP, with and without 10 mM L-malate) assay conditions. Class-2 PEPC (R644A/wt) activity of aliquots from parallel non-radioactive ATP BTPC-K assays performed in the presence of 1 mM EGTA were used as control (dephospho) values to which the phospho-values were compared. All values are the means (± SEM) of $n = 3$ replicate incubations.

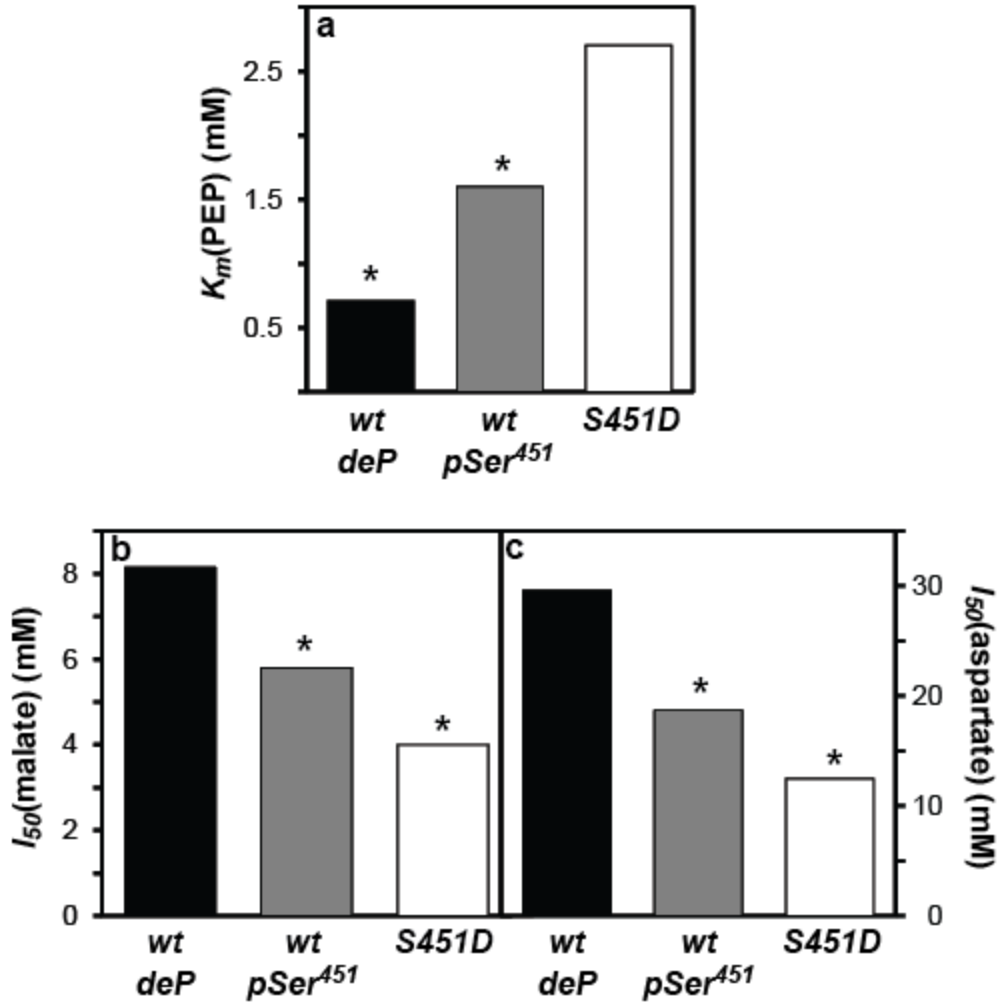

Figure 2.4. Kinetic effect of Ser^{451} phosphorylation on BTPC activity of mutant Class-2 PEPC. Shown are the K_m(PEP) **(a)**, I_{50}(malate) **(b)**, and I_{50}(aspartate) **(c)** values for heterologously expressed Class-2 PEPC complexes containing an inactive PTPC mutant (AtPPC3^{R644A}) and either wild-type (wt) or phosphomimetic castor BTPC (RcPPC4^{S541D}) subunits. Prior to PEPC activity assays, Class-2 PEPC complexes (20 μg) containing wt BTPC subunits were first incubated at 30^{o}C in the standard BTPC-K reaction mixture with BTPC-K (250 ng), 0.1 mM ATP (total reaction volume 50μl), with (wt deP) or without (wt pSer^{451}) 0.5 mM EGTA ([free Ca^{2+}]= 0 μM) for 100 min. PEPC activity was assayed at pH 7.3 **(a-c)** with subsaturating PEP (1 mM) **(b,c)**. All values represent the means of n = 3 separate determinations and are reproducible to within 15% of the mean value. Results for S451D were taken from Dalziel *et al.* (2012). Asterisks denote values that are significantly different from dephospho-wild-type (wt deP) (P < 0.05, Student's t-test).

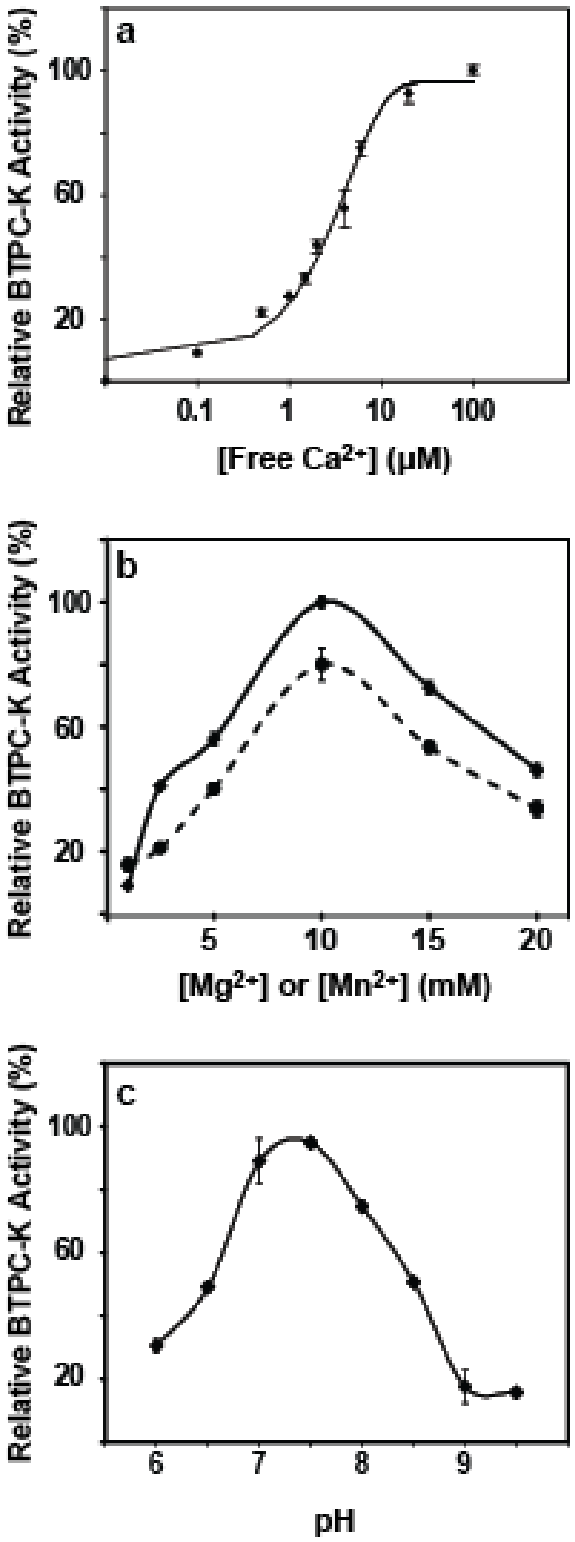

Figure 2.5. Effect of calcium, divalent metal cations, and assay pH, on BTPC-K activity. Pure recombinant Class-2 PEPC (20 µg) was incubated for 30 min at 30 °C with partially purified BTPC-K (250 ng) in the standard phosphorylation assay with 0.1 mM [γ-^{32}P]ATP (specific radioactivity 1000 cpm/pmol) (50 µl total volume) and **(a)** the addition of 0.5 mM EGTA and varying concentrations of free calcium, or **(b)** at varying concentrations of Mg^{2+} (solid line) or Mn^{2+} (dashed line), or **(c)** at different pH values except that the buffer used was a mixture of 25 mM Mes and 25 mM Bis-tris-propane. Reactions were terminated by the addition of 20% (w/v) TCA and 0.2% (w/v) NaPPi, radiolabeled proteins were precipitated as described in "Materials and Methods", and incorporation of ^{32}P into the BTPC subunit determined by Cerenkov counting of the precipitated proteins. All values represent the means ±S.E.M. of n = 3 independent experiments.

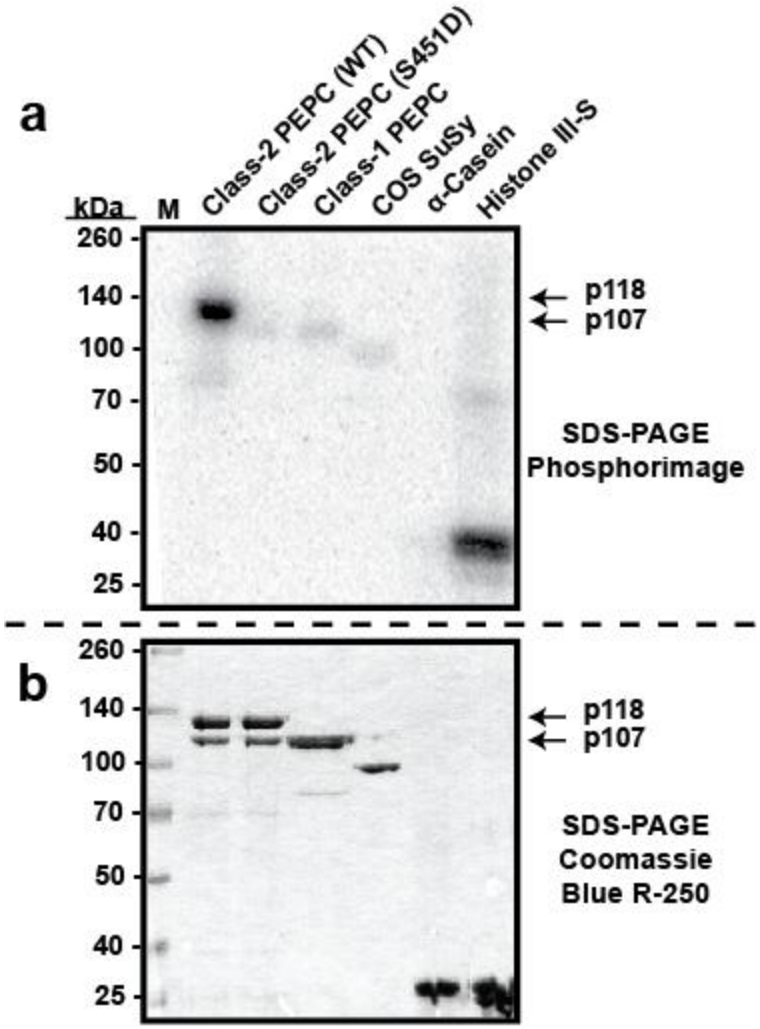

Figure 2.6. Substrate specificity of BTPC-K. Purified recombinant Class-2 PEPCs (wild-type and S451D mutant), purified native *in vitro* dephosphorylated COS Class-1 PEPC (Tripodi *et al.*, 2005) or COS SuSy (Fedosejevs and Plaxton, unpublished data), or dephosphorylated α-casein from bovine milk, or dephosphorylated Histone Type III-S from calf thymus (5 μg each) were incubated for 10 min at 30 °C in the standard [γ-^{32}P]ATP phosphorylation assay in the presence of 250 ng of partially purified BTPC-K. Following SDS-PAGE (1 μg protein per lane), the gel was subjected to **(a)** phosphorimaging and **(b)** stained with Coomassie Blue R-250. Results are representative of n = 3 independent experiments where phosphorylation of S451D, PTPC, SuSy, and α-casein was negligible. M, pre-stained protein molecular weight standards.

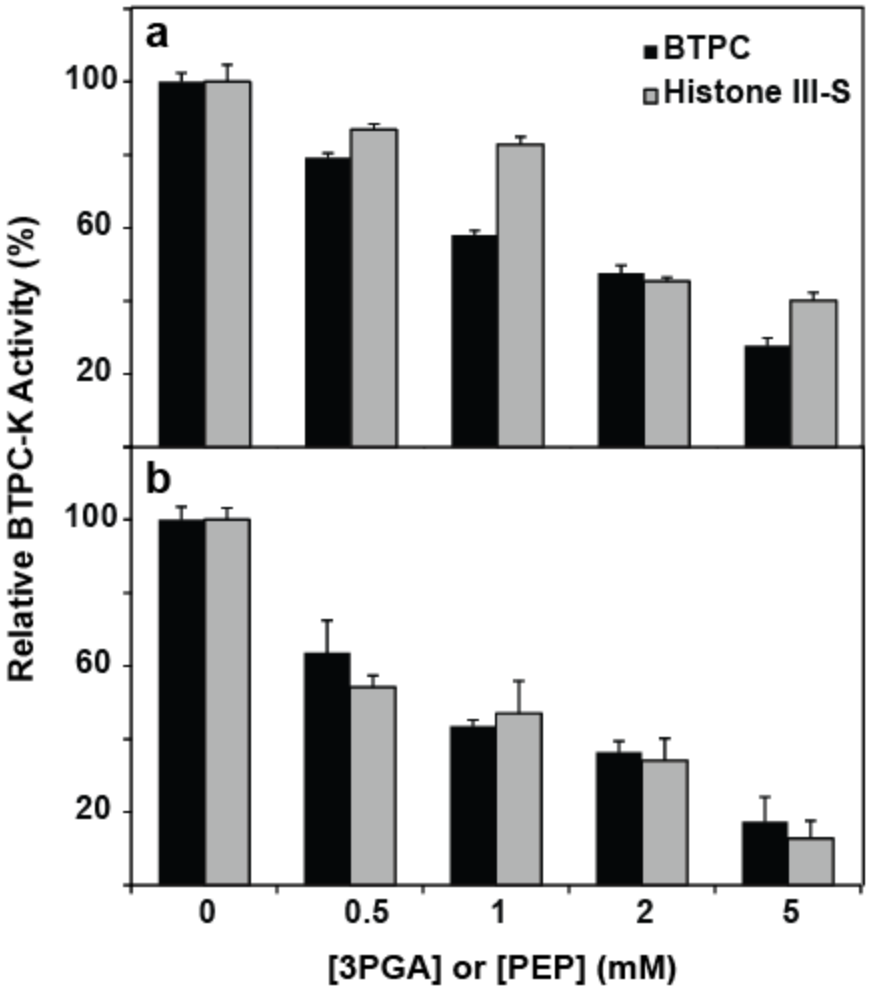

Figure 2.7. Effect of 3-P-glycerate (3PGA) and PEP on BTPC-K activity. Pure recombinant Class-2 PEPC or histone type III-S (10 µg each) were incubated for 10 min at 30°C with partially purified BTPC-K (250 ng) in the standard phosphorylation assay with 0.1 mM [γ-^{32}P]ATP (specific radioactivity 1000 cpm/pmol) (25 µl total volume) in the presence of varying concentrations of **(a)** 3PGA or **(b)** PEP. Reactions were terminated by the addition of 20% (w/v) TCA and 0.2% (w/v) NaPPi, radiolabeled proteins were precipitated as described in "Materials and Methods", and incorporation of ^{32}P into the BTPC subunit determined by Cerenkov counting of the TCA precipitated proteins. Activity is expressed relative to BTPC-K activity with BTPC or histone type III-S respectively in the absence of any metabolite effectors, set at 100%. All values are the means ± S.E.M of *n*= 3 independent experiments.

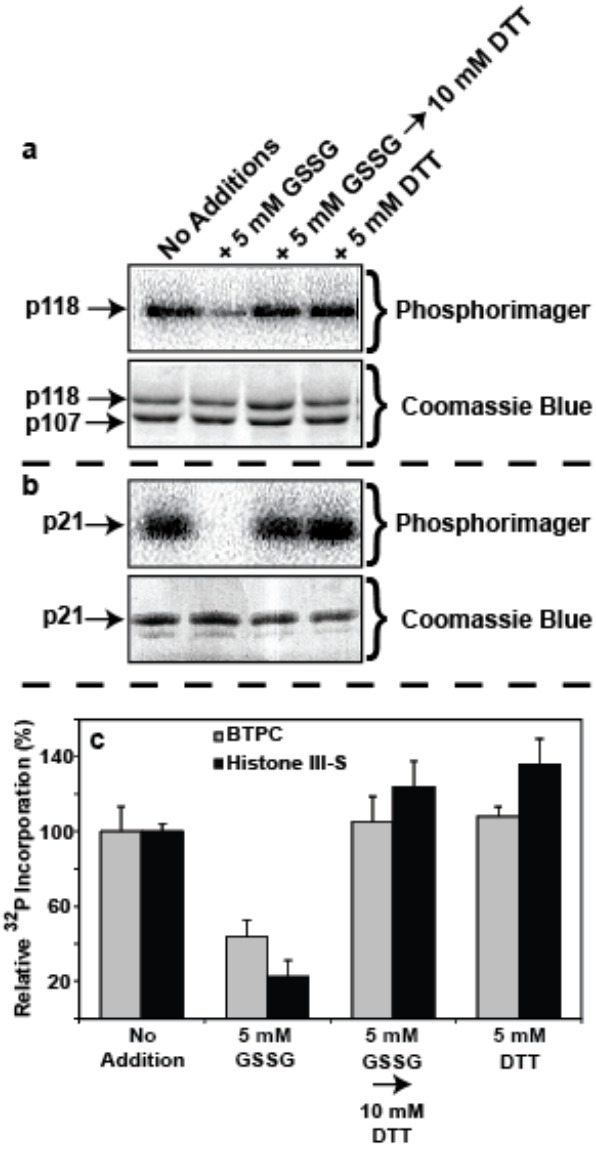

Figure 2.8. BTPC-K is partially inactivated by GSGG and reactivated by DTT. Purified BTPC-K was incubated at 30 °C for 10 min in the presence and absence of 5 mM GSGG or 5 mM DTT. An aliquot of the GSGG-treated BTPC-K was incubated in 10 mM DTT for an additional 10 min. Resultant BTPC-K activity in each sample was estimated by their incubation with **(a)** pure recombinant Class-2 PEPC or **(b)** Histone Type III-S, for 20 min at 30 °C in the standard [γ-^{32}P]-ATP phosphorylation assay. Following SDS-PAGE (1 µg protein/lane), the gel was stained with Coomassie Blue R-250 and subjected to phosphorimaging. **(c)** Separate reactions performed under the same conditions as stated above were terminated with the addition of 20% (w/v) TCA and 0.2% (w/v) NaPPi, radiolabeled proteins were precipitated as is described in "Materials and Methods", and the relative incorporation of ^{32}P into BTPC or Histone Type III-S determined by Cerenkov counting. Mean ^{32}P incorporation under "no additions" reaction conditions were given relative ^{32}P incorporation values of 100%, to which all other values were normalized. All values represent the means ±S.E.M. of *n* = 3 independent experiments.

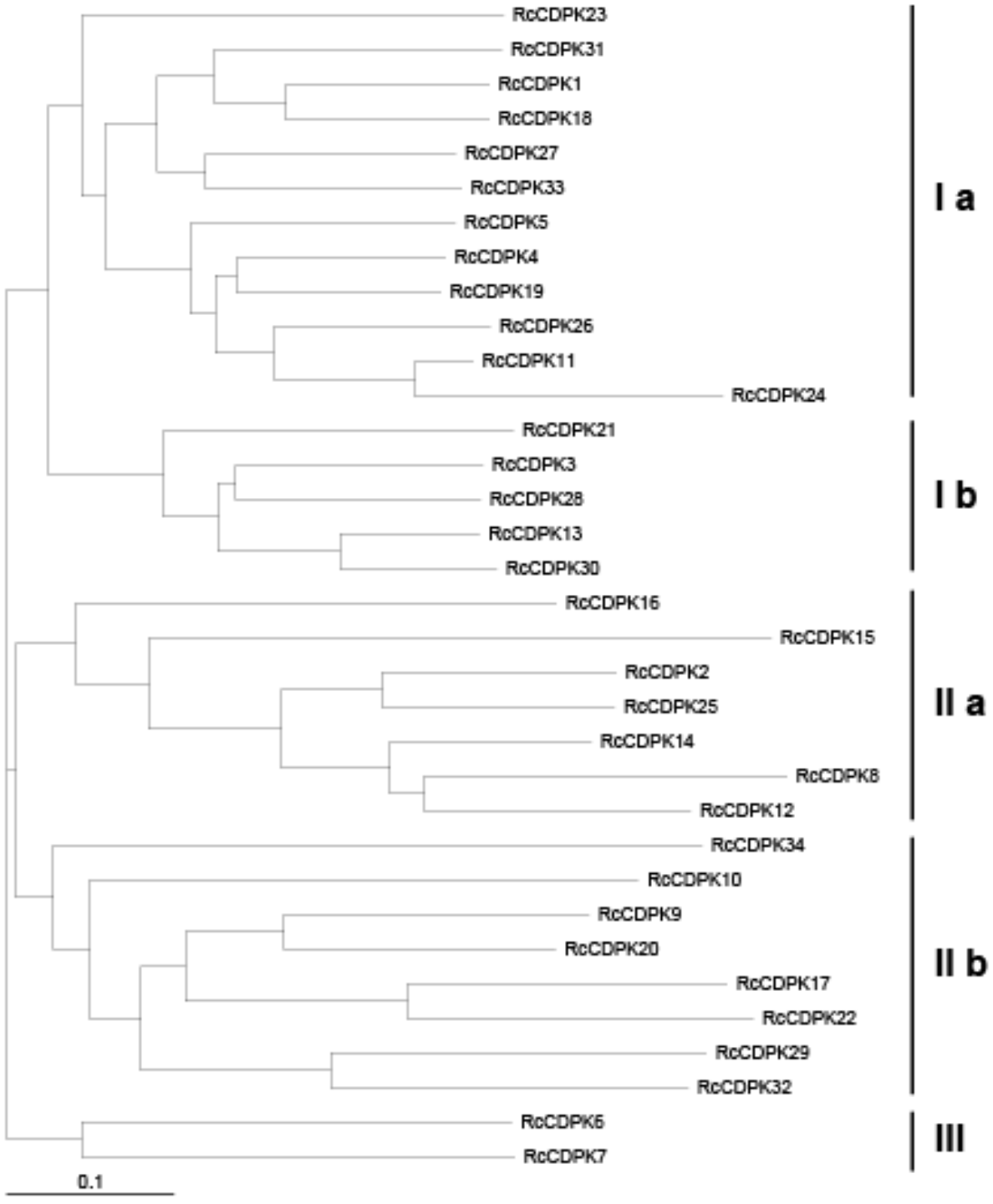

Figure 2.9. Phylogenetic analysis of castor CDPKs. The deduced protein sequences of the RcCDPKs were aligned and analyzed by the ClustalX 1.83 and Treeview 1.6.6 program, respectively. The phylogenetic tree reveals the presence of three distinct, branched subgroups (I–III). The branch lengths are proportional to divergence, with a scale of "0.1" representing 10% change.

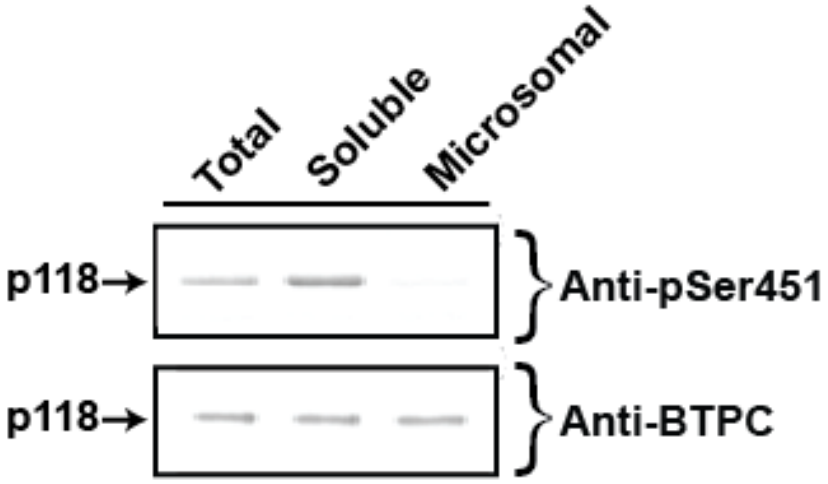

Figure 2.10. BTPC-K is a soluble protein kinase. Purified recombinant Class-2 PEPC (20 µg) was incubated for 25 min at 30°C in reaction mixtures (50 µl final volume) containing 0.1 mM ATP, 50 nM MC-LR and either a Stage VII desalted clarified COS extract (Total), or the soluble or microsomal membrane fractions derived from this clarified COS extract (2 µg protein each) as described in "Materials and Methods". Aliquots were subjected to SDS-PAGE and immunoblotting with either anti-pSer451 (1 µg BTPC/lane) or anti-BTPC (100 ng BTPC/lane) to determine which fraction contained BTPC-K activity.

Table 2.1. Purification of BTPC-K from stage V-VII developing COS endosperm

Step	Protein (mg)	Total Activity (pmol min^{-1})	Specific Activity (pmol min^{-1} mg^{-1})[a]		Ca^{2+}-dependent Specific Activity (pmol min^{-1} mg^{-1})	Ca^{2+} Sensitivity (x-fold)	Purification (x-fold)	Yield (%)
			+ Ca^{2+}	- Ca^{2+}				
(1) Clarified Extract	6500	8667	10.0	8.6	1.4	1	1	100
(2) Butyl-Sepharose	176	8149	65.3	19.0	46.3	3	33	94
(3) Superdex-200	33	4510	160.0	23.3	136.7	7	98	52
(4) Mono-Q	4.8	1394	300.3	10.0	290.3	30	207	16
(5) Blue-Sepharose	0.1	71	713.3	6.7	706.7	107	505	1

[a] Pooled and concentrated fractions were assayed using the radiometric [γ-^{32}P]ATP assay described in Materials and Methods; + Ca^{2+} and – Ca^{2+} assays respectively contained 0.5 mM EGTA with 0.7 mM $CaCl_2$ and 0.5 mM EGTA

Chapter 3. General Discussion

3.1 OVERVIEW

The import of photosynthate and amino acids into developing seeds and the subsequent partitioning of these compounds into the storage end products (starch, proteins and lipids) which will eventually support seed germination is of obvious agronomic concern. PEP-metabolism via PEPC, PK_c and PK_p plays a central role in the partitioning of imported photosynthate to either leucoplast fatty acid biosynthesis or the mitochondrial production of C-skeletons and ATP needed for storage protein biosynthesis (Figure 1.3). In non-green oil seeds such as COS, PEPC is believed to play a critical role in controlling sucrose partitioning at the cytosolic PEP branchpoint to produce C-skeletons (malate) and reductant (NADPH and NADH) required for fatty acid biosynthesis (Figure 1.3b) (O'Leary *et al.*, 2011b). COS PEPC has thus become the focus of intensive research efforts to understand the control of C-metabolism and oil synthesis in non-green oil seeds. In 2001, two physically and kinetically distinct oligomeric classes of PEPC were discovered in the endosperm of developing COS (Blonde and Plaxton, 2001). Class-1 PEPC is a typical homotetramer composed of 107-kDa PTPC subunits, whereas the 910-kDa Class-2 PEPC hetero-octameric complex arises from a tight interaction between Class-1 PEPC and 118-kDa BTPC subunits. BTPC functions as both a catalytic and regulatory subunit of the allosterically-desensitized Class-2 PEPC (O'Leary *et al.*, 2009), which in turn is hypothesized to support PEP-flux to malate for leucoplast fatty acid synthesis.

Work done by Glen Uhrig and Brendan O'Leary to immunopurify native COS BTPC enabled the nearly complete sequencing and phosphoproteomic analysis of BTPC polypeptides, where it was discovered that BTPC subunits of COS Class-2 PEPC are phosphorylated at multiple sites *in vivo* (Uhrig *et al.*, 2008a; O'Leary *et al.*, 2009). This represents the first reported

case of vascular plant BTPC phosphorylation. LTQ-FT MS/MS of co-IP'd COS BTPC was then used to identify its specific phospho-sites to Thr^{4}, Ser^{425} and Ser^{451}. Subsequent work by Brendan O'Leary on the Ser^{425} and Katie Dalziel on Ser^{451} phospho-sites of BTPC using S425D and S451D phosphomimetic mutants, respectively, indicated that phosphorylation at both sites acted as inhibitory regulators of BTPC catalytic activity (O'Leary *et al.,* 2011c; Dalziel *et al.,* 2012).

In a logical progression of COS BTPC research, this thesis strove to purify and characterize the protein kinase (BTPC-K) responsible for *in vivo* BTPC Ser^{451} phosphorylation. A relatively unique non-radioactive, semi-quantitative, immunoassay to monitor BTPC-K activity from developing COS extracts was employed in order to facilitate the successful partial purification of BTPC-K. This assay was based upon the use of phospho-site specific antibodies and immunoblotting to asses P incorporation from unlabeled ATP into the BTPC subunit of Class-2 PEPC at Ser^{451}. A similar approach had previously been used by Murmu and Plaxton (2007) to monitor PPCK activity during its purification from developing COS endosperm. Kinetic and biochemical characterization of partially purified BTPC-K revealed that it differed significantly from other studied PPCKs including COS PPCK. Most notably, BTPC-K activity is strictly dependent on the presence of free Ca^{2+} (K_a= 2.7 μM) (Figure 2.5a), while all known PPCKs are Ca^{2+}-independent (O'Leary *et al.,* 2011; Nimmo, 2003; Chollet *et al.,* 1996). This defining characteristic along with the insensitivity of BTPC-K activity to exogenous CaM, but marked CaM antagonist sensitivity (Appendix 10), led to the conclusion that BTPC-K is a CDPK. BTPC-K displayed a broad pH-activity optima of ~pH 7.3 (Figure 2.5c), and kinetic studies revealed a K_m for Mg^{2+}-ATP of 6.6 μM and a specific activity of 706.7 pmol min^{-1} mg^{-1} (Table 2.1). BTPC-K was also revealed to be soluble (Figure 2.10); thus it likely does not contain N-terminal acylation motifs characteristic of many CDPKs whose function is to localize

them to various cell membranes (Liese and Romeis, 2013, Harper and Harmon, 2005). The narrow substrate specificity displayed by BTPC-K *in vitro* (where its phosphorylation activity was restricted to the Ser^{451} residue of BTPC and Histone Type III-S) (Figure 2.6) implies that: (1) it is likely a dedicated protein kinase of BTPC and (2) there is a specific regulatory role for the kinase as well as for BTPC phosphorylation *in vivo.*

COS BTPC-K did share some kinetic and biochemical similarities with COS PPCK. Both kinases may be subject to redox-regulation *in vivo*, as *in vitro* they each exhibited oxidation-inactivation and reduction-reactivation (Figure 2.8) (Murmu and Plaxton, 2007). COS BTPC-K activity also appears to be attenuated by millimolar amounts of the glycolytic intermediates 3PGA and PEP, in a similar fashion to COS PPCK activity which is also affected by PEP (Figure 2.7) (Murmu and Plaxton, 2007). However, PEP caused apparent inhibition of BTPC-K activity and activation of COS PPCK (Figure 2.7) (Murmu and Plaxton, 2007). Given that PPCK-mediated PEPC phosphorylation activates Class-1 and Class-2 PEPCs while BTPC-K-mediated phosphorylation inhibits Class-2 PEPC, it is logical that increased cytosolic PEP concentrations would serve to simultaneously activate the protein kinase responsible for increasing PEP-flux to malate (i.e. PPCK) via Class-1 PEPC, whilst inhibiting a distinct protein kinase responsible for decreasing PEP-flux through Class-2 PEPC (i.e BTPC-K). Plant CDPKs and PPCKs are classified as belonging to the same superfamily of serine-threonine protein kinases, the "CDPK-SnRK" superfamily, and an analysis of intron placements supports the hypothesis that CDPKs and PPCKs have a common evolutionary origin (Hrabak *et al.*, 2003). Thus the persistence of shared kinetic and biochemical properties would be physiologically relevant, particularly considering the distinct yet similar roles COS BTPC-K and COS PPCK must fulfill in the respective coordinate control of Class-1 and Class-2 PEPCs.

This work has also provided novel insights into the function of plant CDPKs. Most current studies of plant CDPKs entail the purification of a heterologously expressed kinase and its characterization against a variety of synthetic peptides and generic protein kinase substrates, as a means of inferring biochemical and kinetic properties as well as putative roles *in planta* (Leise and Romeis, 2013; Harper and Harmon, 2005; Hrabak *et al.,* 2003). However, even the most fundamental biochemical and kinetic characteristics of plant CDPKs, including their free Ca^{2+} requirements, can change drastically depending on the substrate they are presented with (Boudsocq *et al.*, 2012). This study was able to perform all BTPC-K assays against the bonafide *in vivo* BTPC-K substrate, thus any deduced kinetic parameters or biochemical characteristics are more likely to be physiologically relevant. Furthermore, the result of phosphorylation on the target enzyme (i.e. inhibition of Class-2 PEPC activity) was successfully demonstrated using our approach and this also served to validate previous phosphomimetic mutant Class-2 PEPC studies (Dalziel *et al.,* 2012, O'Leary *et al.,* 2011c). Additionally, BTPC-K was unable to phosphorylate a variety of peptides containing its own phosphorylation motif and phospho-site (Appendix 9). Thus, kinase studies that strictly employ the use of peptides (i.e. high-throughput peptide arrays) to determine kinase recognition motifs likely result in many false-negative results as BTPC-K (and COS PPCK) demonstrate the importance of not only the linear sequence surrounding the phospho-site but also the overall conformation of the target enzyme (Murmu and Plaxton, 2007). This is especially true of kinases which are highly selective for a specific target, one prominent example being the MAP kinase kinases (MEKs) (Hardie *et al.,* 1999). Consequently, our work has identified a novel CDPK recognition motif which is reminiscent of a SnRK1 recognition element, with COS BTPC having a basic Arg residue at position P-2 and hydrophobic residues at P-4 and P+4 (Ile and Leu respectively) (Appendix 13). The Ser^{451} phospho-site as well as these

critical kinase recognition residues are highly conserved amongst several BTPC orthologs which implies an important, conserved function for phosphorylation at this site (Appendix 13). From our work it is obvious that the purification of an endogenous protein kinase based on a known *in vivo* substrate, while considerably more intensive, has several advantages which make this experimental approach worthwhile.

Finally, this study has found novel evidence for the role of Ca^{2+}-signaling in the control of C-metabolism in non-green oilseeds. Unfortunately, most *in vivo* targets of plant CDPKs remain unidentified. However, SuSy provides a good example of another major enzyme with a central role in plant C-metabolism that is phosphorylated *in vivo* by a CDPK that, at least in developing COS, appears to be distinct from the CDPK controlling BTPC phosphorylation at Ser^{451} (Zhang and Chollet, 1997b; E. Fedosejevs and W. Plaxton, unpublished data). Interestingly SnRKs (particularly SnRK1s), have long been implicated in the regulation of plant C-metabolism, as they are known to directly phosphorylate a variety of enzymes involved in C-metabolic pathways (Coello *et al.,* 2011). These targets include, but are not limited to, sucrose phosphate synthase, nitrate reductase, 6-phosphofructo-2-kinase/fructose-2,6-bisphosphatase, and ADP-glucose pyrophosphorylase (Coello *et al.,* 2011). CDPKs and SnRKs are closely related, belonging to the "CDPK-SnRK" superfamily (Hrabak *et al.,* 2003) and work by Huber *et al* (2001) with synthetic peptides has determined that the phosphorylation motifs recognized by many plant CDPKs and SnRK1s are remarkably similar, often only differing by the position of one amino acid. Given the aforementioned false-negatives that are likely associated with using only peptides to determine putative *in vivo* kinase substrates and/or phosphorylation motifs, it is very possible that CDPKs can phosphorylate many of the same or similar targets as SnRKs *in vivo,* perhaps under different physiological conditions. The BTPC Ser^{451} phospho-site itself was

initially predicted to be phosphorylated by a SnRK1 protein kinase (O'Leary *et al.*, 2011b). It is worth considering then, that plant CDPK and SnRK signalling pathways may somehow "link" or converge in the concordant control of plant primary C-metabolism.

3.2 FUTURE DIRECTIONS

Undoubtedly the most critical area of research that should first be addressed following this study is the identification of the castor *CDPK* gene (*RcCDPK*) that encodes BTPC-K. We attempted to identify the BTPC-K polypeptide by subjecting some of the Blue-Sepharose fraction to SDS-PAGE followed by Colloidal Brilliant Blue staining, excision of major protein staining bands and then analysis of the bands via MALDI-TOF MS. Unfortunately, we were unsuccessful as none of the bands were identified as a protein kinase. We are currently in the process of preparing a sample of the Blue-Sepharose fraction for analysis via LC-MS/MS on an Orbitrap. We are hopeful that the increased mass accuracy, sensitivity and dynamic range of this machine will provide fruitful results.

Should this prove unsuccessful, it would be necessary to attempt another purification of BTPC-K. Now that a successful purification scheme has been determined, it would be necessary to scale up the purification; i.e. start with several kg of COS stage V-VII endosperm tissue, in a similar manner to the scale of purification (2.6 kg) that was necessary to purify 0.1 μg of maize leaf PPCK to homogeneity (Saze *et al.*, 2001). It may also be worthwhile to try alternate affinity chromatography resins in place of Blue-Sepharose. However, it should be noted that blue dextran agarose, phospho-cellulose, and γ-linked ATP-Sepharose all proved ineffective for BTPC-K purification (COS BTPC-K activity did not bind to these resins).

After the COS *BTPC-K* gene has been successfully identified, it would then be logical to undertake transcript profiling studies in castor to determine its tissue specific expression as well as any influences of developmental cues or environmental stress (i.e. Pi-deprivation, salt stress, etc.) which might influence *BTPC-K* expression. These studies would serve to further elucidate the roles of both BTPC-K and Class-2 PEPC in COS C-metabolism. While the current thesis only analyzed BTPC-K activity in developing COS endosperm, tissue-specific expression studies have shown that Class-2 PEPC is also present in other biosynthetically active castor tissues including young, expanding leaves (O'Leary *et al.,* 2011a). It would thus be interesting to see if *BTPC-K* transcripts and BTPC-K activity are present in all tissues where Class-2 PEPC is known to be expressed. These studies could also be eventually expanded to include *btpc-k* knock-out plants in order to determine whether: (1) there is an observable phenotype for plants lacking *BTPC-K* expression, and (2) this could be used in tandem with large scale phosphoproteomic analyses to determine whether BTPC-K has targets other than BTPC *in vivo*.

The Ser^{451} phospho-site and basophilic kinase phosphorylation motif is also highly conserved amongst several BTPC orthologues (Appendix 13). It would thus be of merit to explore whether BTPC-K activity and *in vivo* BTPC phosphorylation at residues corresponding to Ser^{451} of COS BTPC occurs in other plant species and tissue types, and if so whether the responsible kinase is also a CDPK.

More broadly in terms of future PEPC research, recent transient co-expression studies of FP (fluorescent protein)-tagged COS PTPC and BTPC subunits in tobacco BY2 cells have demonstrated their *in vivo* interaction, and association with the surface of mitochondria, mediated by BTPC's intrinsically disordered region (Park *et al.,* 2012). While this thesis has demonstrated that Ser^{451} phosphorylation has a significant kinetic effect on Class-2 PEPC, the

phospho-site does occur within BTPC's intrinsically disordered region. Thus it is possible that Ser^{451} phosphorylation may also affect Class-2 PEPC's interaction with the outer mitochondrial envelope or may mediate protein:protein interactions with partners other than PTPC. In order to examine other putative roles of phosphorylation on Class-2 PEPCs *in vivo* function and localization, similar transient expression studies with FP-tagged PTPC and BTPC subunits in tobacco BY2 cells could be employed with the BTPC phosphomimetic S451D mutant and a S451A (alanine) mutant, to mimic both constitutive phosphorylation and constitutive dephosphorylation at this site. Any changes to the dynamic association of Class-2 PEPC with the mitochondrial outer envelope between these two mutants could be readily determined.

Another meaningful avenue of PEPC research would be to definitively determine the K_d value for the association of PTPC and BTPC subunits, and the influence, if any, of Ser^{451} phosphorylation on this interaction. It has now been fairly conclusively established that PTPC is BTPCs constitutive binding partner *in vivo* (Blonde and Plaxton, 2003; O'Leary *et al.,* 2009, O'Leary *et al.*, 2011b, Park *et al.,* 2012). Thus, in order to complete the characterization of this relationship it will be necessary to employ a technique such as isothermal titration calorimetry to determine the affinity with which BTPC binds PTPC. It will also be of great merit to perform structural studies via X-ray crystallography to deduce the crystal structure of Class-2 PEPC. This will provide crucial insights into the subunit architecture of Class-2 PEPC and, in conjunction with site-directed mutagenesis (i.e. the use of phosphomimetic BTPC mutant subunits), will provide information on the influence of BTPC phosphorylation on Class-2 PEPC's structure-function relationships.

Finally, COS BTPC contains two other phospho-sites; Thr^{4} at the N-terminus and Ser^{425} in close proximity to Ser^{451} within the intrinsically disordered region (O'Leary *et al.,* 2009, O'Leary *et al.*, 2011b). This thesis has determined that BTPC-K does not phosphorylate either of these sites. Therefore, there must be distinct protein kinases in developing COS endosperm responsible for regulating their phosphorylation *in vivo.* A similar experimental approach to the one undertaken in this thesis could provide the foundation for purifying, characterizing, and ultimately identifying these important BTPC protein kinases as well.

REFERENCES

Aboelsaad M, Wu R (1995) A rice membrane calcium-dependent protein-kinase is induced by ibberellin. Plant Physiol **108:** 787-793

Agetsuma M, Furumoto T, Yanagisawa S, Izui K (2005) The ubiquitin-proteasome pathway is involved in rapid degradation of phosphoenolpyruvate carboxylase kinase for C4 photosynthesis. Plant Cell Physiol **46:** 389-398

Alonso AP, Goffman FD, Ohlrogge JB, Shachar-Hill Y (2007) Carbon conversion efficiency and central metabolic fluxes in developing sunflower (*Helianthus annuus* L.) embryos. Plant J **52:** 296-308

Alonso AP, Dale VL, Shachar-Hill Y (2010) Understanding fatty acid synthesis in developing maize embryos using metabolic flux analysis. Metab Eng **12:** 488-497

Anil VS, Harmon AC, Rao KS (2003) Temporal association of Ca^{2+}-dependent protein kinase with oil bodies during seed development in *Santalum album* L.: Its biochemical characterization and significance. Plant Cell Physiol **44:**

Anil VS, Rao KS (2001) Purification and characterization of a Ca^{2+}-dependent protein kinase from sandalwood (*Santalum album* L.): evidence for Ca^{2+}-induced conformational changes. Phytochem **58:** 203-212

Antonio Monreal J, Javier Lopez-Baena F, Vidal J, Echevarria C, Garcia-Maurino S (2010) Involvement of phospholipase D and phosphatidic acid in the light-dependent up-regulation of sorghum leaf phosphoenolpyruvate carboxylase-kinase. J Exp Bot **61:** 2819-2827

Antonio Monreal J, Javier Lopez-Baena F, Vidal J, Echevarria C, Garcia-Maurino S (2007) Effect of LiCl on phosphoenolpyruvate carboxylase kinase and the phosphorylation of phosphoenolpyruvate carboxylase in leaf disks and leaves of *Sorghum vulgare*. Planta **225:** 801-812

Baud S, Lepiniec L (2010) Physiological and developmental regulation of seed oil production. Prog Lipid Res **49:** 235-249

Benedict CR, Beevers H (1961) Formation of sucrose from malate in germinating castor beans .1. Conversion of malate to phosphoenol-pyruvate. Plant Physiol **36:** 540-&

Blonde JD, Plaxton WC (2003) Structural and kinetic properties of high and low molecular mass phosphoenolpyruvate carboxylase isoforms from the endosperm developing castor oilseeds. J Biol Chem **278:** 11867-11873

Boudsocq M, Droillard M, Regad L, Lauriere C (2012) Characterization of Arabidopsis calcium-dependent protein kinases: activated or not by calcium? Biochem J **447:** 291-299

Brooks S (1992) A simple computer-program with statistical tests for the analysis of enzyme-kinetics. BioTechniques **13:** 906-911

Cavagnino A, Rossi F, Rizzi M (2011) The potent antiplasmodial calmodulin-antagonist trifluoperazine inhibits *Plasmodium falciparum* calcium-dependent protein kinase 4. Protein Peptide Lett **18:** 1273-1279

Chan AP, Crabtree J, Zhao Q, Lorenzi H, Orvis J, Puiu D, Melake-Berhan A, Jones KM, Redman J, Chen G, Cahoon EB, Gedil M, Stanke M, Haas BJ, Wortman JR, Fraser-Liggett CM, Ravel J, Rabinowicz PD (2010) Draft genome sequence of the oilseed species *Ricinus communis*. Nat Biotechnol **28:** 951-U3

Chang I, Curran A, Woolsey R, Quilici D, Cushman JC, Mittler R, Harmon A, Harper JF (2009) Proteomic profiling of tandem affinity purified 14-3-3 protein complexes in *Arabidopsis thaliana*. Proteomics **9:** 2967-2985

Chen Z, Jenkins GI, Nimmo HG (2008) pH and carbon supply control the expression of phosphoenolpyruvate carboxylase kinase genes in *Arabidopsis thaliana*. Plant Cell Environ **31:** 1844-1850

Chevalier D, Morris ER, Walker JC (2009) 14-3-3 and FHA domains mediate phosphoprotein interactions. Ann Rev Plant Biol **60:** 67-91

Chollet R, Vidal J, OLeary MH (1996) Phosphoenolpyruvate carboxylase: A ubiquitous, highly regulated enzyme in plants. Annu Rev Plant Physiol Plant Mol Biol **47:** 273-298

Chopra J, Kaur N, Gupta AK (2000) Ontogenic changes in enzymes of carbon metabolism in relation to carbohydrate status in developing mungbean reproductive structures. Phytochemistry **53:** 539-548

Coello P, Hey SJ, Halford NG (2011) The sucrose non-fermenting-1-related (SnRK) family of protein kinases: potential for manipulation to improve stress tolerance and increase yield. J Exp Bot **62:** 883-893

Dalziel KJ, O'Leary B, Brikis C, Rao SK, She Y, Cyr T, Plaxton WC (2012) The bacterial-type phosphoenolpyruvate carboxylase isozyme from developing castor oil seeds is subject to in vivo regulatory phosphorylation at serine-451. FEBS Lett **586:** 1049-1054

Dasgupta M (1994) Characterization of a calcium-dependent protein-kinase from *Arachis-hypogea* (groundnut) seeds. Plant Physiol **104:** 961-969

Dong LY, Masuda T, Kawamura T, Hata S, Izui K (1998) Cloning, expression, and characterization of a root-form phosphoenolpyruvate carboxylase from *Zea mays*: Comparison with the C-4-form enzyme. Plant Cell Physiol **39:** 865-873

Eastmond PJ, Dennis DT, Rawsthorne S (1997) Evidence that a malate inorganic phosphate exchange translocator imports carbon across the leucoplast envelope for fatty acid synthesis in developing castor seed endosperm. Plant Physiol **114:** 851-856

Eastmond PJ, Graham IA (2001) Re-examining the role of the glyoxylate cycle in oilseeds. Trends Plant Sci **6:** 72-77

Estruch JJ, Kadwell S, Merlin E, Crossland L (1994) Cloning and characterization of a maize pollen-specific calcium-dependent calmodulin-independent protein-kinase. Proc Natl Acad Sci U S A **91:** 8837-8841

Ettema TJG, Makarova KS, Jellema GL, Gierman HJ, Koonin EV, Huynen MA, de Vos WA, van der Oost J (2004) Identification and functional verification of archaeal-type phosphoenolpyruvate carboxylase, a missing link in archaeal central carbohydrate metabolism. J Bacteriol **186:** 7754-7762

Fukayama H, Tamai T, Taniguchi Y, Sullivan S, Miyao M, Nimmo HG (2006) Characterization and functional analysis of phosphoenolpyruvate carboxylase kinase genes in rice. Plant J **47:** 258-268

Gennidakis S, Rao S, Greenham K, Uhrig RG, O'Leary B, Snedden WA, Lu C, Plaxton WC (2007) Bacterial- and plant-type phosphoenolpyruvate carboxylase polypeptides interact in the hetero-oligomeric Class-2 PEPC complex of developing castor oil seeds. Plant J **52:** 839-849

Goffman FD, Alonso AP, Schwender J, Shachar-Hill Y, Ohlrogge JB (2005) Light enables a very high efficiency of carbon storage in developing embryos of rapeseed. Plant Physiol **138:** 2269-2279

Golombek S, Heim U, Horstmann C, Wobus U, Weber H (1999) Phosphoenolpyruvate carboxylase in developing seeds of *Vicia faba* L.: Gene expression and metabolic regulation. Planta **208:** 66-72

Gonzalez MC, Osuna L, Echevarria C, Vidal J, Cejudo FJ (1998) Expression and localization of phosphoenolpyruvate carboxylase in developing and germinating wheat grains. Plant Physiol **116:** 1249-1258

Greenwood J, Bewley J (1985) Seed development in *Ricinus-communis* Cv Hale (Castor Bean) .3. Pattern of storage protein and phytin accumulation in the endosperm. Can J Bot **63:** 2121-2128

Greenwood J, Bewley J (1982) Seed development in *Ricinus-communis* (Castor Bean) .1. Descriptive morphology. Can J Bot **60:** 1751-1760

Gregory AL, Hurley BA, Tran HT, Valentine AJ, She Y, Knowles VL, Plaxton WC (2009) In vivo regulatory phosphorylation of the phosphoenolpyruvate carboxylase AtPPC1 in phosphate-starved *Arabidopsis thaliana*. Biochem J **420:** 57-65

Hardie, G. (1999) Protein phosphorylation: A practical approach: A practical approach. , Oxford University Press

Harmon AC, Putnam-Evans C, Cormier MJ (1987) A calcium-dependent but calmodulin-independent protein-kinase from soybean. Plant Physiol **83:** 830-837

Harmon A, Yoo B, McCaffrey C (1994) Pseudosubstrate Inhibition of Cdpk, a protein-kinase with a calmodulin-like domain. Biochem (N Y) **33:** 7278-7287

Harper JF, Harmon A (2005) Plants, symbiosis and parasites: A calcium signalling connection. Nature Rev Mol Cell Biol **6:** 555-566

Hartwell J, Gill A, Nimmo GA, Wilkins MB, Jenkins GL, Nimmo HG (1999) Phosphoenolpyruvate carboxylase kinase is a novel protein kinase regulated at the level of expression. Plant J **20:** 333-342

Hetherington A, Trewavas A (1982) Calcium-dependent protein-kinase in pea shoot membranes. FEBS Lett **145:** 67-71

Hibberd JM, Covshoff S (2010) The regulation of gene expression required for C-4 photosynthesis. Ann Rev Plant Biol **61:** 181-207

Houston NL, Hajduch M, Thelen JJ (2009) Quantitative proteomics of seed filling in castor: comparison with soybean and rapeseed reveals differences between photosynthetic and non-photosynthetic seed metabolism. Plant Physiol **151:** 857-868

Hrabak EM, Chan CWM, Gribskov M, Harper JF, Choi JH, Halford N, Kudla J, Luan S, Nimmo HG, Sussman MR, Thomas M, Walker-Simmons K, Zhu JK, Harmon AC (2003) The *Arabidopsis* CDPK-SnRK superfamily of protein kinases. Plant Physiol **132:** 666-680

Huang JZ, Huber SC (2001) Phosphorylation of synthetic peptides by a CDPK and plant SNF1-related protein kinase. Influence of proline and basic amino acid residues at selected positions. Plant Cell Physiol **42:** 1079-1087

Igawa T, Fujiwara M, Tanaka I, Fukao Y, Yanagawa Y (2010) Characterization of bacterial-type phosphoenolpyruvate carboxylase expressed in male gametophyte of higher plants. Bmc Plant Biol **10:** 200

Izui K, Matsumura H, Furumoto T, Kai Y (2004) Phosphoenolpyruvate carboxylase: A new era of structural biology. Ann Rev of Plant Biol **55:** 69-84

Kai Y, Matsumura H, Izui K (2003) Phosphoenolpyruvate carboxylase: three-dimensional structure and molecular mechanisms. Arch Biochem Biophys **414:** 170-179

King SP, Badger MR, Furbank RT (1998) CO_2 refixation characteristics of developing canola seeds and silique wall. Aust J Plant Physiol **25:** 377-386

Lachaud C, Prigent E, Thuleau P, Grat S, Da Silva D, Briere C, Mazars C, Cotelle V (2013) 14-3-3-Regulated Ca^{2+}-dependent protein kinase CPK3 is required for sphingolipid-induced cell death in Arabidopsis. Cell Death Differ **20:** 209-217

Lara-Nunez A, Rodriguez-Sotres R (2004) Characterization of a dicarboxylate exchange system able to exchange pyrophosphate for L-malate in non-photo synthetic plastids from developing maize embryos. Plant Sci **166:** 1335-1343

Law RD, Plaxton WC (1997) Regulatory phosphorylation of banana fruit phosphoenolpyruvate carboxylase by a copurifying phosphoenolpyruvate carboxylase-kinase. E J Biochem **247:** 642-651

Lebouteiller B, Gousset-Dupont A, Pierre J, Bleton J, Tchapla A, Maucourt M, Moing A, Rolin D, Vidal J (2007) Physiological impacts of modulating phosphoenolpyruvate carboxylase levels in leaves and seeds of *Arabidopsis thaliana*. Plant Sci **172:** 265-272

Li B, Chollet R (1994) Salt induction and the partial purification/characterization of phosphoenolpyruvate carboxylase protein-serine kinase from an inducible crassulacean-acid-metabolism (CAM) plant, *Mesembryanthemum-crystallinum* L. Arch Biochem Biophys **314:** 247-254

Liese A, Romeis T (2013) Biochemical regulation of in vivo function of plant calcium-dependent protein kinases (CDPK). Biochim Biophys Acta **1833:** 1582-1589

Lu KP, Liou YC, Zhou XZ (2002) Pinning down proline-directed phosphorylation signaling. Trends Cell Biol **12:** 164-172

Mamedov TG, Moellering ER, Chollet R (2005) Identification and expression analysis of two inorganic C- and N-responsive genes encoding novel and distinct molecular forms of eukaryotic phosphoenolpyruvate carboxylase in the green microalga *Chlamydomonas reinhardtii*. Plant J **42:** 832-843

Marsh JT, Sullivan S, Hartwell J, Nimmo HO (2003) Structure and expression of phosphoenolpyruvate carboxylase kinase genes in *Solanaceae*. A novel gene exhibits alternative splicing. Plant Physiol **133:** 2021-2028

Martin ML, Busconi L (2000) Membrane localization of a rice calcium-dependent protein kinase (CDPK) is mediated by myristoylation and palmitoylation. Plant J**24:** 429-435

Moellering ER, Ouyang Y, Mamedov TG, Chollet R (2007) The two divergent PEP-carboxylase catalytic subunits in the green microalga *Chlamydomonas reinhardtii* respond reversibly to inorganic-N supply and co-exist in the high-molecular-mass, hetero-oligomeric class-2 PEPC complex. FEBS Lett **581:** 4871-4876

Moraes TF, Plaxton WC (2000) Purification and characterization of phosphoenolpyruvate carboxylase from *Brassica napus* (rapeseed) suspension cell cultures - Implications for phosphoenolpyruvate carboxylase regulation during phosphate starvation, and the integration of glycolysis with nitrogen assimilation. E J Biochem **267:** 4465-4476

Mukhopadhyay D, Riezman H (2007) Proteasome-independent functions of ubiquitin in endocytosis and signaling. Science **315:** 201-205

Murmu J, Plaxton WC (2007) Phosphoenolpyruvate carboxylase protein kinase from developing castor oil seeds: partial purification, characterization, and reversible control by photosynthate supply. Planta **226:** 1299-1310

Nhiri M, Bakrim N, Bakrim N, El Hachimi-Messouak Z, Echevarria C, Vidal J (2000) Posttranslational regulation of phosphoenolpyruvate carboxylase during germination of Sorghum seeds: influence of NaCl and L-malate. Plant Sci **151:** 29-37

Nimmo GA, Wilkins MB, Nimmo HG (2001) Partial purification and characterization of a protein inhibitor of phosphoenolpyruvate carboxylase kinase. Planta **213:** 250-257

Nimmo HG (2003) Control of the phosphorylation of phosphoenolpyruvate carboxylase in higher plants. Arch Biochem Biophys **414:** 189-196

Nimmo HG (2000) The regulation of phosphoenolpyruvate carboxylase in CAM plants. Trends Plant Sci **5:** 75-80

Nimmo HG (2006) Control of phosphoenolpyruvate carboxylase in plants. In: Control of Primary Metabolism in Plants (W. Plaxton and M. McManus, Eds.), Annual Plant Revews, Vol. **22:** 219-233

O'Leary B, Rao SK, Kim J, Plaxton WC (2009) Bacterial-type phosphoenolpyruvate carboxylase (PEPC) functions as a catalytic and regulatory subunit of the novel Class-2 PEPC complex of vascular plants. J Biol Chem **284:** 24797-24805

O'Leary B, Fedosejevs ET, Hill AT, Bettridge J, Park J, Rao SK, Leach CA, Plaxton WC (2011a) Tissue-specific expression and post-translational modifications of plant- and bacterial-type phosphoenolpyruvate carboxylase isozymes of the castor oil plant, *Ricinus communis* L. J Exp Bot **62:**

O'Leary B, Park J, Plaxton WC (2011b) The remarkable diversity of plant PEPC (phosphoenolpyruvate carboxylase): recent insights into the physiological functions and post-translational controls of non-photosynthetic PEPCs. Biochem J **436:**

O'Leary B, Rao SK, Plaxton WC (2011c) Phosphorylation of bacterial-type phosphoenolpyruvate carboxylase at Ser^{425} provides a further tier of enzyme control in developing castor oil seeds. Biochem J **433:** 65-74

Osuna L, Pierre JN, Gonzalez MC, Alvarez R, Cejudo FJ, Echevarria C, Vidal J (1999) Evidence for a slow-turnover form of the Ca^{2+}-independent phosphoenolpyruvate carboxylase kinase in the aleurone-endosperm tissue of germinating barley seeds. Plant Physiol **119:** 511-520

Park J, Khuu N, Howard ASM, Mullen RT, Plaxton WC (2012) Bacterial- and plant-type phosphoenolpyruvate carboxylase isozymes from developing castor oil seeds interact in vivo and associate with the surface of mitochondria. Plant J **71:** 251-262

Patel HM, Kraszewski JL, Mukhopadhyay B (2004) The phosphoenolpyruvate carboxylase from *Methanothermobacter thermautotrophicus* has a novel structure. J Bacteriol **186:** 5129-5137

Plaxton WC (1989) Molecular and immunological characterization of plastid and cytosolic pyruvate-kinase isozymes from castor-oil-plant endosperm and leaf. E J Biochem **181:** 443-451

Plaxton WC, Podesta FE (2006) The functional organization and control of plant respiration. Crit Rev Plant Sci **25:** 159-198

Pleite R, Pike M, Garces R, Martinez-Force E, Rawsthorne S (2005) The sources of carbon and reducing power for fatty acid synthesis in the heterotrophic plastids of developing sunflower (*Helianthus annuus* L.) embryos. J Exp Bot **56:** 1297-1303

Putnam-Evans CL, Harmon AC, Cormier MJ (1990) Purification and characterization of a novel calcium-dependent protein-kinase from soybean. Biochemistry **29:** 2488-2495

Radchuk R, Radchuk V, Goetz K, Weichert H, Richter A, Emery RJN, Weschke W, Weber H (2007) Ectopic expression of phosphoenolpyruvate carboxylase in *Vicia narbonensis* seeds: effects of improved nutrient status on seed maturation and transcriptional regulatory networks. Plant J **51:** 819-839

Rawsthorne S (2002) Carbon flux and fatty acid synthesis in plants. Prog Lipid Res **41:** 182-196

Rivoal J, Plaxton WC, Turpin DH (1998) Purification and characterization of high- and low-molecular-mass isoforms of phosphoenolpyruvate carboxylase from *Chlamydomonas reinhardtii* - Kinetic, structural and immunological evidence that the green algal enzyme is distinct from the prokaryotic and higher plant enzymes. Biochem J **331:** 201-209

Rivoal J, Trzos S, Gage DA, Plaxton WC, Turpin DH (2001) Two unrelated phosphoenolpyruvate carboxylase polypeptides physically interact in the high molecular mass isoforms of this enzyme in the unicellular green alga *Selenastrum minutum*. J Biol Chem **276:** 12588-12597

Rivoal J, Turpin DH, Plaxton WC (2002) In vitro phosphorylation of phosphoenolpyruvate carboxylase from the green alga *Selenastrum minutum*. Plant Cell Physiol **43:** 785-792

Rolletschek H, Borisjuk L, Radchuk R, Miranda M, Heim U, Wobus U, Weber H (2004) Seed-specific expression of a bacterial phosphoenolpyruvate carboxylase in *Vicia narbonensis* increases protein content and improves carbon economy. Plant Biotech J **2:** 211-219

Ruuska SA, Schwender J, Ohlrogge JB (2004) The capacity of green oilseeds to utilize photosynthesis to drive biosynthetic processes. Plant Physiol **136:** 2700-2709

Sanchez R, Cejudo FJ (2003) Identification and expression analysis of a gene encoding a bacterial-type phosphoenolpyruvate carboxylase from *Arabidopsis* and rice. Plant Physiol **132:** 949-957

Sangwan RS, Singh N, Plaxton WC (1992) Phosphoenolpyruvate carboxylase activity and concentration in the endosperm of developing and germinating castor-oil seeds. Plant Physiol **99:** 445-449

Saze H, Ueno Y, Hisabori T, Hayashi H, Izui K (2001) Thioredoxin-mediated reductive activation of a protein kinase for the regulatory phosphorylation of C4-form phosphoenolpyruvate carboxylase from maize. Plant Cell Physiol **42:** 1295-1302

Schnell JD, Hicke L (2003) Non-traditional functions of ubiquitin and ubiquitin-binding proteins. J Biol Chem **278:** 35857-35860

Schulz M, Klockenbring T, Hunte C, Schnabl H (1993) Involvement of ubiquitin in phosphoenolpyruvate carboxylase degradation. Botanica Acta **106:** 143-145

Schwender J, Shachar-Hill Y, Ohlrogge JB (2006) Mitochondrial metabolism in developing embryos of *Brassica napus*. J Biol Chem **281:** 34040-34047

Sebei K, Ouerghi Z, Kallel H, Boukhchina S (2006) Evolution of phosphoenolpyruvate carboxylase activity and lipid content during seed maturation of two spring rapeseed cultivars (*Brassica napus* L.). Comptes Rendus Biologies **329:** 719-725

Shane MW, Fedosejevs ET, Plaxton WC (2013) Reciprocal control of anaplerotic phosphoenolpyruvate carboxylase by *in vivo* monoubiquitination and phosphorylation in developing proteoid roots of phosphate-deficient Harsh Hakea. Plant Physiol **161:** 1634-1644

Shearer HL, Turpin DH, Dennis DT (2004) Characterization of NADP-dependent malic enzyme from developing castor oil seed endosperm. Arch Biochem Biophys **429:** 134-144

Shenton M, Fontaine V, Hartwell J, Marsh JT, Jenkins GI, Nimmo HG (2006) Distinct patterns of control and expression amongst members of the PEP carboxylase kinase gene family in C-4 plants. Plant J **48:** 45-53

Simcox P, Garland W, Deluca V, Canvin D, Dennis D (1979) Respiratory pathways and fat synthesis in the developing castor-oil seed. Can J Bot **57:** 1008-1014

Singal HR, Talwar G, Dua A, Singh R (1995) Pod photosynthesis and seed dark CO_2 fixation support oil synthesis in developing *Brassica* seeds. J Biosci **20:** 49-58

Smith RG, Gauthier DA, Dennis DT, Turpin DH (1992) Malate-dependent and pyruvate-dependent fatty-acid synthesis in leukoplastids from developing castor endosperm. Plant Physiol **98:** 1233-1238

Sullivan S, Jenkins GI, Nimmo HG (2004) Roots, cycles and leaves. Expression of the phosphoenolpyruvate carboxylase kinase gene family in soybean. Plant Physiol **135:** 2078-2087

Svensson P, Blasing OE, Westhoff P (2003) Evolution of C4 phosphoenolpyruvate carboxylase. Arch Biochem Biophys **414:** 180-188

Szczegielniak J, Liwosz A, Jurkowski I, Loog M, Dobrowolska GY, Ek P, Harmon AC, Muszynska G (2000) Calcium-dependent protein kinase from maize seedlings activated by phospholipids. Eur J Biochem **267:** 3818-3827

Tripodi KE, Turner WL, Gennidakis S, Plaxton WC (2005) In vivo regulatory phosphorylation of novel phosphoenolpyruvate carboxylase isoforms in endosperm of developing castor oil seeds. Plant Physiol **139:** 969-978

Tsuchida Y, Furumoto T, Izumida A, Hata S, Izui K (2001) Phosphoeno/pyruvate carboxylase kinase involved in C-4 photosynthesis in *Flaveria trinervia*: cDNA cloning and characterization. FEBS Lett **507:** 318-322

Ueoka-Nakanishi H, Sazuka T, Nakanishi Y, Maeshima M, Mori H, Hisabori T (2013) Thioredoxinh regulates calcium dependent protein kinases in plasma membranes. FEBS J **280:** 3220-31

Uhrig RG, O'Leary B, Spang HE, MacDonald JA, She Y, Plaxton WC (2008a) Coimmunopurification of phosphorylated bacterial- and plant-type phosphoenolpyruvate

carboxylases with the plastidial pyruvate dehydrogenase complex from developing castor oil seeds. Plant Physiol **146:** 1346-1357

Uhrig RG, She Y, Leach CA, Plaxton WC (2008b) Regulatory monoubiquitination of phosphoenolpyruvate carboxylase in germinating castor oil seeds. J Biol Chem **283:** 29650-29657

Vidal J, Chollet R (1997) Regulatory phosphorylation of C-4 PEP carboxylase. Trends Plant Sci **2:** 230-237

Wang YH, Chollet R (1993) Partial-purification and characterization of phosphoenolpyruvate carboxylase protein-serine kinase from illuminated maize leaves. Arch Biochem Biophys **304:** 496-502

Weber H, Borisjuk L, Wobus U (2005) Molecular physiology of legume seed development. Ann Rev Plant Biol **56:** 253-279

Xu WX, Zhou Y, Chollet R (2003) Identification and expression of a soybean nodule-enhanced PEP-carboxylase kinase gene (NE-PpcK) that shows striking up-/down-regulation in vivo. Plant J **34:** 441-452

Xu W, Sato SJ, Clemente TE, Chollet R (2007) The PEP-carboxylase kinase gene family in Glycine max (GmPpcK1-4): an in-depth molecular analysis with nodulated, non-transgenic and transgenic plants. Plant J **49:** 910-923

Yoon GM, Dowd PE, Gilroy S, McCubbin AG (2006) Calcium-dependent protein kinase isoforms in Petunia have distinct functions in pollen tube growth, including regulating polarity. Plant Cell **18:** 867-878

Zhang XQ, Chollet R (1997a) Phosphoenolpyruvate carboxylase protein kinase from soybean root nodules: Partial purification, characterization, and up/down-regulation by photosynthate supply from the shoots. Arch Biochem Biophys **343:** 260-268

Zhang XQ, Chollet R (1997b) Seryl-phosphorylation of soybean nodule sucrose synthase (nodulin-100) by a Ca^{2+}-dependent protein kinase. FEBS Lett **410:** 126-130

Zhao L, Shen L, Zhang W, Zhang W, Wang Y, Wu W (2013) Ca^{2+}-dependent protein kinase 11 and 24 modulate the activity of the inward rectifying K^+ channels in *Arabidopsis* pollen tubes. Plant Cell **25:** 649-661

Appendices

Appendix 1

Purification of Recombinant Class-2 PEPC

All purifications were conducted as previously described (O'Leary *et al.*, 2009; O'Leary *et al.*, 2011c). Briefly, *E. coli* cells containing heterologously expressed RcPPC4 or AtPPC3 (or the phosphomimetic mutant RcPPC4^{Ser451D} or the AtPPC3^{R644A} inactive isozyme) were lysed by passage through a French press and cell extracts were subsequently mixed together. The resulting Class-2 PEPCs were purified using PrepEase^{TM} His-Tagged High Yield Purification Ni^{2+}-affinity resin (USB Corp.) followed by Superdex-200 and Superpose-6 gel filtration FPLC (GE Biosciences). Pooled peak fractions were concentrated with an Amicon Ultra-15 centrifugal filter unit (100-kDa cut-off), frozen in liquid N_2, and stored at -80 °C until use. PEPC activity was stable for at least 2 months when stored under these conditions.

Appendix 2

Polyacrylamide gel slice dissolution for quantification of radio-labeled protein by scintillation counting after gel electrophoresis

Protein samples were subjected to SDS-PAGE and staining with Coomassie Blue R-250. Pertinent protein-staining bands were excised from the SDS gel using a razor blade and were incubated in tightly sealed scintillation vials in the presence of 50 µl of 30% H_2O_2 plus 5 µl of 10 mM $CuSO_4$ at 25 ℃ for 16 h. After incubation, vials were uncapped, 200 µl of dH_2O and 3 mL of scintillation cocktail were added, and ^{32}P-radioactivity determined via Cerenkov counting (Donato *et al.*, 1988).

Appendix 3

In vitro phosphorylation of BTPC at Ser^{451} with Protein Kinase A and Dephosphorylation with PP2Ac or λ-Phosphatase

Aliquots (50 µl) of purified recombinant Class-2 PEPC were desalted into the standard dephosphorylation buffer containing 50 mM Tris-HCl (pH 7.5), 5 mM $MgCl_2$, 1 mM DTT, and 20% (v/v) glycerol, using Micro Spin-OUT GT-1200 desalting columns (G-Biosciences) according to the manufacturer's instructions. Desalted Class-2 PEPC (50 µg) was incubated at30 ℃ with 20 units/ml of the catalytic subunit of bovine heart PK-A (Sigma) and 50 nM microcystin-LR ±1 mM ATP. Aliquots of PK-A-treated Class-2 PEPC were subsequently incubated at 30 ℃ in the presence of 15 milliunits/ml of the catalytic subunit of bovine heart PP2A ± 50 nM MC-LR according to Tripodi *et al.,* (2005). Aliquots were withdrawn at specified times and assayed for relative ^{32}P incorporation into Ser^{451} of BTPC subunits by subjecting aliquots of kinase assays to SDS-PAGE and immunoblotting with anti-pSer451 (in the presence of 10 µg/ml dephosphopeptide) and anti-BTPC.

Appendix 4

Protein kinase assay by TCA precipitation (adapted from "Protein Phosphorylation – A practical approach" by Hardie et al., 1999, Book).

1. Run typical 25 or 50 µl BTPC-K assay in 1.5 ml eppendorf tube
2. Stop reaction by adding 1 ml of cold 20% (w/v) TCA containing 0.2% (w/v) NaPPi
3. When all reactions have been stopped, add 30 µl of 10 mg ml^{-1} BSA[1], cap the tube, vortex mix, and leave on ice for at least 2 min.
4. Centrifuge the tubes for 2 min with the tags holding the caps facing radially outwards[2].
5. Remove the supernatant[3] by sliding a glass Pasteur pipette down the face of the tube that was facing radially inwards[4] (opposite to the cap tag). The protein pellet may not be visible; be careful not to scrape the bottom with the pipette tip. A few µl of supernatant will remain but this will be removed in subsequent steps.
6. Add 1 ml cold 20% (w/v) TCA, vortex mix, centrifuge for 2 min, and remove supernatant as before.
7. Repeat step 6 twice more.
8. Count tubes, using Cerenkov effect, by placing the whole tube into a scintillation vial and counting using a scintillation counter.
9. Use appropriate blanks to determine background.

[1] The BSA acts as a carrier for precipitation.
[2] Because the protein pellets may not be visible after subsequent washes, in a fixed angle microcentrifuge rotor the pellet will form a streak near the bottom of the tube on the tube face that was radially outwards. The tag on the tube cap provides the orientation for this.
[3] Initial supernatants and following washes will be radioactive and must be handled with appropriate safety precautions.
[4] This will ensure that the protein pellet is not disturbed.

Appendix 5

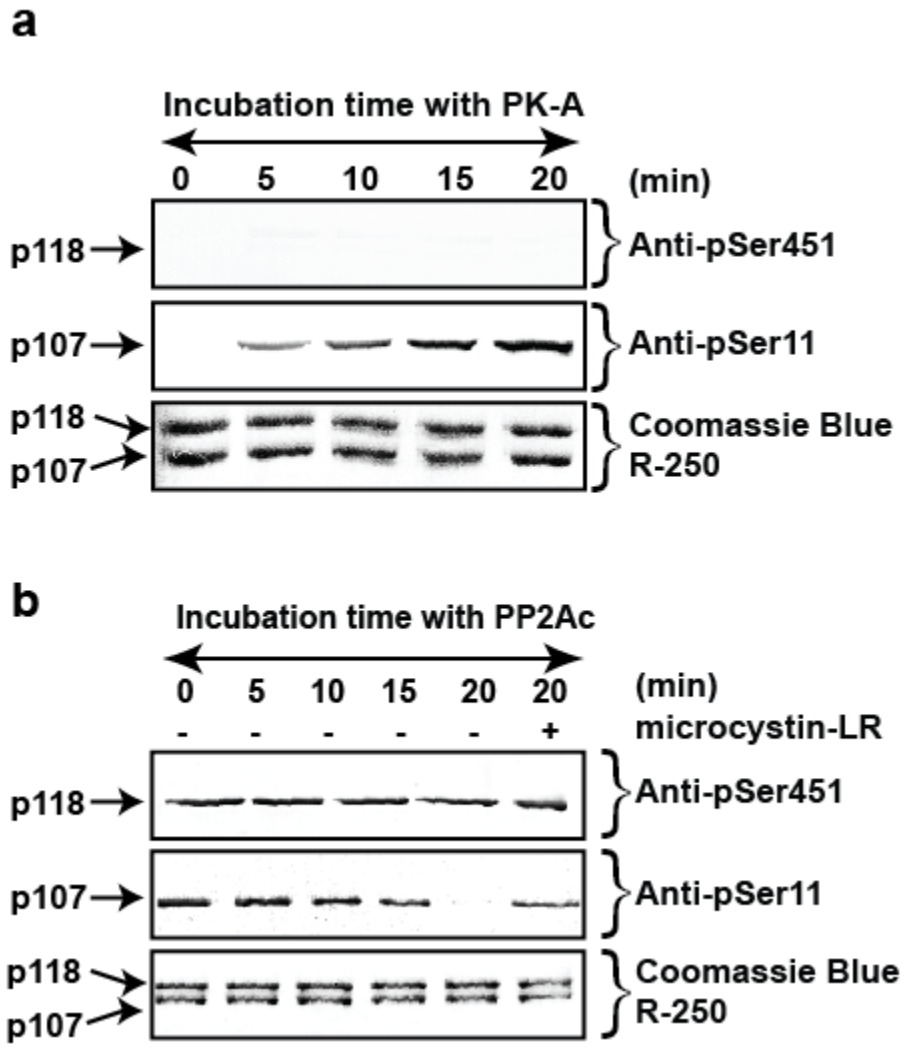

Figure S1. (a) Exogenous bovine PK-A is unable to phosphorylate COS BTPC subunits of Class-2 PEPC at Ser^{451}. (**b)** Exogenous PP2Ac is unable to dephosphorylate phospho-Ser^{451} residues of COS BTPC subunits of Class-2 PEPC. Pure recombinant Class-2 PEPC (50 µg) was incubated at 30 °C in the presence of **(a)** 20 U ml^{-1} of the catalytic subunit of bovine heart PK-A as in Tripodi *et al.* (2005). Aliquots were removed at various time points and subjected to SDS-PAGE, followed by Coomassie blue R-250 staining or immunoblotting with either anti-pSer451 (1 µg BTPC/lane) or anti-PTPC phosphosite-specific (anti-pSer11) (1 µg PTPC/lane) and chromogenic detection as in Tripodi *et al.* (2005). **(b)** Class-2 PEPC previously phosphorylated at Ser^{451} of the BTPC subunit and Ser^{11} of the PTPC subunit was incubated at 30 °C in the presence of 5 mU/ml of the catalytic subunit of bovine heart PP2A as in Gregory *et al., (*2009) in the presence and absence of 50 nM microcystin-LR. Aliquots were withdrawn at specified times and subjected to SDS-PAGE followed by immunoblotting as described in panel **a.**

Appendix 6

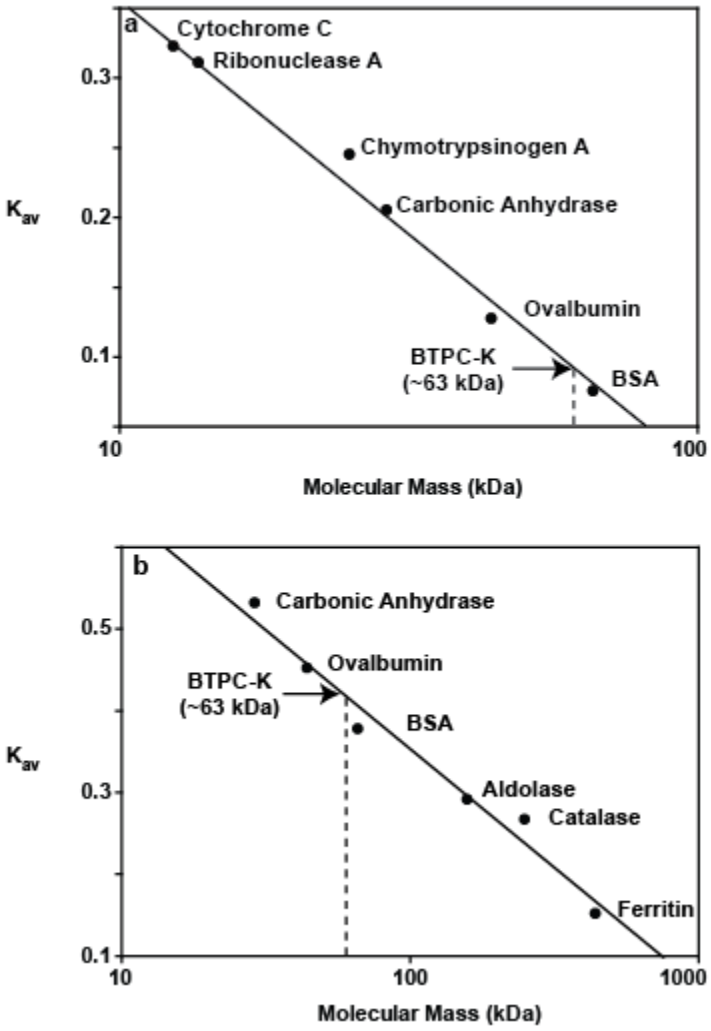

Figure S2. Native molecular mass determination for purified BTPC-K. BTPC native M_r was estimated via gel filtration chromatography on both a calibrated **(a)** Superdex-75 10/30 GL column and **(b)** Superdex-200 10/300 GL column. Results reproducible in three independent repetitions.

Appdendix 7

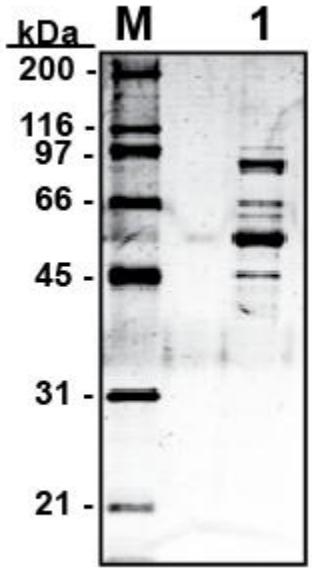

Figure S3. Analysis of purified COS BTPC-K by SDS-PAGE. Proteins from the final pooled and concentrated Blue-Sepharose fraction (1 μg) were resolved on a 10% SDS-PAGE gel, stained with Sypro Red, and protein-staining bands visualized using a Typhoon 6000 (lane 1). M, protein molecular weight standards.

Appendix 8

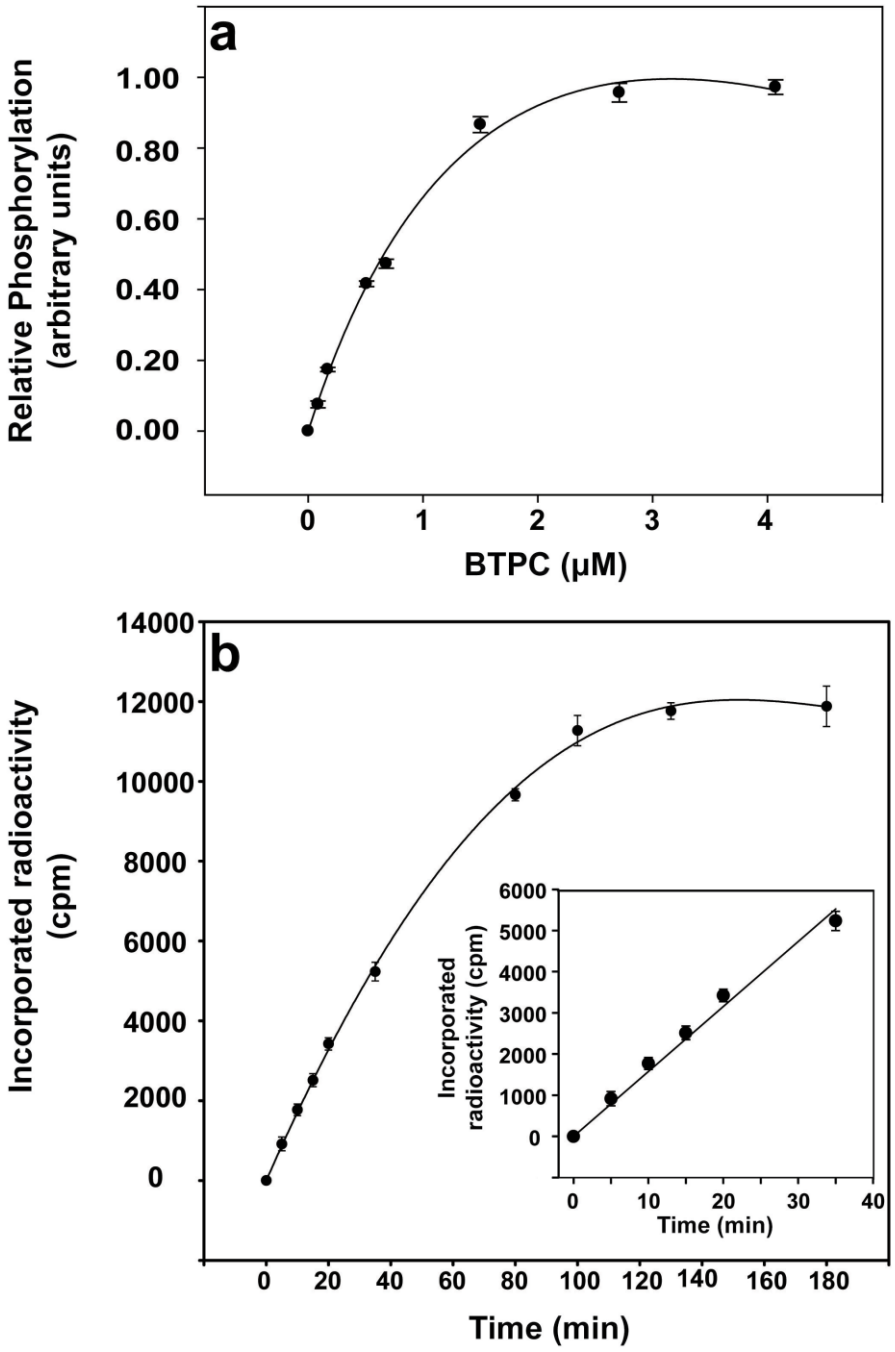

Figure S4. Determination of COS BTPC-K specific activity. **(a)** Saturation curve for BTPC phosphorylation by partially purified BTPC-K (250 ng). All Values were obtained by scintillation counting of the ^{32}P incorporated on BTPC as is described under Materials and Methods. **(b)** Time-course of ^{32}P incorporation (cpm) into BTPC (5 µg) after phosphorylation by purified BTPC-K (250 ng). Values were used to calculate maximal stoichiometric P incorporation into BTPC. Values were obtained by scintillation counting of the ^{32}P incorporated into BTPC as is described under Materials and Methods. **Inset,** linear range for ^{32}P incorporation into BTPC used to calculate specific activity of purified BTPC-K.

Appendix 9

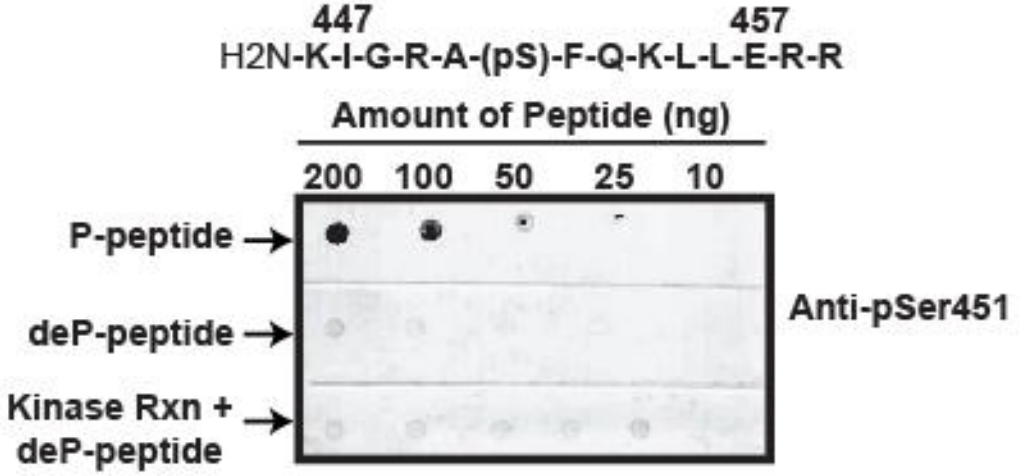

Figure S5. BTPC-K is unable to phosphorylate synthetic peptides containing residues flanking the BTPC Ser^{451} phospho-site. The synthetic peptide was a variant of the phosphorylation motif surrounding BTPC Ser^{451} with the following modifications; (1) Ser^{450} was replaced with Ala in order to ensure that Ser^{451} was the only Ser residue in the peptide, and (2) an additional Arg was added to the N-terminus to improve peptide binding to P81 paper. Synthetic peptide (0.4 mM) was incubated at 30 °C with partially purified BTPC-K (250 ng) (total reaction volume 25µl), in the presence of 0.1 mM of non-radioactive ATP. Reactions were terminated by either dot blotting varying amounts of kinase reactions (along with corresponding phospho- and dephospho-peptides as controls) and probing with anti-pSer451.

Appendix 10

Table S1. Effect of exogenous proteins and a CaM antagonist on BTPC-K activity. Kinase activity was determined in the presence of 1 µM of each compound unless otherwise indicated, using the standard [γ-^{32}P]-ATP radiometric kinase assay. Activity is expressed relative to BTPC-K activity in the absence of any effectors, set at 100%. All values represent the means of triplicate determinations and are reproducible within ± 15 % of the mean value.

Addition	Activity (%)
None	100
CaM	80
14-3-3	87
BSA	85
TFP*	50

*****TFP assayed at 100 µM

Appendix 11

Figure S6. Domain structure of a CDPK. V, N-terminal variable domain; K, kinase domain; CAD, CDPK activation domain; PS, pseudosubstrate segment; CLD; calmodulin-like domain; EF, EF-hand. EF-hand Ca^{2+}-binding loops are represented here as white bars within the EF-hand motifs. This drawn-to-scale scheme is representative of *At*CPK21, which consists of 531 amino acids (Taken from Liese and Romeis, 2013).

Appendix 12

Table S2. Predicted properties of deduced castor CDPKs

Gene Name[a]	Sub-Family	Length (A.A.)	MW (kDa)[b]	pI[b]	Subcellular Distribution[c]	Soluble or Insoluble[c]	Gene ID[a]
RcCDPK1	Ⅰa	533	60.2	6.55	Mitochondrion	Insoluble	16815051_peptide|Rcommunis|29983.t000185|29983.m003286
RcCDPK11	Ⅰa	497	56.0	5.33	Mitochondrion	Insoluble	16815050_peptide|Rcommunis|29983.t000184|29983.m003285
RcCDPK18	Ⅰa	551	62.1	6.44	Other	Insoluble	16806882_peptide|Rcommunis|29728.t000018|29728.m000812
RcCDPK19	Ⅰa	578	64.2	5.40	Chloroplast	Insoluble	16823697_peptide|Rcommunis|30190.t000579|30190.m011343
RcCDPK23	Ⅰa	305	34.3	8.30	Chloroplast	Soluble	16819478_peptide|Rcommunis|30142.t000025|30142.m000651
RcCDPK24	Ⅰa	187	20.8	4.38	Other	Insoluble	16822115_peptide|Rcommunis|30170.t000694|30170.m014282
RcCDPK26	Ⅰa	561	62.8	5.52	Mitochondrion	Soluble	16799163_peptide|Rcommunis|27777.t000008|27777.m000274
RcCDPK27	Ⅰa	536	59.5	5.86	Other	Insoluble	16810728_peptide|Rcommunis|29842.t000094|29842.m003597
RcCDPK31	Ⅰa	529	59.7	6.47	Chloroplast	Insoluble	16817768_peptide|Rcommunis|30100.t000014|30100.m000791
RcCDPK33	Ⅰa	528	59.2	6.35	Other	Soluble	16811562_peptide|Rcommunis|29852.t000019|29852.m002000
RcCDPK4	Ⅰa	641	72.1	6.21	Other	Insoluble	16802702_peptide|Rcommunis|29333.t000051|29333.m001088
RcCDPK5	Ⅰa	584	65.4	5.32	Chloroplast	Soluble	16802692_peptide|Rcommunis|29333.t000041|29333.m001078
RcCDPK13	Ⅰb	529	60.1	6.94	Other	Soluble	16800511_peptide|Rcommunis|28308.t000002|28308.m000065
RcCDPK21	Ⅰb	533	60.4	6.02	Mitochondrion	Insoluble	16808108_peptide|Rcommunis|29761.t000015|29761.m000421
RcCDPK28	Ⅰb	549	62.3	6.67	Other	Soluble	16821242_peptide|Rcommunis|30169.t000219|30169.m006442
RcCDPK3	Ⅰb	525	59.4	5.99	Other	Insoluble	16812395_peptide|Rcommunis|29896.t000003|29896.m000119
RcCDPK30	Ⅰb	536	60.3	6.77	Other	Insoluble	16820071_peptide|Rcommunis|30147.t000328|30147.m014057
RcCDPK12	Ⅱa	512	57.2	7.54	Other	Insoluble	16808371_peptide|Rcommunis|29780.t000025|29780.m001339
RcCDPK14	Ⅱa	598	67.6	9.09	Chloroplast	Soluble	16805369_peptide|Rcommunis|29676.t000013|29676.m001622
RcCDPK15	Ⅱa	148	17.1	8.18	Other	Insoluble	16807073_peptide|Rcommunis|29733.t000003|29733.m000739
RcCDPK16	Ⅱa	575	65.1	8.98	Chloroplast	Insoluble	16810129_peptide|Rcommunis|29830.t000004|29830.m001387
RcCDPK2	Ⅱa	602	67.3	8.84	Other	Insoluble	16817534_peptide|Rcommunis|30089.t000034|30089.m001020
RcCDPK25	Ⅱa	589	66.0	8.85	Other	Insoluble	16799638_peptide|Rcommunis|27964.t000005|27964.m000350
RcCDPK8	Ⅱa	467	51.9	7.75	Chloroplast	Insoluble	16808369_peptide|Rcommunis|29780.t000023|29780.m001337
RcCDPK10	Ⅱb	105	12.3	4.47	Other	Insoluble	16805518_peptide|Rcommunis|29680.t000028|29680.m001685
RcCDPK17	Ⅱb	466	51.5	8.91	Mitochondrion	Insoluble	16805517_peptide|Rcommunis|29680.t000027|29680.m001684

RcCDPK20	IIb	273	30.4	6.80	Other	Soluble	16812383_peptide|Rcommunis|29895.t000006|29895.m000312
RcCDPK22	IIb	490	53.8	7.13	Other	Soluble	16810323_peptide|Rcommunis|29838.t000023|29838.m001653
RcCDPK29	IIb	530	58.2	6.44	Other	Soluble	16823475_peptide|Rcommunis|30190.t000351|30190.m011115
RcCDPK32	IIb	475	52.7	5.25	Other	Soluble	16812933_peptide|Rcommunis|29908.t000164|29908.m006113
RcCDPK34	IIb	508	56.8	5.49	Chloroplast	Soluble	16824290_peptide|Rcommunis|30226.t000071|30226.m002047
RcCDPK9	IIb	162	18.3	6.76	Mitochondrion	Insoluble	16820328_peptide|Rcommunis|30147.t000588|30147.m014317
RcCDPK6	III	309	34.6	5.10	Other	Soluble	16802708_peptide|Rcommunis|29333.t000058|29333.m001095
RcCDPK7	III	284	32.9	7.62	Other	Soluble	16802707_peptide|Rcommunis|29333.t000056|29333.m001093

[a]Source of protein coding transcripts was Phytozome (http://www.phytozome.net/). [b]Molecular masses in kilodaltons and pI predicted using DNAStar software. [c]Subcellular distribution was predicted using TargetP (http://www.cbs.dtu.dk/services/TargetP/). [d]Solubility predicted using PROSO II (http://mips.helmholtz-muenchen.de/prosoII/prosoII.seam).

Appendix 13

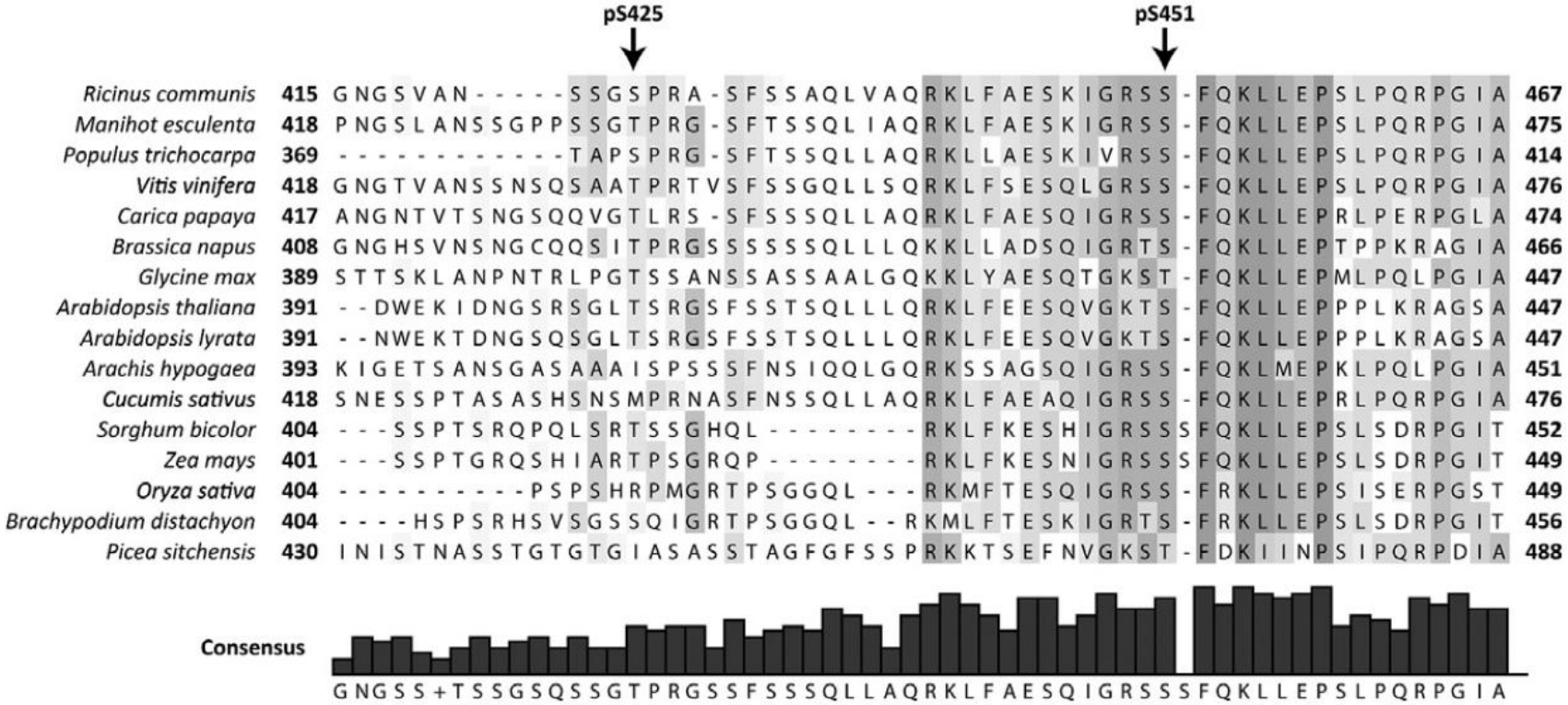

Figure S7. Partial alignment of COS BTPC Ser[425] and Ser[451] phosphorylation domains with other vascular plant BTPCs. Available full length plant BTPC amino acid sequences were aligned using the TCoffee program (available online at http://www.tcoffee.org/). Ser[425] and Ser[451] phospho-sites are indicated by the arrows. *****, **:** and **.** indicate decreasing degrees of conservation. The protein sequences were identified using NCBI's BLAST program and the NCBI (http://www.ncbi.nlm.nih.gov/) or Phytozome (www.phytozome.org) databases (taken from Dalziel *et al.*, 2012).